MOLECULAR CONSTANTS OF NO_2 FROM HIGH-RESOLUTION ABSORPTION SPECTRA AND MAGNETIC CIRCULAR DICHROISM AND MAGNETIC CIRCULAR BIREFRINGENCE OF NO AND NO_2

Thesis for the Degree of Ph. D.

MICHIGAN STATE UNIVERSITY
RICHARD E. BLANK

1970

This is to certify that the

thesis entitled

MOLECULAR CONSTANTS OF NO_2 FROM HIGH-RESOLUTION ABSORPTION SPECTRA AND MAGNETIC CIRCULAR DICHROISM AND MAGNETIC CIRCULAR BIREFRINGENCE OF NO AND NO_2

presented by

RICHARD E. BLANK

has been accepted towards fulfillment
of the requirements for

Ph.D. degree in PHYSICS

C. D. Hause

Major professor

Date April 17, 1970

ABSTRACT

MOLECULAR CONSTANTS OF NO_2 FROM
HIGH-RESOLUTION ABSORPTION SPECTRA
AND
MAGNETIC CIRCULAR DICHROISM AND MAGNETIC
CIRCULAR BIREFRINGENCE OF NO AND NO_2

by Richard E. Blank

High-resolution, near-infrared absorption spectra of the (0,0,3), (1,0,3), and (3,0,1) vibration-rotation bands of $^{14}N^{16}O_2$ and $^{15}N^{16}O_2$ have been analyzed. Ground state constants have been given by Olman and Hause as well as vibration-rotation interaction constants from which initial values for A, B, and C in the upper states were predicted. Improved values for the upper state constants including centrifugal distortion and empirical P^6 terms have been obtained. Prediction of improved ground state constants showed no significant difference from those previously reported.

Spin splitting was observed and analyzed for a number of transitions in the (0,0,3) band of both isotopes since the splitting was large and resolution favorable in that region ($\sim$0.03 cm^{-1}). Effective spin-rotation coupling constants were obtained for the excited state. No spin splitting was observed in either of the (1,0,3) or (3,0,1) bands due to weakness of absorption and reduced resolution ($\sim$0.05 cm^{-1}) in that region.

Richard E. Blank

The (1,0,1) and (2,0,1) bands previously analyzed in this laboratory combined with the results from the (0,0,3), (1,0,3), and (3,0,1) bands have been used to calculate vibrational and vibration-rotation interaction constants.

Finally methods based on those described by Stalder and Eberhardt for measurement of magnetic circular dichroism and magnetic circular birefringence were used to obtain these spectra for the (0,0,3) band of NO_2. Magnetic circular birefringence spectra were also observed for the 3-0 band of NO.

The Jones-Mueller matrix mathematics of polarized light is discussed, and a general matrix describing the effect of a dichroic, birefringent sample on any incident state of polarization has been derived. The Jones-Mueller calculus was then used to derive intensity expressions for magnetic circular dichroism and magnetic circular birefringence.

MOLECULAR CONSTANTS OF NO_2 FROM HIGH-RESOLUTION ABSORPTION SPECTRA AND MAGNETIC CIRCULAR DICHROISM AND MAGNETIC CIRCULAR BIREFRINGENCE OF NO AND NO_2

By

Richard E. Blank

A THESIS

Submitted to
Michigan State University
in partial fulfillment of the requirements
for the degree of

DOCTOR OF PHILOSOPHY

Department of Physics

1970

TO KAREN

ACKNOWLEDGMENTS

It has been a privilege to work and study under the patient guidance of Professor C. D. Hause. His dedication to teaching and research is evident to all who know him. I am grateful to Professor T. H. Edwards who has given freely of his time and who has provided many good ideas. I appreciate the aid of Professor P. M. Parker who has taken the time to answer many questions. My thanks also to Professor R. D. Spence for the help that he has given.

I would like to thank Dr. Melvin Olman who contributed much to the development of this work. I appreciate the assistance received from Dr. Donald Keck and Dr. Lamar Bullock who contributed computer programs which were very useful in reducing the data. I wish also to thank Dr. Peter Willson, Dr. Richard Peterson, Dr. Lewis Snyder, Dr. Tom Barnett, and Dr. Kent Moncur for their stimulating discussions and various contributions.

I am grateful to the Department of Physics and the National Science Foundation for their support of this work through assistantships, fellowships and grants. My thanks to the Michigan State University Computer Center staff for their assistance and consideration.

I am deeply grateful to my parents, Mr. and Mrs. E. H. Blank, for their encouragement. My father contributed

several ideas for experimental apparatus.

A special thanks to my wife, Karen, for her help in the preparation of this thesis and for making it all worthwhile.

TABLE OF CONTENTS

LIST OF FIGURES

LIST OF TABLES

LIST OF APPENDICES

INTRODUCTION

Nitrogen dioxide and nitric oxide have been of interest in molecular spectroscopy because they are among the very few stable, paramagnetic molecules. The single unpaired electron possessed by these molecules produces unique spin coupling and magnetic effects.

This work is primarily concerned with studies of vibration-rotation bands and magnetic effects in NO_2(1)-(6). Also included are experimental magnetic circular birefringence spectra of NO which are of interest in themselves. The NO spectra, because of their intensity, were useful in refining the experimental techniques for the weaker magnetic circular birefringence and dichroism spectra of NO_2.

The first section of this work details the analysis of the (0,0,3), (1,0,3), and (3,0,1) vibration-rotation spectra of $^{14}N^{16}O_2$ and $^{15}N^{16}O_2$ in the near-infrared. The spectra are analyzed on the basis of the slightly asymmetric rotor with the spin-rotation interaction as a perturbation. From these results combined with the previously analyzed (1,0,1) and (2,0,1) bands are derived the upper state constants, spin-rotation coupling constants, vibrational and vibration-rotation interaction constants.

The second part of this work details the experimental

results of recent techniques (7) (8) for obtaining separation of magnetic circular birefringence and magnetic circular dichroism effects which have generally been measured in a combined form in magnetic rotation studies (9) (10). An introduction to the Jones-Mueller mathematics of polarization is given which is used to derive intensity expressions for the two experimental arrangements. Experimental spectra are presented for NO_2 and NO as well as an indication of the methods by which predicted spectra may eventually be generated and compared to the observed.

CHAPTER I

THEORY

ENERGY EXPRESSIONS

This part of the work is a continuation of the investigations begun by Olman and Hause on the absorption spectra of $^{14}N^{16}O_2$ and $^{15}N^{16}O_2$. A discussion of the theory of energy levels, selection rules, and spin-rotation interaction is presented.

GEOMETRY

Nitrogen dioxide is a slightly asymmetric, non-linear, triatomic molecule whose geometry is illustrated in Figure 1. The assignment of axes a, b, and c is as shown. Each axis has associated with it a moment of inertia I_a, I_b, and I_c respectively. It is conventional to define reciprocal quantities:

$$R = \frac{h}{8\pi^2 c I_r}$$

where R = A,B,C and r = a,b,c respectively. Molecules are classified according to the relative value of the reciprocal moments:

A = B = C	Spherical Top
A > B = C	Prolate Symmetric Top

$\measuredangle$O-N-O = $134^{o}4'$, r_s = 1.1934 Å

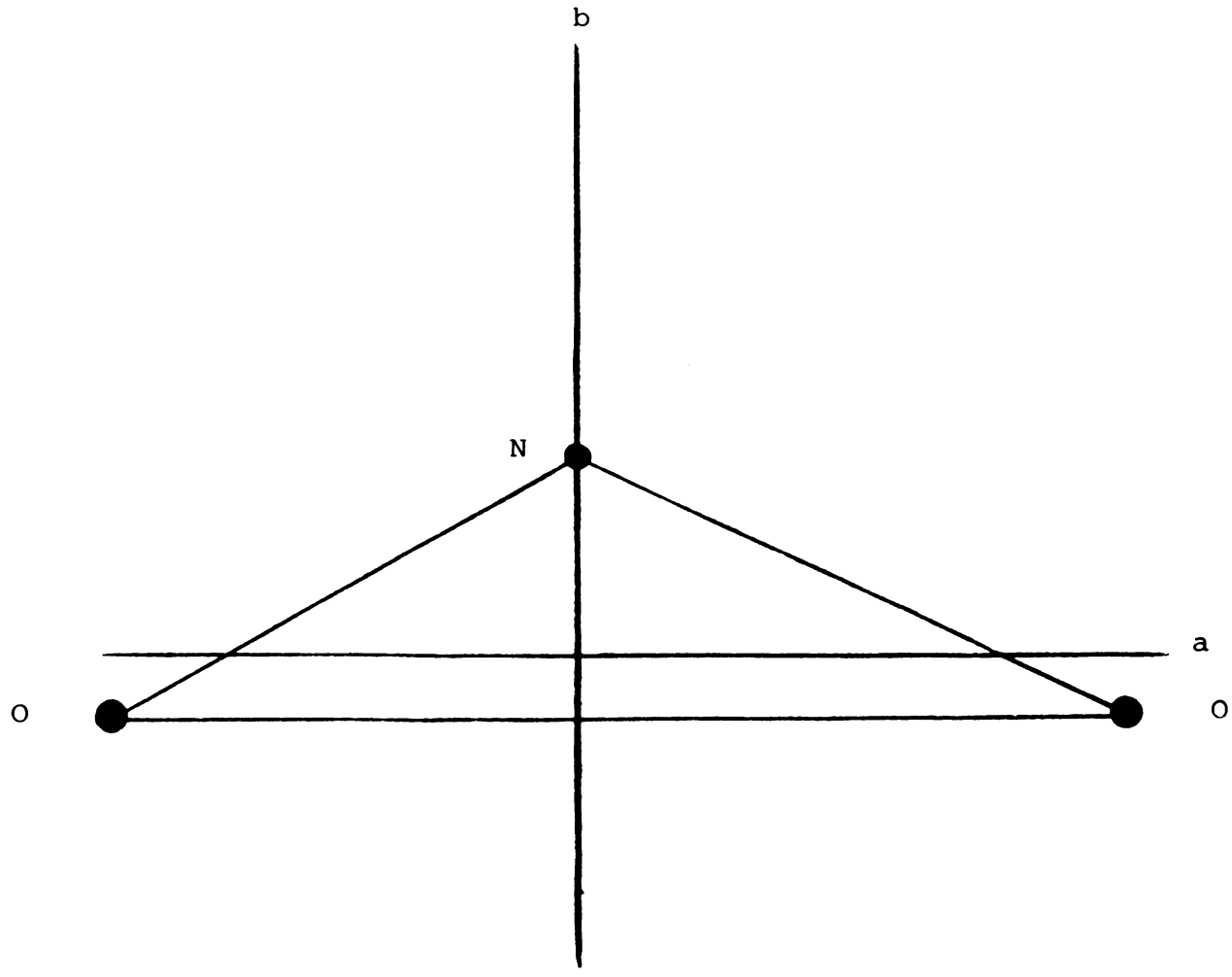

Figure 1
Geometry of the NO_2 molecule.

$A = B > C$ Oblate Symmetric Top

$A > B > C$ Asymmetric Top

In each case the axes have been assigned to the molecule such that $A \geq B \geq C$.

Nitrogen dioxide closely approaches the prolate symmetric top since B and C are nearly equal. One method of denoting the degree of asymmetry is by the value of Ray's asymmetry parameter

$$\kappa = \frac{2B - A - C}{A - C}$$

where $\kappa = +1$ (-1) for an oblate (prolate) symmetric top. Nitrogen dioxide is found to have $\kappa = -0.994$ so that it is a close approximation to the prolate symmetric top. This is an aid in analysis since energy levels for symmetric tops can be expressed in closed form, and perturbation theory yields excellent values for levels of slightly asymmetric tops.

SYMMETRY CONSIDERATIONS

As can be seen from Figure 1, nitrogen dioxide belongs to the C_{2v} group with the b-axis corresponding to the symmetry axis. This symmetry has an important consequence in that if the two identical nuclei have zero or integral spin the total eigenfunction for the state must be symmetric and the molecule follow Bose statistics. This means that even though the symmetric top energy levels are split by the asymmetry of the molecule, only the totally symmetric levels are populated i.e. half of the levels are missing.

The missing levels can be determined as follows. All transitions discussed here are within the $^2\Sigma$ ground state which is symmetric. If the vibrational state is denoted by (v_1,v_2,v_3) then the vibrational eigenfunction is symmetric (antisymmetric) as v_3 is even (odd), and all upper states observed here have v_3 odd. Finally the nature of a rotation about the b-axis is such that the rotational eigenfunction is symmetric under a 180° rotation about the b-axis if K_{-1} and K_{+1} are both odd or both even, and antisymmetric if one is odd and one is even (11). Thus the rotational wavefunction is symmetric if $K_{-1} + K_{+1}$ is even and antisymmetric if $K_{-1} + K_{+1}$ is odd. Since the total eigenfunction

$$\Psi = \Psi_E \Psi_V \Psi_R$$

must be symmetric, we have for the ground state

(Symmetric)x(Symmetric)x(Symmetric) → Symmetric

and for the upper state

(Symmetric)x(Antisymmetric)x(Antisymmetric) → Symmetric

Thus Ψ_R must be symmetric in the ground state and antisymmetric in the upper state. As a consequence of the missing levels symmetric rotor notation, $^{\Delta K}\Delta N_K(N)$, may be used without ambiguity where K is K_{-1}.

SELECTION RULES

All observed bands were of Type A which correspond to parallel bands in the near-by prolate limit. For such bands the selection rules are

$$\Delta K_{-1} = 0$$
$$\Delta N = 0,\pm 1 \quad \text{if } K_{-1} \neq 0 \qquad (1)$$
$$\Delta N = \pm 1 \quad \text{if } K_{-1} = 0$$

$\Delta K_{-1} = \pm 2$ transitions which would be allowed by the finite asymmetry of the molecule were not observed presumably due to the very low intensity of such lines.

ASYMMETRIC ENERGY EXPRESSIONS

The energy levels have been determined from the perturbation expansion:

$$E = E_0 + E_1 + E_2 + E_{SR}$$

E_{SR} represents the spin-rotation interaction energy and will be given in detail in the next section.

E_o is the rigid rotor energy for the slightly asymmetric molecule based on the Wang reduced energies(12).

$$E_0 = \left(\frac{B+C}{2}\right)N(N+1) + \left(A-\left(\frac{B+C}{2}\right)\right)\omega \qquad (2)$$

A,B, and C are the molecular rotational constants, and ω is the Wang reduced energy. The method used to obtain the Wang energies is based on the diagonalization of the Wang reduced energy matrices by numerical techniques(13).

E_1 includes P^4 or centrifugal distortion terms of the form:

$$E_1 = \sum_{i=1}^{4} \tau_i X_i = \tau_{aaaa}X_1 + \tau_{bbbb}X_2 + \tau_{aabb}X_3 + \tau_{abab}X_4 \qquad (3)$$

The τ's are treated as parameters and account is taken of

possible vibrational dependence by allowing the τ's to be determined independently in the upper and lower states. It was found that there is a strong correlation between τ_{aabb} and τ_{abab} in each of the bands studied. In order to determine a significant estimate of τ_{aabb} the value of τ_{abab} was calculated from the expression of Chung and Parker (27).

$$\tau_{abab} = \frac{-16\ A_e B_e C_e}{\omega_3^2}$$

Explicit expressions for the χ's are given by Hill (14)(21).

$$\chi_1 = \frac{1}{16}\Big\{r^2[N^2(N+1)^2-\delta_1-2N(N+1)\delta_2] - (r-2)[2rN(N+1)\langle P_z^2\rangle + 2r\delta_3 - (r-2)\langle P_z^4\rangle]\Big\}$$

$$\chi_2 = \frac{1}{16}\Big\{(1+s)^2[N^2(N+1)^2-2N(N+1)\langle P_z^2\rangle + \langle P_z^4\rangle] - (1-s)^2\delta_1 + 2(1-s^2)[N(N+1)\delta_2 + \delta_3]\Big\} \qquad (4)$$

$$\chi_3 = \frac{1}{8}\Big\{(1+s)[rN^2(N+1)^2 - 2(r-1)N(N+1)\langle P_z^2\rangle + (r-2)\langle P_z^4\rangle] + r[(1-s)\delta_1 - 2sN(N+1)\delta_2] - 2[1+s(1-r)]\delta_3\Big\}$$

$$\chi_4 = \frac{1}{2}\Big\{N(N+1)\langle P_z^2\rangle - \langle P_z^4\rangle - \delta_3\Big\}$$

$$\delta_1 = (2\omega\langle P_z^2\rangle - \langle P_z^4\rangle - \omega^2)/b_p^2$$

$$\delta_2 = (\langle P_z^2\rangle - \omega)/b_p$$

$$\delta_3 = (\omega\langle P_z^2\rangle - \langle P_z^4\rangle)/b_p$$

and

$$r = C_e^2/A_e^2 \qquad s = C_e^2/B_e^2$$

Since the equilibrium rotational constants A_e, B_e, and C_e are not known it is necessary to use the ground state values for those constants in the calculation of r and s.

P^6 TERMS

E_2 consists of P^6 terms as described by Pierce, DiCianni, and Jackson (15). These terms are of the form

$$E_2 = H_N N^3(N+1)^3 + H_{NK} N^2(N+1)^2 \langle P_z^2 \rangle + H_{KN} N(N+1) \langle P_z^4 \rangle + H_K \langle P_z^6 \rangle \quad (5)$$

Where the H's are empirical constants and the $\langle P_z^n \rangle$ are expectation values of the operator $P_z \equiv P_a$. $\langle P_z \rangle$ is very nearly K_{-1} since in the prolate limit the wavefunctions are eigenfunctions of P_z.

THE COMPLETE ENERGY EXPRESSION

Thus combining E_0, E_1, and E_2 the complete energy expression exclusive of the spin-rotation interaction can be written

$$E = \frac{(B+C)}{2} N(N+1) + \left[A - \frac{(B+C)}{2}\right] \omega + \sum_{i=1}^{4} \tau_i \chi_i + H_N N^3(N+1)^3 + H_{NK} N^2(N+1)^2 \langle P_z^2 \rangle + H_{KN} N(N+1) \langle P_z^4 \rangle + H_K \langle P_z^6 \rangle \quad (6)$$

SPIN-ROTATION INTERACTION

The only angular momentum of an electronic character in non-linear molecules is a spin momentum since the orbital motion of electrons is generally "quenched" or suppressed. Thus the primary perturbation on the energy levels of the non-linear NO_2 molecule is an $\underline{N}\cdot\underline{S}$ interaction where $\underline{N}$ is the rotational and $\underline{S}$ the spin angular momentum. The spin magnetic moment interacts with the magnetic field due to molecular rotation which gives an interaction energy proportional to $\underline{N}\cdot\underline{S}$. The field arises partly from the motion of charges in the molecule due to simple rotation, and partly from the transfer of a small amount of angular momentum from end-over-end rotational motion to electronic orbital motion(16). The spin splitting is small compared to the differences in rotational energy levels. The result is a doubling of the spectral lines for $K_{-1} \neq 0$.

A detailed treatment is discussed by Lin (17) in which the spin-rotation Hamiltonian can be represented in the form:

$$H_{SR} = \frac{\underline{N}\cdot\underline{S}}{N(N+1)} \sum_{i,j} \varepsilon_{ij} N_i N_j \qquad i,j = a,b,c \qquad (7)$$

The spin splitting observed in this work is at most 0.2 cm^{-1} so the symmetric rotor approximation may be used. In this approximation $\varepsilon_{ij} = 0$ for $i \neq j$ and $\varepsilon_{bb} = \varepsilon_{cc}$. So H_{SR} can be written in the form

$$H_{SR} = \frac{\underline{N}\cdot\underline{S}}{N(N+1)}\left[\varepsilon_{aa}N_a^2 + \varepsilon_{bb}(N_b^2 + N_c^2)\right] = \frac{\underline{N}\cdot\underline{S}}{N(N+1)}\left[\varepsilon_{aa}N_a^2 + \varepsilon_{bb}(N^2-N_a^2)\right] \tag{8}$$

Since the symmetric top eigenfunctions are eigenfunctions of N_a^2 and N^2 and since

$$\langle J|\underline{N}\cdot\underline{S}|J\rangle = \frac{J(J+1) - N(N+1) - S(S+1)}{2} \tag{9}$$

we have

$$E_{SR} = \left[\varepsilon_{bb} + (\varepsilon_{aa}-\varepsilon_{bb})\frac{K^2}{N(N+1)}\right]\langle J|\underline{N}\cdot\underline{S}|J\rangle \tag{10}$$

Then neglecting ε_{bb} in comparison to the second term in Eq. (10) and defining an effective ε and a K_{SR} such that

$$\varepsilon = \varepsilon_{aa} - \varepsilon_{bb} \tag{11}$$

and

$$K_{SR} = \frac{K^2\varepsilon}{N(N+1)} \tag{12}$$

we can write

$$E_{SR} = K_{SR}\frac{[J(J+1) - N(N+1) - S(S+1)]}{2} \tag{13}$$

Since there is one electron and one unit of spin angular momentum, S = 1/2, J can assume only the values

$$J^+ = N + 1/2$$
$$J^- = N - 1/2 \tag{14}$$

then

$$E^{+}_{SR} = K_{SR}N/2$$
$$E^{-}_{SR} = -K_{SR}(N+1)/2 \qquad (15)$$

thus the magnitude of the splitting of a given level is

$$E^{+}_{SR} - E^{-}_{SR} = K_{SR}(N+1/2) = \frac{K^2(N+1/2)\varepsilon}{N(N+1)} \qquad (16)$$

The only transitions observed have $\Delta J = \Delta N$ so that the spin splitting is not directly measurable as seen in Figure 2. Denoting the $J^{+"}$ to $J^{+'}$ and $J^{-"}$ to $J^{-'}$ transitions by ν^{+} and ν^{-} respectively we have for $\Delta K = 0$

$$\nu^{+} - \nu^{-} = \frac{K^2(N'+1/2)\varepsilon'}{N'(N'+1)} - \frac{K^2(N"+1/2)\varepsilon"}{N"(N"+1)} \qquad (17)$$

It is important to note that even if $\varepsilon' = \varepsilon"$ splitting will occur in the P and R branches due to the dependence on N. In the more typical case the effective spin splitting constants differ so that splitting also arises in the Q branch. Then as can be seen in Figure 3, it is possible for the spin splitting to be increased in the R(P) branch and decreased in the P(R) branch. In addition the spin splitting is not symmetrical about the asymmetric energy levels so one need not expect symmetrical splitting in the observed transitions.

If one makes the assumption that the electronic structure is unchanged by isotopic substitution it follows (18) that

Figure 2

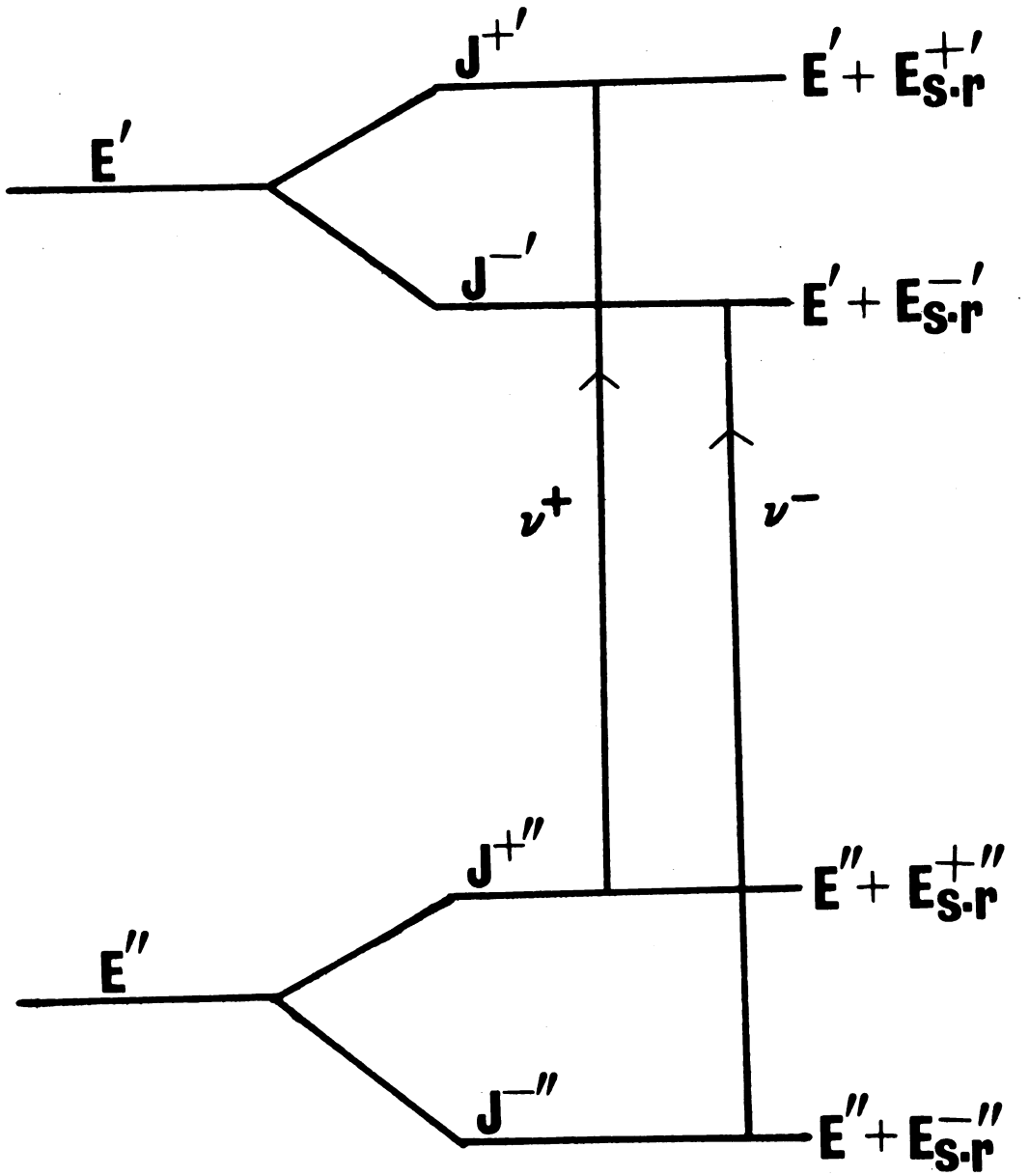

A schematic diagram of the observed transitions giving rise to spin doubling.

Figure 3

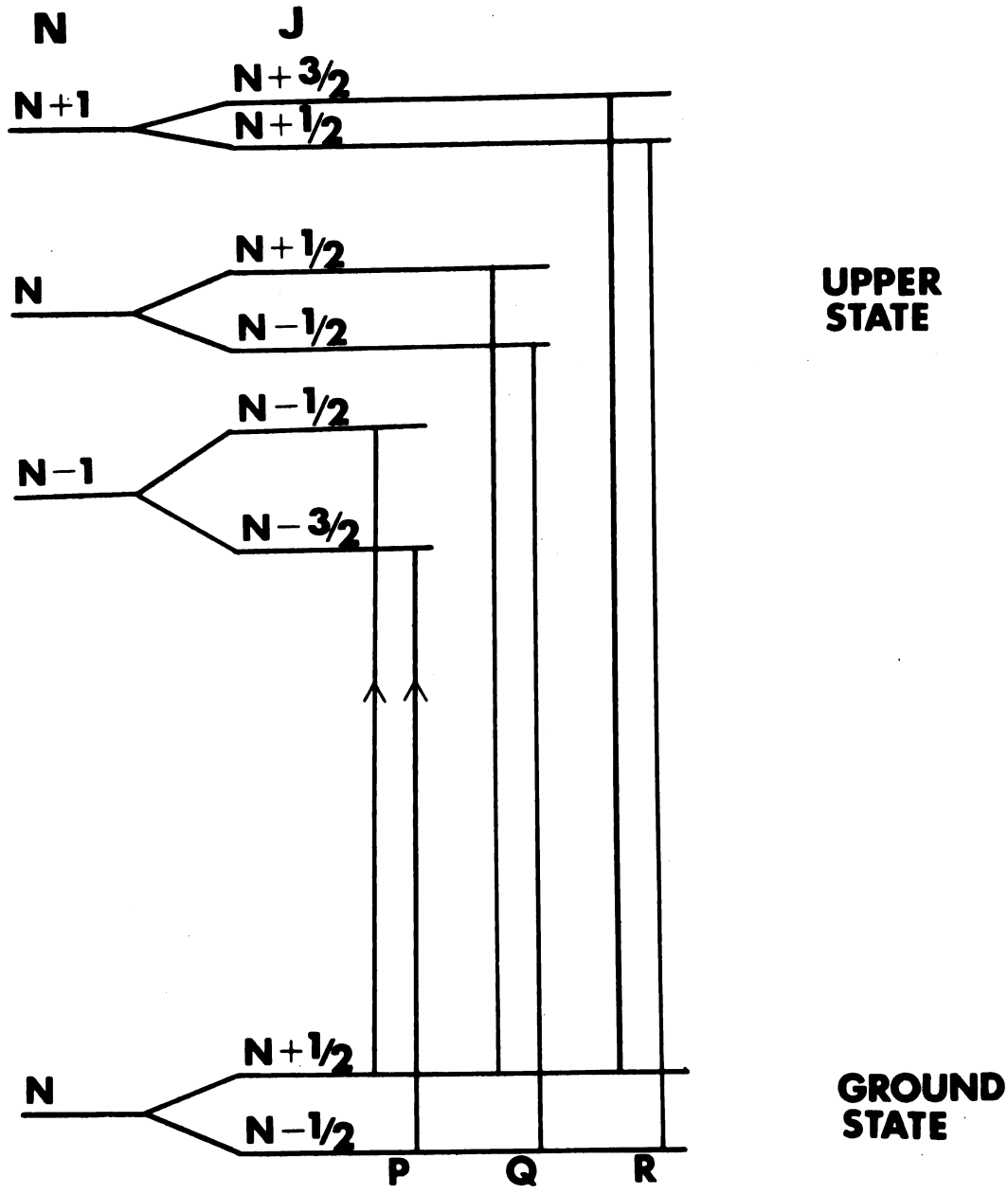

A schematic diagram of spin splitting in the P, Q, and R branches.

$$\frac{^{14}\varepsilon_{rr}}{^{15}\varepsilon_{rr}} = \frac{^{14}R}{^{15}R} \tag{18}$$

where R assumes the values A,B,and C as r assumes a,b, and c. Since ε_{aa} is so nearly equal to the effective ε in NO_2, it is a valid approximation to write

$$\frac{^{14}\varepsilon}{^{14}A} = \frac{^{15}\varepsilon}{^{15}A} \tag{19}$$

This makes it possible to combine the spin data from isotopes of the molecule for a particular band. Constants determined from the combined data agree very closely with those determined from each isotope separately. Conversely one can use this as a verification of the premise that the electronic structure is unchanged by isotopic substitution.

CHAPTER II

EXPERIMENTAL METHODS AND ANALYSIS

The Michigan State University high-resolution, near-infrared spectrometer as previously described (9)(10)(19), was employed to produce absorption, Zeeman, and magnetic rotation spectra of the (1,0,3),(3,0,1) and (0,0,3) bands of $^{14}N^{16}O_2$ and $^{15}N^{16}O_2$. The spectra were recorded on strip charts utilizing a dual pen recorder in which one pen traced the spectrum of NO_2, and the other recorded calibration fringes for the purpose of accurate interpolation between calibration lines of known frequency. The spectra were photographed and measured on the Hydel system (30), and each chart was measured twice to reduce measuring error. Two runs were made of the (1,0,3) of $^{15}NO_2$ and the (3,0,1) and (0,0,3) bands of both isotopes. The (1,0,3) of $^{14}NO_2$ required additional runs because the only available calibration lines were situated directly above the band.

The (0,0,3) band was run at a pressure of 15-18 Torr and an absorbing pathlength of 6.3 meters. The (1,0,3) and (3,0,1) bands were run at 50 Torr and 40 Torr respectively with a 15.75 meter pathlength. The method of calibration has been described by Rao et. al. (20). The spectra were calibrated using the precise near-infrared absorption frequencies measured by Rank and co-workers (20).

The standard errors of the least squares fits to obtain calibration constants averaged 0.002 cm^{-1} for the (0,0,3) band and 0.003 cm^{-1} for the (1,0,3) and (3,0,1) bands. The effective resolution obtained was approximately 0.05 cm^{-1} for the (1,0,3) and (3,0,1) bands and 0.03 cm^{-1} for the (0,0,3) band where conditions were favorable.

IDENTIFICATION OF TRANSITIONS

The individual transitions were identified through the use of ground state combination differences. These differences have been determined by microwave authors and Olman and Hause (1) (22). For a given band all possible differences of the frequencies were formed and compared to the known ground state combination differences. Those which agreed within a given tolerance were tabulated and were extremely useful in identifying series of lines and consequently subbands. Once a few transitions had been identified the predicted frequencies from the least squares fits could be used in conjunction with the ground state combination differences in order to identify additional lines.

ANALYSIS OF ASYMMETRIC ENERGY LEVELS

GROUND STATE

The ground state energy levels and molecular constants are assumed known from previous work. Attempts to refine

the ground state constants employing the data from the (1,0,3), (3,0,1), and (0,0,3) bands yielded no significant changes in the values reported by Olman and Hause (1). Thus these ground state values are accepted and for completeness are listed in Table I.

UPPER STATE CONSTANTS

Analysis of the upper state rotational, centrifugal distortion, empirical P^6 terms, and spin splitting constants proceeded as follows:

1. A sufficient number of unperturbed lines were identified to enable prediction of the entire unperturbed spectrum of the band.

2. Spin split lines were identified and analyzed yielding effective spin splitting constants.

3. A single unperturbed frequency was determined for each spin split line and these values, in addition to the unsplit lines, were entered in the least squares fits of the unperturbed spectrum.

The upper state constants may be determined by forming upper state combination differences or by using ground state constants plus observed transitions to determine the set of upper state vibrational and rotational energy levels. The latter method was used because it is difficult to determine A and H_K from combination differences, and furthermore, series deviating from the predicted spectrum are clearly

Table I

Ground State Constants for NO_2 (cm^{-1})

	$^{14}NO_2$ a	$^{15}NO_2$ a
A	8.00251 ± 0.00010 [b]	7.63062 ± 0.00029
B	0.433665 ± 0.000004	0.433717 ± 0.000016
C	0.410493 ± 0.000014	0.409492 ± 0.000030
τ_{aaaa}	$(-11.37 \pm 0.28) \times 10^{-3}$	$(-9.15 \pm 0.5) \times 10^{-3}$
τ_{bbbb}	$(-1.418 \pm 0.023) \times 10^{-6}$	$(-1.40 \pm 0.04) \times 10^{-6}$
τ_{aabb}	$(6.91 \pm 0.24) \times 10^{-5}$	$(5.87 \pm 0.4) \times 10^{-5}$
τ_{abab}	-8.215×10^{-6}	-8.175×10^{-6}
H_{KN}	$(-1.1 \pm 0.6) \times 10^{-7}$	0.0
H_K	$(2.8 \pm 1.1) \times 10^{-5}$	0.0

a Ref. (1)
b 95% Simultaneous confidence intervals throughout

The 95% confidence interval is approximately 4.5 times as large as the standard deviation. The ground state constants were obtained by forming ground state combination differences.

defined.

The complete asymmetric energy level expression given by Eq.(6) is not in a form directly suitable for least squares and iterative procedures. The expression was linearized by Hill (21) by writing the approximation

$$E_0 \simeq \zeta A + \xi\left(\frac{B+C}{2}\right) + \eta\left(\frac{B-C}{2}\right) \tag{20}$$

After some manipulation (22) one finds the expressions

$$\begin{aligned} \zeta &= \langle P_z^2 \rangle \\ \xi &= N(N+1) - \langle P_z^2 \rangle \\ \eta &= (\langle P_z^2 \rangle - \omega)/b_p \end{aligned} \tag{21}$$

where

$$b_p = \frac{C-B}{2A-B-C} \tag{22}$$

So the complete linearized energy expression can be written

$$E = \zeta A + \xi\left(\frac{B+C}{2}\right) + \eta\left(\frac{B-C}{2}\right) + \sum_i \chi_i \tau_i + H_N N^3 (N+1)^3 + H_{NK} N^2 (N+1)^2 \langle P_z^2 \rangle + H_{KN} N(N+1) \langle P_z^4 \rangle + H_K \langle P_z^6 \rangle \tag{23}$$

Corrections to the energy levels in a given vibrational state can be expressed as:

$$\Delta E = \zeta\Delta A + \xi\Delta\left(\frac{B+C}{2}\right) + \eta\Delta\left(\frac{B-C}{2}\right) + \sum_i \chi_i \Delta\tau_i + N^3(N+1)^3\Delta H_N + \tag{24}$$

$$N^2(N+1)^2\langle P_z^2\rangle\Delta H_{NK} + N(N+1)\langle P_z^4\rangle\Delta H_{KN} + \langle P_z^6\rangle\Delta H_K$$

Experimentally one observes not energy levels but transitions between energy levels so we can write the frequency of an observed line as

$$\nu = \nu_o + E' - E'' \tag{25}$$

where ν_o is the band origin, and a prime indicates the upper state while a double prime indicates the lower state. One finds corrections in the molecular parameters by using least squares to minimize the differences between the observed and predicted frequencies. This can be written

$$\nu_{obs} - \nu_{pred} = \Delta\nu_o + \Delta E' - \Delta E'' \tag{26}$$

If the ground state is known $\Delta E''$ vanishes and

$$\nu_{obs} - \nu_{pred} = \Delta\nu_o + \Delta E' \tag{27}$$

In order to employ iterative methods it was necessary to provide initial values for A, B, and C in the upper state from which ζ, ξ, η, and $\langle P_z^n\rangle$ could be calculated. The least squares fits were done utilizing program Specfit contributed by Olman (22). The resulting upper state constants are given in the following tables.

(0,0,3) Table II

(1,0,3) Table III

(3,0,1) Table IV

SPIN SPLITTING ANALYSIS

Least squares methods were used to analyze the spin splitting data. Since ε' and ε'' occur linearly in Eq. (17) least squares methods can be applied directly to determine values for these constants. The data was analyzed utilizing program SPINFIT contributed by Olman (22). The values of ε derived from the various fits are given in Table VI.

The combined fits agree very closely with the separate fits which may also be used as a confirmation that the electronic structure is unchanged by isotopic substution.

GENERAL FEATURES OF THE BANDS

(0,0,3) of NO_2

The (0,0,3) is a strongly absorbing band located in the region from 4695 cm^{-1} to 4775 cm^{-1} for $^{14}NO_2$ and from 4611 cm^{-1} to 4676 cm^{-1} for $^{15}NO_2$. A previous analysis ascribed the observed structure to the overlapping of a type A and a type B band, but with the exception of one weak series underlying the (0,0,3) of $^{15}NO_2$ we have found that at room temperature the structure can be accounted for entirely by the type A band. Analysis has produced fits of nearly all observed lines with K_{-1} as high as 7 and N as high as 48. The branches of differing subbands

Table II

Upper State Constants for NO_2 (cm^{-1})

	003	
	$^{14}NO_2$	$^{15}NO_2$
ν_o	4754.209±0.006	4655.228±0.009
A	7.3427±0.0012	7.0217±0.0019
B	0.425457±0.000032	0.425781±0.000046
C	0.402916±0.000024	0.402214±0.000036
τ_{aaaa}	$(-0.992\pm0.025)\times10^{-2}$	$(-0.836\pm 0.044)\times10^{-2}$
τ_{bbbb}	$(-1.51\pm0.14) \times 10^{-6}$	$(-1.58\pm0.19) \times 10^{-6}$
τ_{aabb}	$(9.06\pm0.38) \times 10^{-5}$	$(7.26\pm0.81) \times 10^{-5}$
τ_{abab}[b]	-8.215×10^{-6}	-8.175×10^{-6}
H_{KN}	$(-1.77\pm0.31) \times 10^{-7}$	0.0
H_K	$(2.961\pm0.093)\times10^{-5}$	$(0.29\pm0.17) \times 10^{-5}$
No. Lines Identified	550	466
No. Lines Used	416	308
SD of Fit	0.0082	0.0092

a 95% simultaneous confidence intervals throughout
b Calculated values

The value of τ_{abab} is in all cases fixed at the theoretical value given by Chung and Parker (27).

Table III

Upper State Constants for NO_2 (cm^{-1})

	103	
	$^{14}NO_2$	$^{15}NO_2$
ν_o	5984.705±0.004[a]	5874.951±0.010
A	7.4140±0.0087	7.0791±0.0057
B	0.423211±0.000039	0.42355±0.00016
C	0.399358±0.000017	0.398728±0.000065
τ_{aaaa}	$(-1.20\pm0.19) \times 10^{-2}$	$(-0.99\pm0.15) \times 10^{-2}$
τ_{bbbb}	$(-1.540\pm0.076)\times10^{-6}$	$(-1.39\pm0.40) \times 10^{-6}$
τ_{aabb}	$(8.6\pm2.1) \times 10^{-5}$	$(6.8\pm1.0) \times 10^{-5}$
τ_{abab}[b]	-8.215×10^{-6}	-8.175×10^{-6}
H_{KN}	0.0	0.0
H_K	0.0	$(1.07\pm0.71) \times 10^{-5}$
No. Lines Identified	301	323
No. Lines Used	214	233
SD of Fit	0.0065	0.0199

a 95% simultaneous confidence intervals throughout
b Calculated values

Table IV

Upper State Constants for NO_2 (cm^{-1})

	301	
	$^{14}NO_2$	$^{15}NO_2$
ν_o	5437.540±0.012[a]	5367.316±0.026
A	8.0140±0.0056	7.5328±0.0090
B	0.42384±0.00011	0.42452±0.00027
C	0.399519±0.000079	0.39911±0.00019
τ_{aaaa}	$(-3.97\pm0.31)\times10^{-2}$	$(4.86\pm0.895)\times10^{-2}$
τ_{bbbb}	0.0	0.0
τ_{aabb}	$(1.16\pm0.37)\times10^{-4}$	0.0
τ_{abab}[b]	-8.215×10^{-6}	-8.175×10^{-6}
H_N	0.0	0.0
H_{NK}	0.0	$(4.6\pm3.6)\times10^{-8}$
H_{KN}	0.0	$(-9.4\pm3.3)\times10^{-6}$
H_K	$(2.22\pm0.24)\times10^{-4}$	$(-2.700\pm0.097)\times10^{-3}$
No. Lines Identified	228	152
No. Lines Used	171	121
SD of Fit	0.009	0.016

a 95% simultaneous confidence intervals throughout

b Calculated values

Table V

(0,0,3) Band Spin-Splittings (cm^{-1})

			$^{14}NO_2$		$^{15}NO_2$	
Branch	K_{-1}	N	OBS	PRED	OBS	PRED
P	2	3	+0.0515	+0.0594		
P	3	4	+0.0642	+0.0595		
P	5	6			+0.0491	+0.0425
Q	3	3			-0.0652	-0.0465
Q	3	4			-0.0459	-0.0359
Q	4	8	-0.0440	-0.0356		
Q	5	5	-0.0995	-0.0865		
Q	5	8			-0.0626	-0.0523
Q	6	6			-0.1105	-0.0987
Q	6	11	-0.0571	-0.0592		
Q	6	12			-0.0569	-0.0511
R	1	1			-0.0593	-0.0651
R	2	3	-0.0630	-0.0654		
R	2	4	-0.0428	-0.0441		
R	3	4	-0.1008	-0.0992	-0.1049	-0.0942
R	3	5	-0.0755	-0.0730		
R	3	6	-0.0552	-0.0568		
R	3	7	-0.0440	-0.0460	-0.0431	-0.0436
R	4	4			-0.1845	-0.1674
R	4	6	-0.1080	-0.1010	-0.0982	-0.0957
R	4	7	-0.0873	-0.0818	-0.0673	-0.0785

Table V (con't)

(0,0,3) Band Spin-Splittings (cm^{-1})

			$^{14}NO_2$		$^{15}NO_2$	
Branch	K_{-1}	N	OBS	PRED	OBS	PRED
R	4	8			-0.0542	-0.0642
R	4	9	-0.0652	-0.0582	-0.0534	-0.0551
R	4	10	-0.0444	-0.0505	-0.0461	-0.0478
R	4	11	-0.0286	-0.0445		
R	4	12	-0.0260	-0.0397		
R	4	13	-0.0224	-0.0357		
R	5	6	-0.1351	-0.1578		
R	5	9			-0.0835	-0.0860
R	5	10	-0.0876	-0.0789	-0.0556	-0.0747
R	5	11	-0.0636	-0.0695		
R	5	12	-0.0729	-0.0620	-0.0448	-0.0586
R	5	13	-0.0592	-0.0559	-0.0491	-0.0528
R	5	14	-0.0384	-0.0507	-0.0419	-0.0479
R	5	15	-0.0407	-0.0464		
R	5	16	-0.0422	-0.0427	-0.0269	-0.0404
R	6	10			-0.1027	-0.1093
R	6	12	-0.1036	-0.0983		
R	6	15	-0.0626	-0.0668		
R	6	16	-0.0440	-0.0615		
R	6	17	-0.0524	-0.0570		
R	6	18			-0.0461	-0.0501

Table V

(0,0,3) Band Spin-Splitting (cm^{-1})

			$^{14}NO_2$		$^{15}NO_2$	
Branch	K_{-1}	N	OBS	PRED	OBS	PRED
R	6	19			-0.0437	-0.0468
R	6	20			-0.0403	-0.0439
R	6	21	-0.0416	-0.0437	-0.0354	-0.0413
R	6	22	-0.0403	-0.0413		
R	6	23			-0.0447	-0.0369

Table VI

Effective Spin-Rotation Coupling Constants

For the (0,0,3) Band of NO_2

	$^{14}NO_2$	$^{15}NO_2$
ε_{000} [a]	0.181644	0.173210
ε_{201} [b]	0.1782 ± 0.0014	0.1693 ± 0.0016
$(\varepsilon_{000} - \varepsilon_{201})$ [b]	0.0036 ± 0.0010	0.0038 ± 0.0010
ε_{003} [c]	0.1629 ± 0.0013	0.1555 ± 0.0010
$(\varepsilon_{000} - \varepsilon_{003})$ [c]	0.0187 ± 0.0013	0.0177 ± 0.0010
ε_{003} [d]	0.1627 ± 0.0012	0.1556 ± 0.0019
$(\varepsilon_{000} - \varepsilon_{003})$ [d]	0.0189 ± 0.0012	0.0176 ± 0.0019

a. From microwave values

b. From Ref. (1)

c. Fitting $^{14}NO_2$ and $^{15}NO_2$ separately

d. $^{14}NO_2$ and $^{15}NO_2$ data combined

overlap considerably, and the Q branches of the various subbands are widely separated. In the (0,0,3) of $^{14}NO_2$ the Q lines for $K_{-1} = 1$ are grouped about 4752 cm^{-1} while for $K_{-1} = 6$ they occur about 4730 cm^{-1}. Figure 4 displays the complete picture of the (0,0,3) band of $^{14}NO_2$ and Figure 5 shows a detailed picture of a portion of the (0,0,3) showing the $K_{-1} = 0$ subband.

A perturbation was found affecting the $K_{-1} = 5$ subband in the (0,0,3) of $^{14}NO_2$. The deviation of observed from predicted frequencies increased with N and was as large as 0.16 cm^{-1} at N = 42. A similar perturbation was noted in the $K_{-1} = 4$ subband of $^{15}NO_2$ and of approximately the same deviation.

Spin splitting has been observed and analyzed in the (0,0,3) band. The high resolution, strong absorption, and large splittings permitted observation of 32 resolved or nearly resolved spin doublets in $^{14}NO_2$ and 27 such doublets in $^{15}NO_2$. Splitting is small in the P branch, intermediate in the Q branch, and large in the R branch. The possibility of this was considered previously. The maximum observed splitting was 0.135 cm^{-1} for $R_5(6)$ in $^{14}NO_2$ and 0.185 cm^{-1} for $R_4(4)$ in $^{15}NO_2$. Very few doublets were observed in the P branch due to the small splitting, overlapping, and weakness of the spin split lines. A list of the observed doublets is given in Table V. A small region of the (0,0,3) of $^{14}NO_2$ is shown in Figure 6 with

several resolved spin doublets. Effective spin rotation splitting constants are listed in Table VI.

(1,0,3) of NO_2

The (1,0,3) is a weakly absorbing band located in the region from 5923 to 6000 cm^{-1} for $^{14}NO_2$ and from 5825 to 5890 cm^{-1} for $^{15}NO_2$. The complete (1,0,3) band is shown in Figure 7, and a portion of the (1,0,3) is seen in Figure 8 where the $K_{-1} = 0$ and the $K_{-1} = 1$ transitions are indicated. Note the missing lines in the $K_{-1} = 0$ series. Q branches of the subbands were present but too weak to be analyzed. Transitions have been identified with K_{-1} as high as 5 and N as high as 46. Good fits were obtained for series through $K_{-1} = 3$. The $K_{-1} = 5$ series was very weak, and the $K_{-1} = 4$ series was perturbed.

Spin splitting was not observed due to overlapping, low resolution ($\sim$0.05 cm^{-1}) in the region, and weak absorption of the low N lines.

(3,0,1) of NO_2

The (3,0,1) is a Type A band extending from 5380 cm^{-1} to 5456 cm^{-1} for $^{14}NO_2$ and from 5330 to 5387 cm^{-1} for $^{15}NO_2$. P, Q, and R branches were observed in both bands. P and R lines were identified and analyzed by least squares methods to yield molecular constants. This also led to correct predicted positions for the Q subbranches which are present.

The weakness and overlapping of the Q subbranches prevented identification of individual lines. Figure 9 shows the K_{-1} = 0 subband of the (3,0,1) of $^{14}NO_2$. Lines were identified through K_{-1} = 5 for $^{14}NO_2$ and K_{-1} = 4 for $^{15}NO_2$. The K_{-1}= 4 subband was perturbed.

Due to the weak absorption and overlapping of band lines spin splitting was not observed in the (3,0,1) bands.

VIBRATIONAL CONSTANTS

The vibrational energy levels can be expressed as a sum of harmonic oscillator energy levels linear in the v_i quantum numbers and quadratic anharmonic terms in the form

$$G(v_1,v_2,v_3) = \sum_i \omega_i (v_i+\frac{1}{2}) + \sum_{i=1}^{3} \sum_{j=1}^{i} X_{ij} (v_i+\frac{1}{2})(v_j+\frac{1}{2}) \quad (28)$$

with a zero point energy of

$$G(0,0,0) = \frac{1}{2} \sum_i \omega_i + \frac{1}{4} \sum_{i=1}^{3} \sum_{j=1}^{i} X_{ij} \quad (29)$$

Thus the band origins of the measured bands are given by

$$\nu_o(v_1,v_2,v_3) = G(v_1,v_2,v_3) - G(0,0,0) \quad (30)$$

This equation is in a form adaptable to least squares analysis.

In addition to the (1,0,3), (3,0,1), and (0,0,3) bands the (1,0,1) and (2,0,1) bands of $^{14}NO_2$ and $^{15}NO_2$ analyzed by Olman and Hause (1) were included in the least

Figure 4

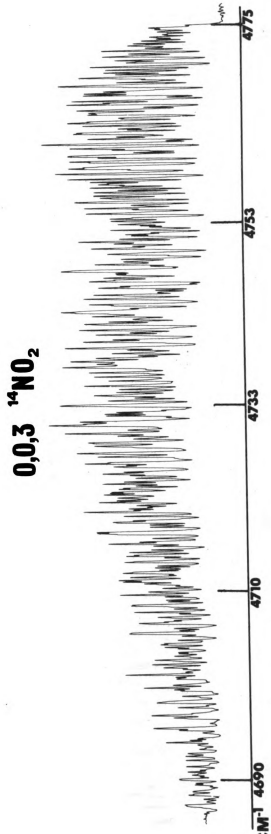

The complete (0,0,3) band of $^{14}NO_2$.

Figure 5

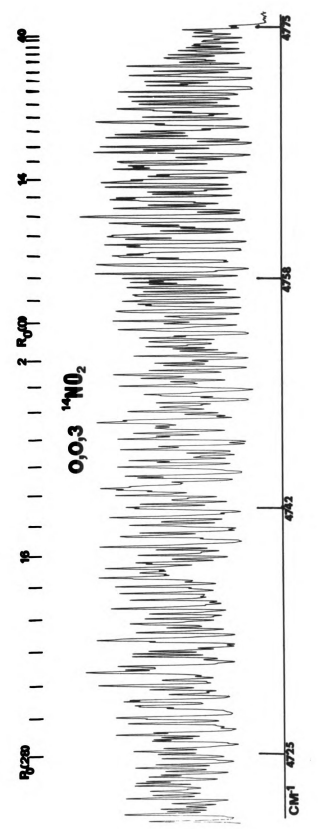

A portion of the (0,0,3) band of $^{14}NO_2$
showing part of the $K_{-1} = 0$ subband.

(0,0,3) $^{14}NO_2$

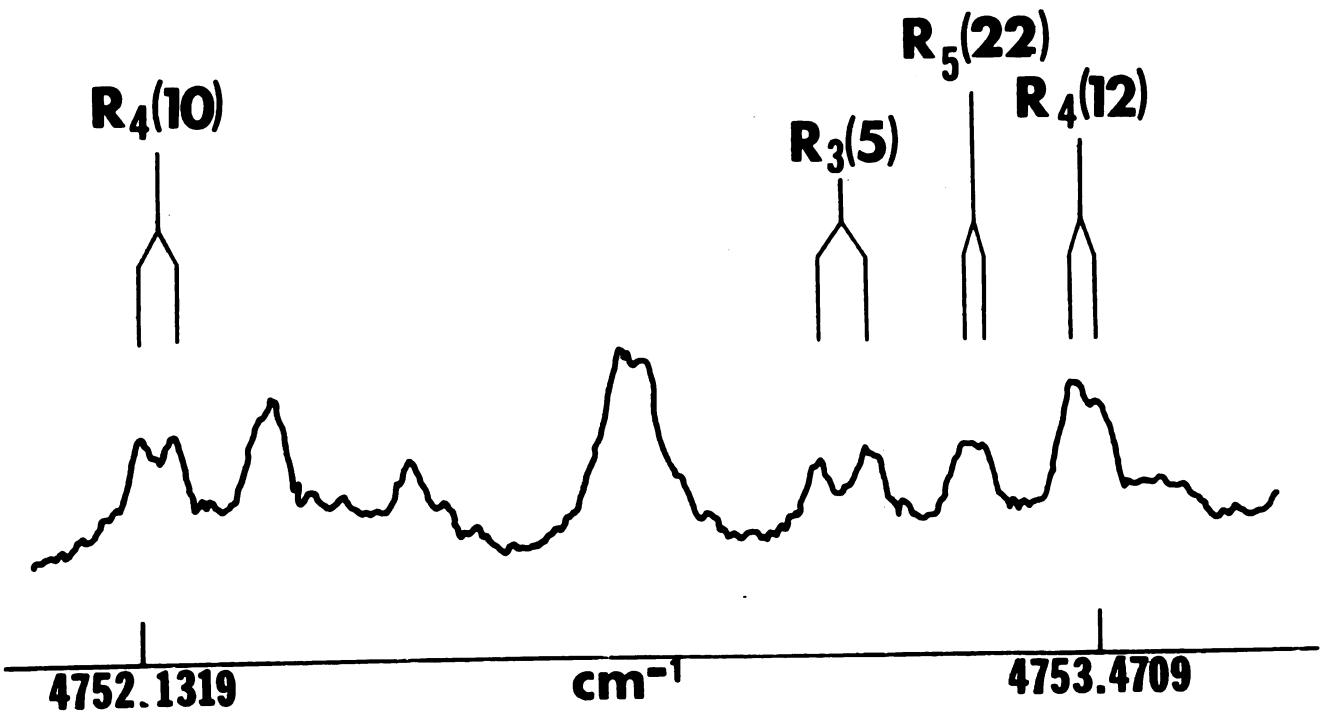

Figure 6: Spin doublets ranging from broadened lines such as $R_5(22)$ to resolved doublets such as $R_3(5)$ in which the splitting is 0.073 cm^{-1}.

Figure 7

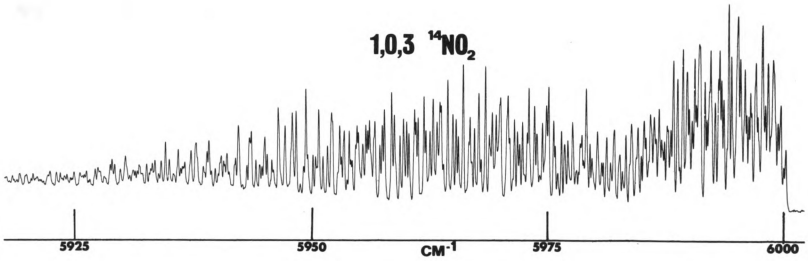

The complete (1,0,3) band of $^{14}NO_2$.

Figure 8

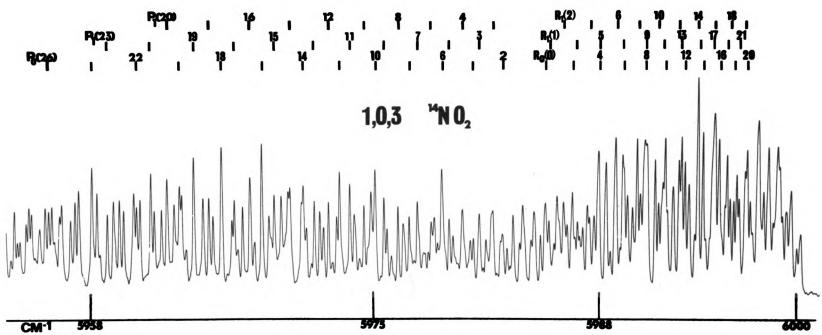

A portion of the (1,0,3) band of $^{14}NO_2$ showing part of the $K_{-1} = 0$ and $K_{-1} = 1$ subbands. Due to the asymmetry of the molecule and the presence of two identical oxygen nuclei there are two subbands for $K_{-1} = 1$ and higher: an even subband with odd N lines missing and an odd one with even N lines missing. For $K_{-1} = 0$ only the even N lines are present.

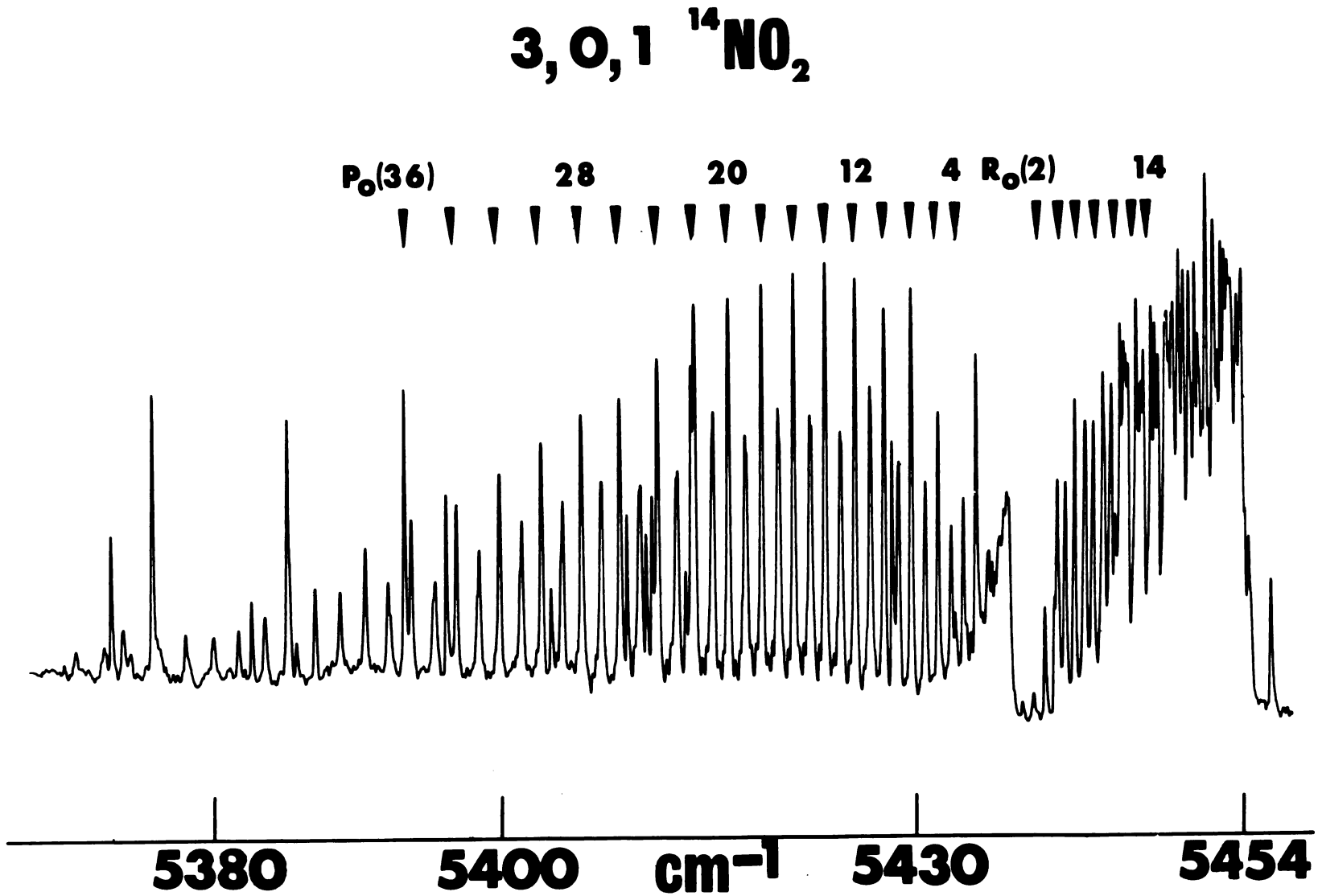

Figure 9: The (3,0,1) band of $^{14}NO_2$ is shown with the $K_{-1} = 0$ subband indicated.

squares analysis. Note that in each of the bands $v_2 = 0$. Thus it was necessary to supply values for X_{12} and X_{23} from the work of Arakawa and Nielsen (5). The accuracy of the results thus depends on the accuracy of that work.

Program VIBCON was written to perform the fits utilizing the Efroymson least squares subroutine. The resulting vibrational constants as well as all the constants from Arakawa and Nielsen are given in Table VII and a listing of VIBCON is given in Appendix I.

VIBRATION-ROTATION INTERACTION CONSTANTS

The rotational constants A, B, and C depend on the vibrational state as follows:

$$R_{v_1 v_2 v_3} = R_{000} - \sum_{i=1}^{3} \alpha_i^R v_i \qquad (31)$$

where R = A, B, or C and the v_i are the vibrational quantum numbers. This equation is easily adapted to least squares analysis and program ROTCON listed in Appendix I, was written to perform the desired fits. Values of α_1^R and α_3^R for both isotopes of NO_2 are given in Table VIII.

TABLE VII

VIBRATIONAL CONSTANTS (cm^{-1})

Constant	$^{14}NO_2$ [a]	$^{14}NO_2$ [b,c]	$^{15}NO_2$ [a]	$^{15}NO_2$ [b,c]
ω_1	1357.8	1355.9	1342.5	1338.5
ω_2	756.8	756.8	747.1	747.1
ω_3	1665.8	1663.5	1628.0	1628.3
X_{11}	-9.0	-8.1	-8.8	-7.4
X_{12}	-9.7	-9.7	-9.5	-9.5
X_{13}	-28.7	-29.8	-27.7	-28.4
X_{22}	-0.5	-0.5	-0.4	-0.4
X_{23}	-2.7	-2.7	-2.6	-2.6
X_{33}	-16.4	-15.6	-15.6	-15.3

a Arakawa and Nielsen's values

b Present work

c ω_2, X_{12}, X_{22}, and X_{23} are fixed at the values given by Arakawa and Nielsen

TABLE VIII

VIBRATION-ROTATION INTERACTION CONSTANTS

	$^{14}NO_2$	$^{15}NO_2$
α_1^A	-0.0753±0.0083	-0.042±0.038
α_1^B	0.002354±0.000094	0.00222±0.00019
α_1^C	0.00282±0.00050	0.00269±0.00058
α_3^A	0.2208±0.0070	0.199±0.032
α_3^B	0.002718±0.000079	0.00265±0.00015
α_3^C	0.00264±0.00042	0.00256±0.00049

CHAPTER III

THE MATHEMATICS OF POLARIZED LIGHT

In the discussion which follows it is interesting and economical to apply the powerful methods of matrix algebra which have been developed to describe the polarization state of electromagnetic radiation and the changes introduced by various optical elements such as polarizers and retarders. Since these methods are not generally common knowledge it is thought desirable to include a brief description of the mathematics and some useful matrices. More complete information is available in POLARIZED LIGHT by Shurcliff (23) and the RCA Institute Lecture Notes entitled MODERN OPTICS by Sutton and Panati (24). Also references to several papers are found within these references.

THE JONES-MUELLER CALCULUS

Two forms of matrix algebra have been developed to aid computation in dealing with phase relationships, intensity, and polarization of light. One form, the Mueller calculus utilizes 4x4 matrices and the Stokes vector as its basic units. It is most useful in dealing with incoherent beams and partially polarized light. The matrices in this

theory have been derived empirically, and thus have a firm experimental basis.

Jones calculus is based on 2x2 matrices and the Jones vector which is simply a vector of the amplitudes and phases of the x and y vibrations for a beam propagating along the z axis. Jones calculus is suited to completely polarized light and addition of coherent beams. Thus Jones calculus is best suited for this work and will be discussed briefly.

The general Jones vector can be written

$$J = \begin{bmatrix} E_x e^{i\varepsilon_x} \\ E_y e^{i\varepsilon_y} \end{bmatrix} \tag{31}$$

for some particular amplitudes of the electric vector E_x and E_y with some definite phase angle ε_x and ε_y. An harmonic time variation is assumed. The type of polarization depends on E_x, E_y, and the relative phase difference. There is no Jones vector for unpolarized light or partially polarized light.

Where absolute phases and intensities are unnecessary one uses standard normalized Jones vectors. For example the complete vector for light plane polarized along the x axis is

$$J = \begin{bmatrix} E_x e^{i\varepsilon_x} \\ 0 \end{bmatrix} \tag{32}$$

The normalized Jones vector is

$$\frac{J}{(J^{\dagger}J)^{1/2}} = \begin{bmatrix} e^{i\varepsilon_x} \\ 0 \end{bmatrix} \tag{33}$$

where $J^{\dagger}$ is the Hermitian conjugate of J.

Since ε_x is arbitrary one writes the standard normalized Jones vector

$$J' = \begin{bmatrix} 1 \\ 0 \end{bmatrix} \tag{34}$$

A Jones matrix can be associated with each optical element which alters the polarization state but leaves the direction of propagation unaltered. These matrices when operating on the Jones vector of the incident light yield the Jones vector of the emergent radiation. A list of useful Jones vectors is found in Table IX and Jones instrument matrices are found in Table X.

As an example consider the case of a polarizer-analyzer assembly with the axis of the analyzer making an angle θ with the polarizer axis. Suppose the polarizer produces linearly polarized light with a Jones vector

$$\begin{bmatrix} 1 \\ 0 \end{bmatrix} \tag{35}$$

The Jones matrix of the analyzer (Table X) operating on the incident Jones vector can be written

$$\begin{bmatrix} \mathrm{Cos}^2\theta & \mathrm{Cos}\theta\mathrm{Sin}\theta \\ \mathrm{Cos}\theta\mathrm{Sin}\theta & \mathrm{Sin}^2\theta \end{bmatrix} \begin{bmatrix} 1 \\ 0 \end{bmatrix} = \begin{bmatrix} \mathrm{Cos}^2\theta \\ \mathrm{Cos}\theta\mathrm{Sin}\theta \end{bmatrix} \tag{36}$$

so the amplitudes are

$$E_x = \mathrm{Cos}^2\theta$$
$$E_y = \mathrm{Sin}\theta\mathrm{Cos}\theta \tag{37}$$

and they are in phase. The intensities are found from

$$I = J^{\dagger}J = E_x^{*}E_x + E_y^{*}E_y = \mathrm{Cos}^2\theta \tag{38}$$

in agreement with the Law of Malus.

In this way the theory of polarization is reduced to a series of matrix multiplications often with great simplification of the problem. Note that if light described by a Jones vector, [J] , is incident on a series of elements in the order A,B,C, to yield a Jones vector, [J'] , then the matrix multiplication takes the form

$$[J'] = CBA\ [J] \tag{39}$$

The Mueller calculus is similar in application since the Stokes vectors and Mueller matrices are tabulated. The Mueller calculus deals directly with intensities and is useful only where phase information is not required.

TABLE IX JONES VECTORS

POLARIZATION FORM	JONES VECTOR	
	FULL	STANDARD NORMALIZED
LINEAR POLARIZATION		
Horizontal $\theta = 0^{o}$ ——	$\begin{bmatrix} A_x e^{i\varepsilon_x} \\ 0 \end{bmatrix}$	$\begin{bmatrix} 1 \\ 0 \end{bmatrix}$
Vertical $\theta = 90^{o}$ |	$\begin{bmatrix} 0 \\ A_y e^{i\varepsilon_y} \end{bmatrix}$	$\begin{bmatrix} 0 \\ 1 \end{bmatrix}$
Oblique $\theta = \pm 45^{o}$ X	$A_x e^{i\varepsilon_x} \begin{bmatrix} 1 \\ \pm 1 \end{bmatrix}$	$\frac{1}{\sqrt{2}} \begin{bmatrix} 1 \\ \pm 1 \end{bmatrix}$
CIRCULAR POLARIZATION		
Right Circular	$\begin{bmatrix} A_x e^{i\varepsilon_x} \\ A_x e^{i(\varepsilon_x + \pi/2)} \end{bmatrix}$	$\frac{1}{\sqrt{2}} \begin{bmatrix} -i \\ 1 \end{bmatrix}$
Left Circular	$\begin{bmatrix} A_x e^{i\varepsilon_x} \\ A_x e^{i(\varepsilon_x - \pi/2)} \end{bmatrix}$	$\frac{1}{\sqrt{2}} \begin{bmatrix} i \\ 1 \end{bmatrix}$
ELLIPTICAL POLARIZATION		
General Elliptical	$\begin{bmatrix} A_x e^{i\varepsilon_x} \\ A_y e^{i\varepsilon_y} \end{bmatrix}$	$\begin{bmatrix} (\mathrm{Cos}R)\, e^{-i\gamma/2} \\ (\mathrm{Sin}R)\, e^{i\gamma/2} \end{bmatrix}$

$\mathrm{Tan}R = A_y/A_x \qquad \gamma = \varepsilon_x + \varepsilon_y$

TABLE X JONES INSTRUMENT MATRICES

AZIMUTH OF TRANSMISSION AXIS, θ	MATRIX
LINEAR POLARIZERS	
0°	$\begin{bmatrix} 1 & 0 \\ 0 & 0 \end{bmatrix}$
90°	$\begin{bmatrix} 0 & 0 \\ 0 & 1 \end{bmatrix}$
General θ	$\begin{bmatrix} \mathrm{Cos}^2\theta & \mathrm{Cos}\theta\mathrm{Sin}\theta \\ \mathrm{Cos}\theta\mathrm{Sin}\theta & \mathrm{Sin}^2\theta \end{bmatrix}$
IDEAL LINEAR RETARDERS OF RETARDANCE $\delta = 90^\circ$	
AZIMUTH OF FAST AXIS, θ	
0°	$\begin{bmatrix} e^{i\pi/4} & 0 \\ 0 & e^{-i\pi/4} \end{bmatrix}$
90°	$\begin{bmatrix} e^{-i\pi/4} & 0 \\ 0 & e^{i\pi/4} \end{bmatrix}$
$\theta = \pm 45^\circ$	$\frac{1}{\sqrt{2}}\begin{bmatrix} 1 & \pm i \\ \pm i & 1 \end{bmatrix}$
CIRCULAR POLARIZERS	
Right Circular	$\frac{1}{2}\begin{bmatrix} 1 & -i \\ i & 1 \end{bmatrix}$
Left Circular	$\frac{1}{2}\begin{bmatrix} 1 & i \\ -i & 1 \end{bmatrix}$

CHAPTER IV

PHASE SENSITIVE DETECTION OF MAGNETIC CIRCULAR DICHROISM (MCD) AND MAGNETIC CIRCULAR BIREFRINGENCE (MCB) IN NO AND NO_2

Conventional magnetic rotation spectra are obtained by inserting a sample of gas between a crossed polarizer-analyzer pair, applying a magnetic field, and recording the intensity of the radiation emerging from the analyzer. These spectra are a combination of contributions from magnetic circular dichroism and birefringence.

In this series of experiments adaptations of the techniques described by Eberhardt and Stalder of the Georgia Institute of Technology (7)(8) have been applied to separate and record magnetic circular dichroism (MCD) and magnetic circular birefringence (MCB).

The techniques for the measurement of MCB were applied to the 3-0 band of NO and the (0,0,3) band of NO_2. Measurement of MCD requires production of right and left circularly polarized light. This can be accomplished with quarter-wave plates and properly oriented polarizers or by electro-optical techniques such as Pockel's effect. In these initial experiments quartz quarter-wave plates were selected as being the simplest method to verify that MCD signals could be detected. The quarter-wave plates were purchased from

Carl Lambrecht Co. and were centered at 2.11 microns which is the center of the (0,0,3) band of NO_2. The radiation at 2.11 microns was essentially circularly polarized and MCD could be measured, however, the radiation at the 3-0 of NO at 1.8 microns showed such ellipticity that measurement was not feasible.

THE JONES INSTRUMENT MATRIX OF THE SAMPLE

A general Jones matrix to describe a sample with circular dichroism and circular birefringence may be determined as follows.

Assume that there exists a matrix which describes the way in which the sample operates on any incident state of polarization. Further assume that the matrix has the circular polarization states as eigenvectors. Thus we have an eigenvalue problem. For right circularly polarized light

$$\begin{bmatrix} A & B \\ C & D \end{bmatrix} \frac{1}{\sqrt{2}} \begin{bmatrix} -i \\ 1 \end{bmatrix} = (T^+)^{1/2} e^{i\delta/2} \frac{1}{\sqrt{2}} \begin{bmatrix} -i \\ 1 \end{bmatrix} \tag{40}$$

where T^+ is the right circular transmission fraction and δ is the relative phase shift between the right and left circularly polarized components. Likewise for left circularly polarized light

$$\begin{bmatrix} A & B \\ C & D \end{bmatrix} \frac{1}{\sqrt{2}} \begin{bmatrix} i \\ 1 \end{bmatrix} = (T^-)^{1/2} e^{-i\delta/2} \frac{1}{\sqrt{2}} \begin{bmatrix} i \\ 1 \end{bmatrix} \tag{41}$$

where T^- is the left circular transmission fraction. Solution yields the matrix

$$\begin{bmatrix} A & B \\ -B & A \end{bmatrix} \tag{42}$$

where

$$A = \frac{(T^+)^{1/2} e^{i\delta/2} + (T^-)^{1/2} e^{-i\delta/2}}{2} \tag{43}$$

and

$$B = \frac{(T^+)^{1/2} e^{i\delta/2} - (T^-)^{1/2} e^{-i\delta/2}}{2i} \tag{44}$$

This matrix operating on the incident Jones vector gives the emergent Jones vector. This permits the following work to be described completely in terms of Jones calculus.

CONVENTIONAL MAGNETIC ROTATION (MR)

The signal observed when a sample in a magnetic field is placed between crossed polarizers may be readily derived. The first polarizer generates a horizontal beam described by

$$\begin{bmatrix} 1 \\ 0 \end{bmatrix}$$

then the sample and final polarizer operate to give

$$\begin{bmatrix} J_x' \\ J_y' \end{bmatrix} = \begin{bmatrix} 0 & 0 \\ 0 & 1 \end{bmatrix} \begin{bmatrix} A & B \\ -B & A \end{bmatrix} \begin{bmatrix} 1 \\ 0 \end{bmatrix}$$

which simplifies to

$$\begin{bmatrix} J'_x \\ J'_y \end{bmatrix} = \begin{bmatrix} 0 \\ -B \end{bmatrix} \tag{46}$$

and

$$I \propto J^{\dagger}J = B^{*}B \tag{47}$$

B is evaluated from Eq.(44) so the intensity becomes

$$I \propto \frac{1}{4}[T^{+} + T^{-} - 2(T^{+}T^{-})^{1/2}\mathrm{Cos}\delta] \tag{48}$$

Assume an exponential absorption law

$$T^{\pm} = e^{-\alpha^{\pm}L}$$

where α^{+} (α^{-}) is the absorption coefficient for right (left) circularly polarized light and δ is the relative phase shift between right and left circularly polarized components. This is usually expressed in terms of the Faraday angle

$$\theta = \delta/2 \tag{49}$$

where

$$0 = \frac{\pi}{\lambda}(n^{-} - n^{+})L \tag{50}$$

Then Eq.(48) may be rewritten

$$I \propto \frac{[(T^{+})^{1/2} - (T^{-})^{1/2}]^{2}}{4} + (T^{+}T^{-})^{1/2}\mathrm{Sin}^{2}\theta \tag{51}$$

which separates into a magnetic circular dichroism term

$$MCD = \frac{[(T^{+})^{1/2} - (T^{-})^{1/2}]^2}{4} \qquad (52)$$

and a magnetic circular birefringence term

$$MCB = (T^{+}T^{-})^{1/2}\sin^2\theta \qquad (53)$$

Magnetic rotation spectra are composed of the combined effects of dichroism and birefringence.

MAGNETIC CIRCULAR DICHROISM (MCD)

The MCD of the (0,0,3) band of NO_2 was measured using the experimental setup of Figure 10.

Figure 10

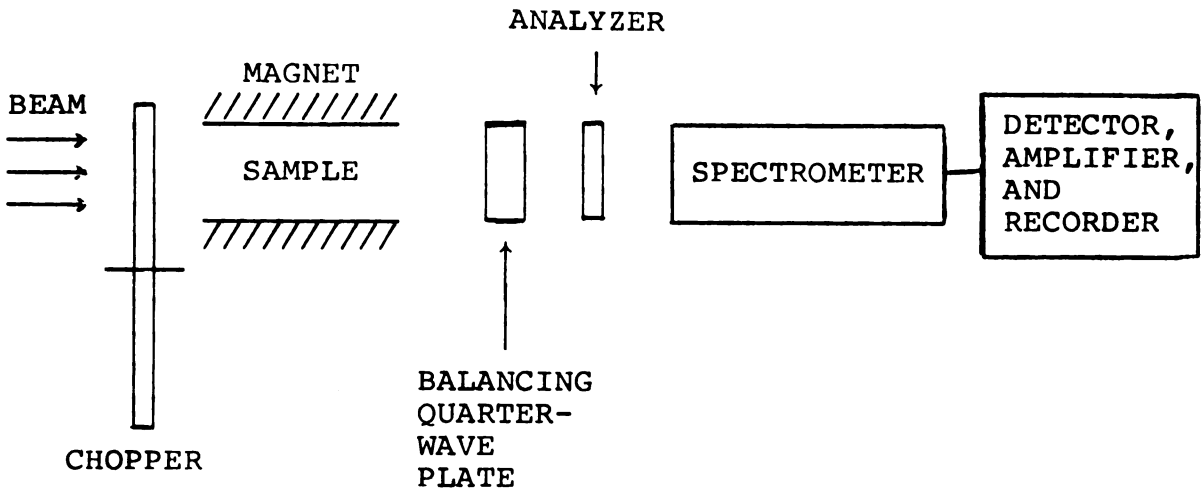

The construction of the chopper is shown if Figure 11

Figure 11

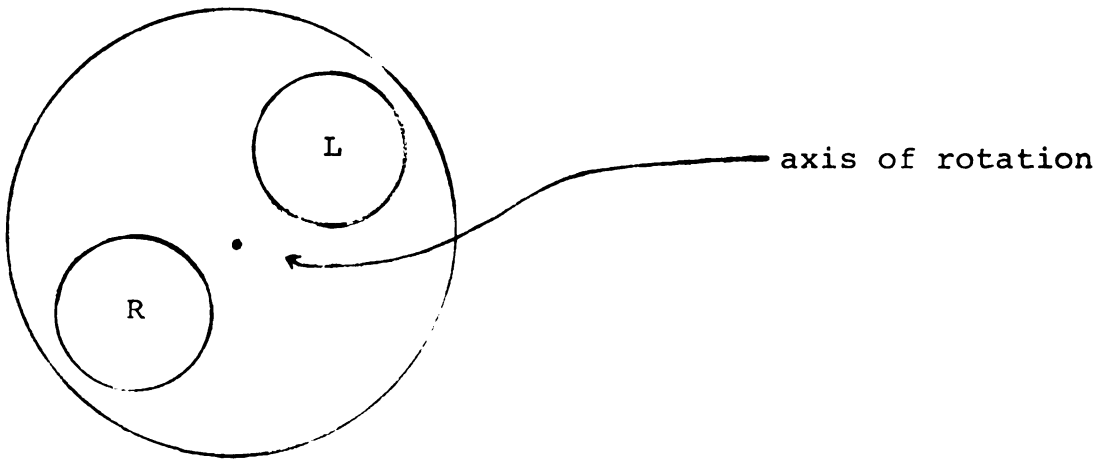

where R stands for the right circular polarizer and

L stands for the left circular polarizer.

The right and left circular polarizers were constructed by mounting a quartz quarter-wave plate preceeded by an HR polarizer in a teflon assembly. The axis of the HR polarizer was mounted at an angle of $\pm 45^{\circ}$ to the fast axis of the quarter-wave plates which generates left and right circularly polarized light respectively.

The relative orientation of the circular polarizers was not important since circular polarization has no unique axis. As the chopper rotates the incident beam is alternately converted to right and left circularly polarized pulses. It is therefore possible to look for a difference in the right and left signals directly. This is accomplished by observing that the primary signal occurs at a frequency

2ν where ν is the frequency of rotation. Also present is a difference signal at ν which is proportional to the difference in intensities of the right and left pulses after passing through the sample. The origin of the signal can be schematically visualized by reference to Figure 12

Figure 12

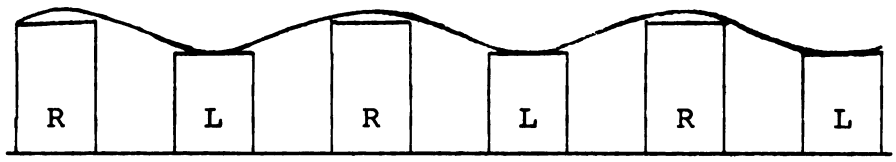

R represents right circular pulses

L represents left circular pulses

This difference signal is a direct measure of the circular dichroism and can be expressed as

$$D = (I_R - I_L)\mathrm{Sin}(\omega t + \gamma) \qquad (54)$$

where $\omega = 2\pi\nu$ and γ is an arbitrary phase angle.

The signal was detected using a Princeton HR-8 lock-in amplifier which is a sensitive tuned amplifier plus a phase sensitive detector. The phase sensitive detector requires an externally generated reference signal which has a definite phase relationship to the actual signal. The reference for convenience was generated by reflecting a laser beam from a half blackened disk mechanically locked to the chopper disk. The beam was detected by a photo detector, amplified, and used to provide the reference

required by the HR-8. The lock-in amplifier effectively selects a frequency, converts the output of the detector to a sinusoidal wave form at the desired frequency whose amplitude is proportional to the signal, rectifies the resultant AC signal utilizing the reference signal as a timer or gate, and filters the output to generate a DC voltage. Appropriate time constants can be selected for the filtering in order to smooth out the high frequency noise while retaining the signal.

In practice the right and left circular polarizers do not pass precisely the same intensity of radiation, and the grating is polarization sensitive. Any imbalance in the right and left signals produces an absorption spectrum which could mask the desired circular dichroism. Thus a compensating scheme was necessary. Balancing was accomplished by inserting a quarter-wave plate and a linear polarizer into the optical train after the sample as shown in Figure 13. The quarter-wave plate converts the right and left circularly polarized light to linearly polarized light at $\pm 45^{o}$ to the fast axis of the plate.

In practice the final polarizer is aligned with the grating to give maximum sensitivity and the fast axis of the quarter-wave plate is rotated until balancing is achieved as shown is Figure 13.

The initial imbalance was small but compensation was required and this scheme allowed effective balancing. The

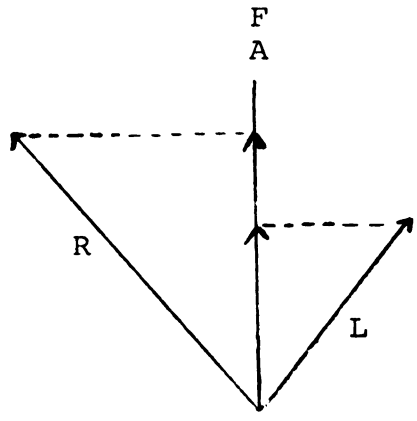

UNBALANCED

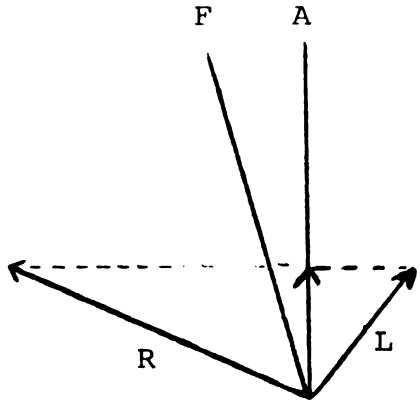

BALANCED

Figure 13

The linearly polarized pulses emerging from the balancing quarter-wave plate are shown resolved along the axis of the analyzer.

R is the result of conversion of the right circular pulse to linear polarization.

L is the result of conversion of the left circular pulse to linear polarization.

F is the fast axis of the balancing quarter-wave plate.

A is the axis of the analyzer.

Both cases are for zero applied field.

Balancing is achieved when the components along the analyzer axis are equal in the absence of a field.

method is also useful because small rotations of the quarter-wave plate produce a difference which can be used as a test signal when tuning and phasing the electronics even in the absence of a sample. The net result of the balancing scheme is to reduce the signal slightly but to retain the same dependence of the signal on (I_R-I_L).

The overall result of a change in the relative values of (I_R-I_L) is to introduce a negative sign $-(I_R-I_L)$ which is equivalent to a 180^o phase shift.

$$D = -(I_L-I_R)\ \mathrm{Sin}(\omega t + \gamma) = (I_L-I_R)\ \mathrm{Sin}(\omega t + \gamma + \pi) \qquad (56)$$

In a lock-in amplifier a 180^{o} phase shift inverts the output voltage which makes it possible to record positive and negative deflections.

MAGNETIC CIRCULAR BIREFRINGENCE (MCB)

Magnetic circular birefringence is usually measured by the degree of rotation of a linearly polarized beam of radiation in passing through a sample subjected to a longitudinal magnetic field. A linearly polarized beam can be thought of as composed of a right and a left circularly polarized component of equal magnitudes. Thus mathematically the Jones vector of a vertical linearly polarized beam can be represented as

$$\begin{bmatrix} 0 \\ 1 \end{bmatrix} = \frac{1}{2}\begin{bmatrix} -i \\ 1 \end{bmatrix} + \frac{1}{2}\begin{bmatrix} i \\ 1 \end{bmatrix} \qquad (57)$$

From a classical point of view the right and left components can have different indices of refraction denoted by $n_R = n^+$ and $n_L = n^-$ which yields a difference in relative phase as the components traverse the sample.

The following is a description of an experimental arrangement which can measure the relative difference $n_R - n_L$. The experimental setup for measurement of MCB is shown in Figure 14. The polarizer and analyzer were crossed and the rotating polarizer was mounted on a cylinder set in a 1.75 inch I.D. ball bearing. The assembly was rotated

Figure 14

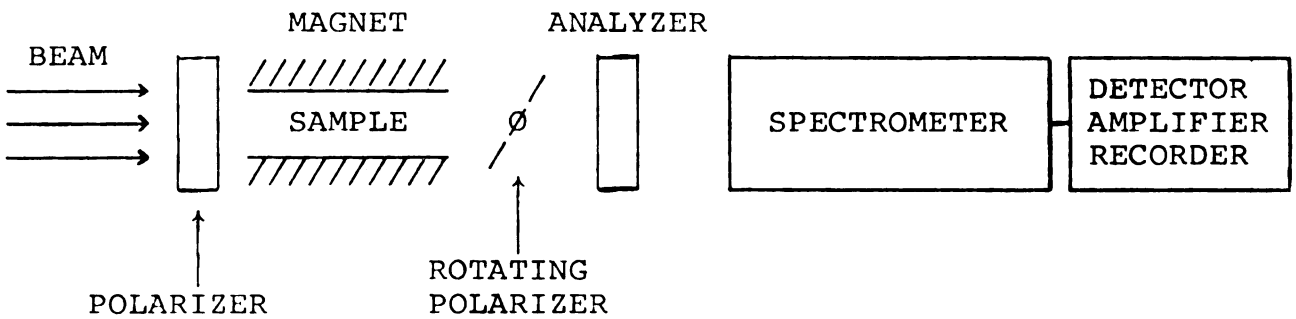

using pulleys and a belt drive powered by a 1/20 H.P. synchronous motor. The reference required for the lock-in was derived by aligning a laser beam with a hole bored in the cylinder which produced two brief pulses per revolution. The pulses were detected with a photo detector and amplified in a tuned circuit then sent to the tuned reference amplifier of the HR-8 lock-in amplifier. The tuned circuits converted the brief pulses into sinusoidal waves suitable as a reference.

A mathematical analysis of the system is required to find the form of the radiation emerging from the analyzer, but a brief physical picture may be useful. If one neglects circular dichroism then the result of magnetic circular birefringence on a linearly polarized beam is to produce a

rotation of the plane of polarization. This occurs because the relative phase of the two equal amplitude circular components into which the linearly polarized beam can be decomposed is changed due to their differing indices of refraction. Thus neglecting dichroism we have a linearly polarized beam emergent from the sample and incident on the rotating polarizer but at different angles depending on the MCB.

In the experimental arrangement of Figure 14 and in the absence of a sample one has a primary signal at 4ν where ν is the rotational frequency of the polarizer. The maxima of the signal occur at $\theta = 45^{o}$, 135^{o}, 225^{o}, and 315^{o} where θ is the angle of rotation of the polarizer measured from the horizontal. When the sample is introduced and the beam is rotated by $+\varepsilon$ degrees alternate pulses increase and the remaining pulses decrease, and for $-\varepsilon$ the relative pulse difference is reversed. This means that going from $+\varepsilon$ to $-\varepsilon$ changes the phase of the signal impressed at 2ν by 180^{o}. This is the reason that positive and negative deflections can be observed.

The following calculation with Jones calculus shows how the observed signal is related to the angle of rotation. Assume that the first polarizer produces a horizontal beam

$$\begin{bmatrix} 1 \\ 0 \end{bmatrix}$$

which is incident on the sample. Then we have the following multiplication of Jones matrices for the experimental

arrangement of Figure 14.

$$\begin{bmatrix} 0 & 0 \\ 0 & 1 \end{bmatrix} \begin{bmatrix} C_1^2 & C_1S_1 \\ C_1S_1 & S_1^2 \end{bmatrix} \begin{bmatrix} A & B \\ -B & A \end{bmatrix} \begin{bmatrix} 1 \\ 0 \end{bmatrix} \tag{58}$$

where C_1 and S_1 are $\cos\phi$ and $\sin\phi$ and the angle ϕ is the azimuthal angle of the rotating polarizer measured from the horizontal. A and B were defined previously. This reduces to

$$J = \begin{bmatrix} 0 \\ C_1S_1A - S_1^2B \end{bmatrix} \tag{59}$$

The emergent intensity is found from

$$I \propto J^{\dagger}J \tag{60}$$

which after appropriate simplification gives

$$I \propto \frac{\sin^2\phi}{4}(T^+ + T^- + 2(T^+T^-)^{1/2}\cos(2\phi + \delta)) \tag{61}$$

where $\phi = \omega_o t$ is the rotating polarizer angle. Recall ϕ is measured from the horizontal. If we wish to measure from the vertical

$$\phi \rightarrow \phi + \pi/2$$

and the expression becomes

$$I \propto \cos^2\phi(T^+ + T^- - 2(T^+T^-)^{1/2}\cos2(\phi + \theta)) \tag{62}$$

where $\theta = \delta/2$ which reduces in the appropriate limits to the conventional magnetic rotation signal (10). This intensity is converted to an equivalent electrical signal at the detector.

The remaining problem is to show that if the lock-in amplifier is tuned to twice the rotational frequency one gets a signal proportional to the angle of rotation of the beam or the Faraday angle. For this to be true two conditions must be met:

(a) The MCD must be very small compared to the MCB and

(b) The rotation of the beam in the sample must be a few degrees or less.

These conditions have been experimentally verified for NO_2 and theoretically for NO (10).

The terms dependent on 2ϕ may be found as follows. First expand

$$\mathrm{Cos}(2\phi + \delta) = \mathrm{Cos}2(\phi + \theta) = 1 - 2\mathrm{Sin}^2(\phi + \theta) \qquad (63)$$

so

$$I \propto \frac{[(T^+)^{1/2} - (T^-)^{1/2}]^2}{4}\mathrm{Cos}^2\phi + (T^+T^-)^{1/2}\mathrm{Cos}^2\phi\mathrm{Sin}^2(\phi+\theta) \qquad (64)$$

The first term is the MCD which is assumed small. Then complex exponentials can be used to reduce $\mathrm{Cos}^2\phi\mathrm{Sin}^2(\phi+\theta)$ into simple trigonometric functions. The only term in 2ϕ which remains is $\mathrm{Sin}\theta\mathrm{Sin}(2\phi+\theta)$. The observed intensity then assumes the form

$$I_{2\phi} \propto (T^{+}T^{-})^{1/2}\mathrm{Sin}\theta\mathrm{Sin}(2\phi + \theta) \qquad (65)$$

or in terms of the absorption coefficients

$$I_{2\phi} = I_{o}e^{[-(\alpha^{+}+ \alpha^{-})L]/2}\mathrm{Sin}\theta\mathrm{Sin}(2\phi + \theta) \qquad (66)$$

The signal depends on an amplitude factor and a phase shift. The $\mathrm{Sin}(2\phi + \theta)$ term introduces a small phase shift but the dominant signal arises from the $\mathrm{Sin}\theta$ term. As θ goes from + to -, $I_{2\phi}$ changes sign which corresponds to a 180^{o} phase shift in the lock-in amplifier. This makes it possible to observe positive and negative deflections of the recorder about some relative base line.

MCD AND MCB SPECTRA

NO 3-0 BAND

Magnetic circular birefringence spectra were observed in the 3-0 band of $^{14}N^{16}O$ utilizing the Michigan State University near-infrared spectrometer. The spectra are shown in Figure 15. The absorption and magnetic rotation spectra have been observed previously and are included in Figure 15 for comparison. The MCB spectra were run at a pressure of 10 cmHg and with an absorbing pathlength of 18.9 meters at fields of 2000 and 4000 Gauss. The signal was detected at a frequency of 47 Hz with a lead sulfide detector.

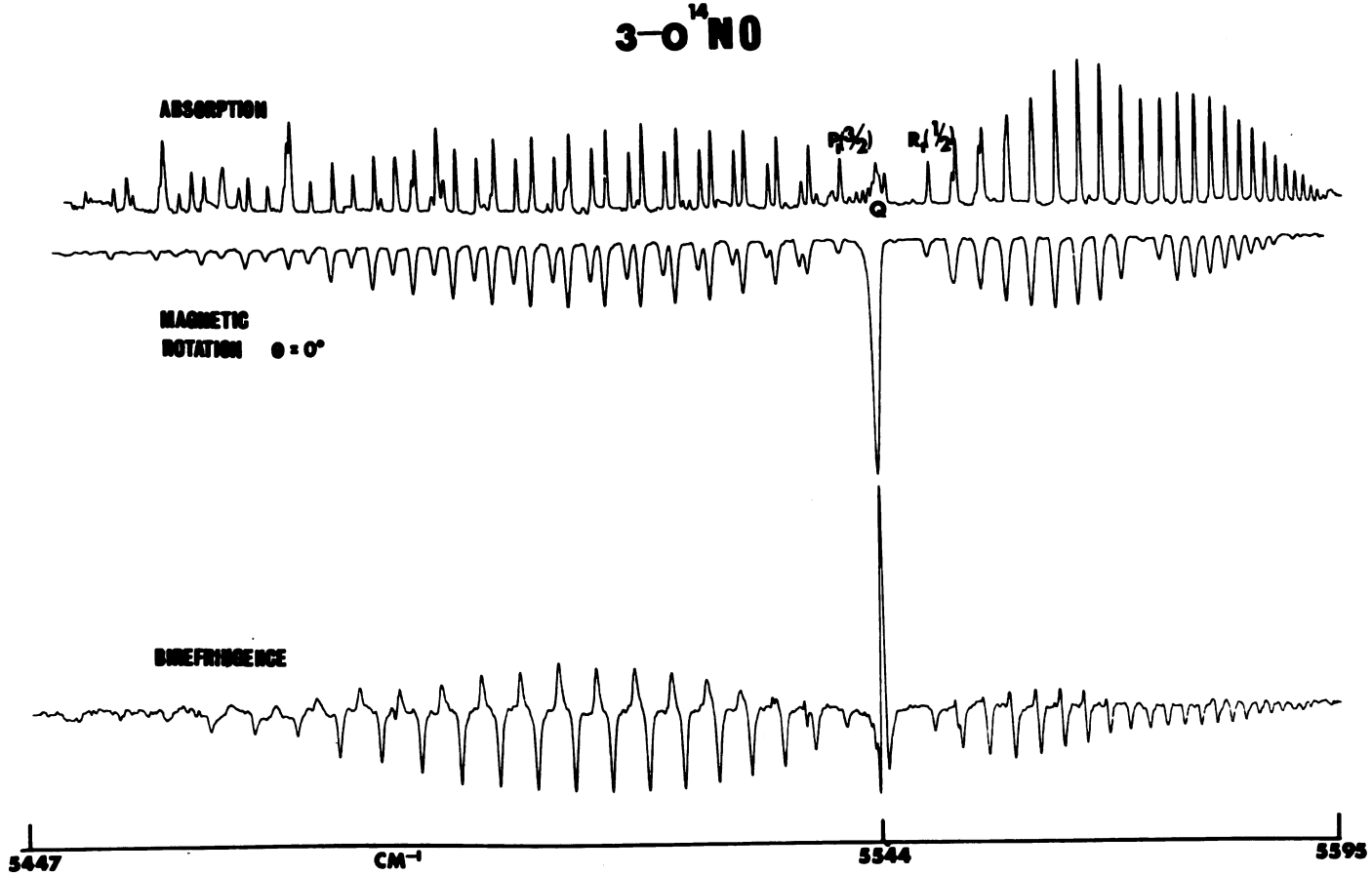

Figure 15: Absorption, MR, MCB spectra in the 3-0 band of $^{14}N^{16}O$ with a field of 4000 Gauss.

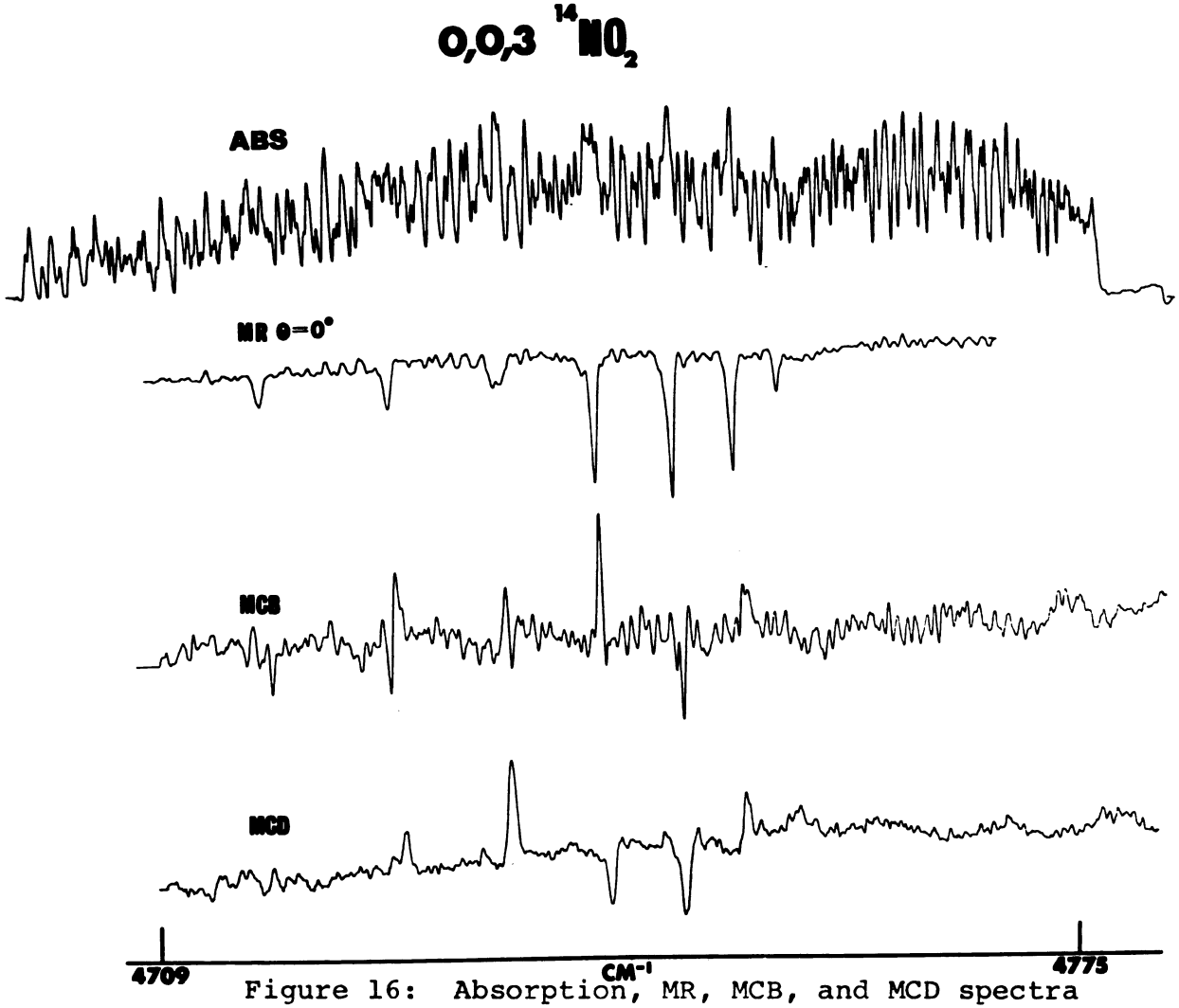

Figure 16: Absorption, MR, MCB, and MCD spectra of $^{14}N^{16}O_2$ at a field of 4000 Gauss.

The spectra at once prove that for the P and R branches the $^2\Pi_{1/2}$ and $^2\Pi_{3/2}$ lines are rotated in opposite directions. The direction of rotation is positive for the $^2\Pi_{1/2}$ P and R lines and negative for the $^2\Pi_{3/2}$ lines. The Q branch shows a very strong signal which is predominantly rotated in the negative direction. The directions of rotation are in agreement with the work of Aubel (9) and Keck (10). A complete explaination of the spectrum awaits a detailed analysis.

(0,0,3) of NO_2

It was possible to observe both MCB and MCD signals in the (0,0,3) band of $^{14}N^{16}O_2$. Absorption and magnetic rotation spectra were also run for camparison. Typical absorption, MR, MCB, and MCD spectra are shown in Figure 16.

MCB and MCD spectra were run at a pressure of 3 cm Hg and a pathlength of 18.9 meters at fields of 2000 and 4000 Gauss. The MCD signals were much weaker than the MCB and required that the entrance and exit slits of the spectrometer be opened from 100 microns to 200 microns. Furthermore it was necessary to increase the gain by a factor of 2.5. This supports the premise that the MCD signals are much smaller than the MCB signals.

The strongest MR, MCB, and MCD signals occur around the Q branch lines which are closely spaced in N and widely separated according to the value of K_{-1}. The MR lines from right to left in Figure 16 arise from K_{-1} = 2,3,4,5,6,7 and 8.

The theory required for prediction of Zeeman patterns for NO_2 has been detailed by Olman (22), and it is hoped that a detailed study of these patterns will lead to further meaningful interpretation of these spectra.

SUGGESTIONS FOR CONTINUED WORK

Much work has already been done on the magnetic rotation spectra of paramagnetic molecules. Mann and Hause (25) (26), Aubel (9), and Keck (10) have developed a considerable body of information about the MR of NO and NO_2. The calculation of MR spectra requires prediction of both magnetic circular birefringence and dichroism terms. In principle calculation of either birefringence or dichroism signals should be simpler than the MR signals where they are combined.

A semiclassical approach to the calculation of birefringence and dichroism effects has been outlined by Aubel (9) and continued by Keck (10) with application to the NO molecule. Briefly, in this approach one calculates the absorption coefficients, α^+ and α^-, from expressions which apply to Doppler, Lorentz, or intermediate line shapes. Then the indices of refraction, n^+ and n^-, are related to the absorption coefficients through the Kramers-Kronig relations.

Once n^+ and n^- are known θ is determined and can be inserted into Eqs. (66) and (56) which are the intensity expressions for birefringence and dichroism. This enables computation of an ideal predicted spectrum. To compare this

with the observed spectrum the effect of the spectrometer slit function must be included. Semi-quantative agreement between predicted and observed signals provides strong support for the validity of the Zeeman and dispersion theories.

It is hoped that this approach will be fruitful for interpretation of the observed MCB and MCD spectra of NO and NO_2.

SUMMARY

The (0,0,3), (1,0,3), and (3,0,1) vibration-rotation bands of $^{14}N^{16}O_2$ and $^{15}N^{16}O_2$ have been analyzed on the basis of the slightly asymmetric top molecule. Least squares methods were used to compare the observed to predicted transitions and by iterative procedures yielded the upper state constants for those bands. This information in conjunction with the previously analyzed (1,0,1) and (2,0,1) bands was used to predict improved vibrational and vibration-rotation interaction constants.

Spin splitting was observed in the (0,0,3) band and was analyzed to give spin-rotation interaction constants.

Magnetic circular birefringence and dichroism studies were undertaken for NO and NO_2. Experimental spectra were obtained which are qualitatively in agreement with previous experimental work and theoretical predictions. Finally a method was suggested whereby the experimental spectra may be compared to theoretical predictions.

REFERENCES

1. M. D. Olman and C. D. Hause, J. Mol. Spectry. 26, 241 (1968).
2. M. D. Olman and C. D. Hause, J. Chem. Phys. 49, 4575 (1968).
3. G. R. Bird et al., J. Chem. Phys. 40, 3378 (1964).
4. R. M. Lees, R. F. Curl, Jr., and J. G. Baker, J. Chem. Phys. 45, 2037 (1966).
5. E. T. Arakawa and A. H. Nielsen, J. Mol. Spectry. 2, 413 (1958).
6. G. E. Moore, J. Opt. Soc. Amer. 43, 1045 (1953).
7. A. F. Stalder, Thesis, Georgia Institute of Technology (1967).
8. A. F. Stalder and W. H. Eberhardt, J. Chem. Phys. 47, 1445 (1967).
9. J. L. Aubel, Thesis, Michigan State University (1964).
10. D. B. Keck, Thesis, Michigan State University (1967).
11. C. H. Townes and A. L. Schawlow, Microwave Spectroscopy (McGraw-Hill Book Co., New York, 1955), p. 93.
12. Ibid., p. 84.
13. Swalen and Pierce, Journal of Math. Phys. 2, 736 (1961).
14. R. A. Hill and T. H. Edwards, J. Mol. Spectry. 9, 494 (1962).
15. L. Pierce, N. DiCianni, and R. H. Jackson, J. Chem. Phys. 38, 730 (1963).

16. Townes and Schawlow, op. cit., p. 175.

17. C. C. Lin, Phys. Rev. 116, 903 (1959).

18. W. T. Raynes, J. Chem. Phys. 41, 3020 (1964).

19. D. B. Keck et al., "Symposium on Molecular Structure and Spectroscopy," Columbus, Ohio, 1966, Paper H-2.

20. K. Narahari Rao, C. J. Humphreys, and D. H. Rank, Wavelength Standards in the Infrared, Appendix III and pp. 160, 161, 171. Academic Press, New York, 1966.

21. R. A. Hill, Thesis, Michigan State University (1963).

22. M. D. Olman, Thesis, Michigan State University (1967).

23. W. A. Shurcliff, Polarized Light (Harvard University Press, Cambridge, Mass., 1962).

24. A. M. Sutton and C. F. Panati, Modern Optics (RCA Institute, Inc. Lecture Notes, 1969).

25. G. Mann, Thesis, Michigan State University (1959).

26. G. A. Mann and C. D. Hause, J. Chem. Phys. 33, 1117 (1960).

27. K. T. Chung and P. M. Parker, J. Chem. Phys. 43, 3869 (1965).

28. G. Herzberg, Infrared and Raman Spectra of Polyatomic Molecules, Molecular Spectra and Molecular Structure II (D. Van Nostrand Company Ltd., New York, 1945).

29. M. A. Efroymson, Mathematical Methods for Digital Computers (John Wiley and Sons, Inc., New York, 1960), Ch. 17, pp. 191-203.

30. T.L. Barnett, Thesis, Michigan State University (1967).

APPENDIX I

COMPUTER PROGRAMS

Several computer programs were utilized in the course of this work. Several programs were contributed as previously acknowledged. The following programs were written to perform least squares fits based on a least squares routine by M. A. Efroymson (29). Typical data decks are listed as well as the programs.

VIBCON

This program performs a least squares fit on Eq. (30) using the experimentally determined band origins as data points to determine vibrational constants. It is necessary to input approximate values of the vibrational constants and any or all of the constants may be fixed or varied as indicated in the data deck.

ROTCON

This program performs a least squares fit on Eq. (31) using the experimentally determined rotational constants A, B, and C as data points to determine vibration-rotation interaction constants. The program is otherwise similar in operation to VIBCON.

```
      PROGRAM VIBCON
      COMMON/123/NK(30), NDELMAX, XDEVMAX
      COMMON/12/ INFO1,INFO2, INFO3,NUMCON,JUMP,CONST(30),EFIN,EFOUT,TOL
     1, IDENT(2)
      COMMON/A/ NAME(30)
      DIMENSION NU1(50), NU2(50), NU3(50)
      DIMENSION CON(10,50),FOBS(50),FCALC(50),WT(50),NUSE(50)
      READ 20, III
   20 FORMAT(I2)
      PRINT 21, III
   21 FORMAT(* THE FOLLOWING VIBRATIONAL CONSTANTS ARE FOR *I2*NO2*)
  100 READ1, NUMCON,JUMP, XDEVMAX, NDELMAX
      PRINT 1, NUMCON,JUMP, XDEVMAX, NDELMAX
    1 FORMAT(2I5,F10.4,I5)
      READ5,INFO1,INFO2,INFO3,TOL,EFIN,EFOUT
      PRINT 5 , INFO1, INFO2, INFO3, TOL,EFIN,EFOUT
    5 FORMAT( 3I5, 3F10.5)
      N = 0
  102 N = N + 1
      READ 2, CONST(N), NK(N)
    2 FORMAT(F19.4, I1)
      PRINT12 , CONST(N), NK(N)
   12 FORMAT(1X, F19.4,2X,I1)
      IF(CONST(N).NE.0)  GO TO 102
      NCOUNT = N - 1
      NN = 0
  104 NN = NN + 1
      READ 4, NU1(NN),NU2(NN),NU3(NN), FOBS(NN),WT(NN)
      PRINT 4,NU1(NN),NU2(NN),NU3(NN), FOBS(NN),WT(NN)
    4 FORMAT(3I3, 2F10.4)
      IF(FOBS(NN).NE.0)  GO TO 104
      INDATA = NN - 1
      PRINT6, INDATA
    6 FORMAT( * INDATA IS* I5)
      NAME(1) = 6HOMEGA1
      NAME(2) = 6HOMEGA2
      NAME(3) = 6HOMEGA3
      NAME(4) = 3HX11
      NAME(5) = 3HX22
      NAME(6) = 3HX33
      NAME(7) = 3HX12
      NAME(8) = 3HX13
      NAME(9) = 3HX23
      NCONP1 = NUMCON + 1
      DO 110,NN = 1, INDATA
      CON(1,NN) = NU1(NN)
      CON(2,NN) = NU2(NN)
      CON(3,NN) = NU3(NN)
      CON(4,NN) = ((NU1(NN) + 0.5)*(NU1(NN) + 0.5)) - 0.25
      CON(5,NN) = ((NU2(NN) + 0.5)*(NU2(NN) + 0.5)) - 0.25
      CON(6,NN) = ((NU3(NN) + 0.5)*(NU3(NN) + 0.5)) - 0.25
      CON(7,NN) = ((NU1(NN) + 0.5)*(NU2(NN) + 0.5)) - 0.25
      CON(8,NN) = ((NU1(NN) + 0.5)*(NU3(NN) + 0.5)) - 0.25
      CON(9,NN) = ((NU2(NN) + 0.5)*(NU3(NN) + 0.5)) - 0.25
```

```
110  CONTINUE
     PRINT 1000, CON
000  FORMAT(F10.4)
     PRINT 1001, NAME
001  FORMAT(A8)
     DO 200, NN = 1, INDATA
     FCALC(NN) = CONST(1)*CON(1,NN) + CONST(2)*CON(2,NN) + CONST(3)*
    1CON(3,NN) + CONST(4)*CON(4,NN) + CONST(5)*CON(5,NN) + CONST(6)*
    2CON(6,NN) + CONST(7)*CON(7,NN) + CONST(8)*CON(8,NN) + CONST(9)*
    3CON(9,NN)
     PRINT 10, NU1(NN),NU2(NN),NU3(NN),FCALC(NN)
 10  FORMAT(3I3, F10.4)
200  CONTINUE
     CALL STEPFIT (CON,FOBS,FCALC,NUSE, WT, NCONP1, INDATA)
     END
     SUBROUTINE PRINTOUT(DATA,FOBS,FCALC,NUSE,WT,NCONP1,INDATA)
     COMMON/123/ NK(30),NDELMAX,XDEVMAX
     COMMON/23/NODATA,NOVMI,AVEWHT,STDY,NOSTEP, N, WTN, FREQPRD, YPRED,
    1 DEV
     COMMON/100/JJ(900), KK(900), JDEL(900), KDEL(900), NUDEL(900)
     DIMENSIONDATA(NCONP1,INDATA),FOBS(INDATA),FCALC(INDATA),WT(INDATA)
    1, NUSE(INDATA)
     ENTRY PRINT 2
     PRINT166
     RETURN
     ENTRY PRINT 3
     PRINT 165, N, KDEL(N), JDEL(N), KK(N), JJ(N), WTN, FOBS(N), FCALC(
    1N), FREQPRD, DATA(NCONP1, N), YPRED, DEV
     RETURN
165  FORMAT (I5,X, 2R1, I2, 1H,, I2, 3X, F6.2, 6F11.4)
166  FORMAT (*1  NO.              WT    OBS FREQ   CALC FREQ   PRED FREQ
    1OBS-CALC   PRED-CALC    OBS-PRED*)
     END
     SUBROUTINE STEPFIT(DATA,FOBS,FCALC,NUSE, WT, NCONP1,INDATA)
     COMMON/123/ NK(30),NDELMAX,XDEVMAX
     COMMON/12/INFO1,INFO2,INFO3,NUMCON,JUMP,CONST(30),FFIN,EFOUT,TOL,
    1IDENT(2)
     COMMON/23/NODATA,NOVMI,AVEWHT,STDY,NOSTEP, N, WTN, FREQPRD, YPRED,
    1 DEV
     COMMON/A/ NAME(30)
     DIMENSION N1(30),VECTOR(31,31),INDEX(30),IDEX(30),SIGMA(30),
    1COEN(30),SIGMCO(30),NOTIN(30),XCONST(30)
     DIMENSIONDATA(NCONP1,INDATA),FOBS(INDATA),FCALC(INDATA),WT(INDATA)
    1, NUSE(INDATA)
     TYPE INTEGER SS,VV
     TYPE DOUBLE VECTOR,SIGMA,COEN,SIGMCO,SIGY,DEFR,VAR
     IF(IDENT(1)) 9100,9110
9100 IDENT(1)=8HINPUT DA
     IDENT(2) =2HTA
9110 CONTINUE
     IF(.NOT.EFOUT) EFOUT=1.E-8
     IF(.NOT.EFIN) FFIN=EFOUT=1.E-8
     IF(TOL.EQ.0.0) TOL=0.001
 175 NOVAR = 1
```

```
      DO 157 I=1,NUMCON
      IF(NK(I))158,157
  158 N1(NOVAR)=NAME(I)
      IF(JUMP) 8158,8159
 8158 XCONST(NOVAR)=CONST(I)
 8159 NOVAR=NOVAR+1
  157 CONTINUE
      NODATA=0
      DO254 N=1,INDATA
      IF(WT(N))252,253
  253 NUSE(N)=0
      GO TO 254
  252 NUSE(N)=1
      NODATA=NODATA+1
  254 CONTINUE
      NDEL=0
  495 NOIN=K=NOENT=NOMIN=NOMAX=VAR=FLEVEL=0.0
      LOOP=0
      NOVMI = NOVAR - 1
      NOVPL = NOVAR + 1
      DO 176 I = 1,NOVPL
      DO 176 J = 1,NOVPL
  176 VECTOR(I,J) = 0.0
      IF(NDEL)501,500
  500 SUMWHT=0.0
      IDEX(NOVAR)=NCONP1
      DO525N=1,INDATA
      NUM=0
      DO 512 I=1,NUMCON
      IF(NK(I))511,512
  511 NUM=NUM+1
      IDEX(NUM)=I
  512 CONTINUE
      DATA(NCONP1,N)=FOBS(N)-FCALC(N)
  525 SUMWHT=SUMWHT+WT(N)
  501 AVEWHT=SUMWHT/NODATA
      DO510N=1,INDATA
      IF(NUSE(N))146,510
  146 WHT=WT(N)/AVEWHT
      DO 540 I = 1, NOVAR
      VECTOR(I,NOVPL)=VECTOR(I,NOVPL)+DATA(IDEX(I),N)*WHT
      DO 540 J = I,NOVAR
  540 VECTOR(I,J)=VECTOR(I,J)+DATA(IDEX(I),N)*DATA(IDEX(J),N)*WHT
      VECTOR(NOVPL,NOVPL) = VECTOR(NOVPL,NOVPL) + WHT
  510 CONTINUE
      IF(INF01)580,650
  580 PRINT 1115
 1115 FORMAT(*1SUM OF VAR*/)
      NOMAX=NOVMI
      IF(NOVMI.GT.7) NOMAX = 7
      PRINT 15, (I,I=1,NOMAX)
      PRINT 17, VECTOR(NOVAR,NOVPL),(VECTOR(I,NOVPL),I=1,NOMAX)
 9581 IF(NOVMI.EQ.NOMAX) GO TO 581
      MOMAX = NOMAX + 1 $  NOMAX = MOMAX + 7
```

```
      IF(NOMAX.GT.NOVMI) NOMAX = NOVMI
      PRINT 1116, (I,I=NOMAX,NOMAX)
      PRINT 17, (VECTOR(I,NOVPL), I = NOMAX,NOMAX)
      GO TO 9581
 81   CONTINUE
      NOMIN = 1  $  NOMAX = NOVMI  $  NGO = 5
 02   IF(NOVMI.GT.NGO) NOMAX = NGO
 99   PRINT 152,(I,I = NOMIN, NOMAX)
      DO 180  J = NOMIN, NOVMI
      JJJ = J
      IF(JJJ.GT.NOMAX)  JJJ = NOMAX
 80   PRINT 153, J, (VECTOR(I,J), I = NOMIN, JJJ)
      PRINT 154, (VECTOR(I,NOVAR), I = NOMIN, NOMAX)
      IF(NOMAX.EQ.NOVMI) GO TO 603
      NOMIN = NOMAX + 1  $  NGO = NGO + 5  $  NOMAX = NOVMI
      GO TO 602
 03   CONTINUE
      PRINT155, VECTOR(NOVAR,NOVAR)
 650  NOSTEP = -1
      ASSIGN 1320 TO NUMREP
      DEFR   = VECTOR(NOVPL,NOVPL) - 1.0
      DO 800  I = 1,NOVAR
      IF(VECTOR(I,I)) 792,794,810
 792  PRINT  793, I
      GOTO172
 794  PRINT 795, I
      SIGMA(I) = 1.0
      GO TO 800
 810  SIGMA(I) =DSQRT  (VECTOR (I,I))
 800  VECTOR(I,I) = 1.0
      DO 830 I = 1,NOVMI
      IP1 = I + 1
      DO 830 J = IP1, NOVAR
      VECTOR(I,J) = VECTOR(I,J) /( SIGMA(I)* SIGMA(J))
 830  VECTOR(J,I) = VECTOR(I,J)
      IF(INFO2) 870,1001
870   NOMIN = 1  $  NOMAX = NOVMI  $  NGO = 15  $  NOMINP = 2
602   IF(NOVMI.GT.NGO) NOMAX = NGO
      PRINT 159, (I,I = NOMIN, NOMAX)
      DO 885 I = NOMINP, NOVMI
      III = I - 1
      IF(III.GT.NOMAX) III = NOMAX
 885  PRINT 160, I,(VECTOR(I,J), J = 1, III)
      PRINT 161,(VECTOR(I,NOVAR), I = NOMIN, NOMAX)
      IF(NOMAX.EQ.NOVMI) GO TO 1001
      NOMIN = NOMAX + 1  $  NOMINP = NOMIN + 1
      NGO = NGO + 15  $  NOMAX = NOVMI
      GO TO 1602
1001  NOSTEP = NOSTEP + 1
      IF (VECTOR( NOVAR,NOVAR)) 1002,1002,1010
1002  NSTPM1 = NOSTEP - 1
      PRINT 1004, NSTPM1
      GO TO 1381
1010  SIGY =  SIGMA(NOVAR) *DSQRT  (VECTOR(NOVAR,NOVAR)/ DEFR)
```

```
      DEFR =DEFR-1.0
      IF (DEFR )  1017,1017, 1020
1017  PRINT  1019 ,NOSTEP
      GO TO 1381
1020  VMIN=VMAX=NOIN=0
      DO 1050 I = 1,NOVMI
      IF (VECTOR(I,I)) 1042, 1050, 1060
1042  PRINT 1044, I, NOSTEP
      GO TO 1381
1060  IF(VECTOR(I,I)-TOL) 1050, 1080, 1080
1080  VAR=VECTOR(I,NOVAR)*VECTOR(NOVAR,I)/VECTOR(I,I)
      IF(VAR)1100, 1050, 1110
1100  NOIN = NOIN + 1
      INDEX(NOIN) = I
      COEN(NOIN)  = VECTOR(I,NOVAR) * SIGMA(NOVAR) / SIGMA (I)
      SIGMCO(NOIN) = (SIGY / SIGMA(I)) *DSQRT (VECTOR(I,I))
      IF (VMIN) 1160,1170,904
  904 PRINT 906
      GOTO172
1170  VMIN = VAR
      NOMIN = I
      GO TO 1050
1160  IF(VAR - VMIN)1050,1050,1170
1110  IF (VAR - VMAX)1050,1050,1210
1210  VMAX = VAR
      NOMAX = I
1050  CONTINUE
      IF (NOIN) 903,1240,1300
  903 PRINT 907
      GO TO 172
1240  STDY=SIGY
      GO TO 1350
1300  IF(INFO3)1310,1320
1310  IF (NCENT) 1311,1311,1313
1311  PRINT168, NOSTEP, K
      GO TO 1314
1313  PRINT169, NOSTEP, K
1314  IF(LOOP) FLEVEL=FL
      PRINT 162,K,FLEVEL,SIGY
      DO1301J=1,NOIN
      N=INDEX(J)
1301  PRINT163,N,N1(N),COEN(J),SIGMCO(J)
      IF(JUMP) 8302,8304
8302  IF(LOOP) 8303,8304
8303  PRINT 8305
8305  FORMAT(*2FINAL CONSTANTS AFTER CORRECTIONS WERE ADDED*/)
      DO 8306 J=1,NOIN
      N=INDEX(J)
      XNEWCON=COEN(J)+XCONST(N)
8306  PRINT 163,N,N1(N),XNEWCON,SIGMCO(J)
8304  GO TO NUMBER,(1320,1580)
1320  FL=FLEVEL
      FLEVEL=VMIN*DEFR/VECTOR(NOVAR,NOVAR)
      IF(EFOUT + FLEVEL) 1350, 1350, 1340
```

```
1340 K =  NOMIN
1345 NOENT = 0
     GO  TO  1391
1350 FLEVEL = VMAX * DEFR / (VECTOR(NOVAR,NOVAR)-  VMAX)
     IF (EFIN - FLEVEL) 1370,1361,1380
1361 IF (EFIN) 1380,1380,1370
1370 K = NOMAX
     NOENT = K
1391 IF(K) 1392,1392,1400
1392 PRINT 1395, NOSTEP
     GOTO172
1400 DO 1410   I = 1,NOVAR
     IF (I-K) 1430,1410,1430
1430 DO 1440   J = 1, NOVAR
     IF (J-K) 1460,1440,1460
1460 VECTOR(I,J)=VECTOR(I,J)-VECTOR(I,K)*VECTOR(K,J)/VECTOR(K,K)
1440 CONTINUE
1410 CONTINUE
     DO 1480  I = 1, NOVAR
     IF (I-K) 1500,1480,1500
1500 VECTOR (I,K)  =  -  VECTOR (I,K) / VECTOR (K,K)
1480 CONTINUE
     DO 1520 J = 1, NOVAR
     IF (J-K) 1540,1520,1540
1540 VECTOR(K,J) =   VECTOR (K,J) / VECTOR (K,K)
1520 CONTINUE
     VECTOR(K,K) =  1.0 / VECTOR(K,K)
     GOTO1001
1380 PRINT 167,IDENT(1),IDENT(2),NODATA,NOVMI,NDELMAX,XDEVMAX,AVEWHT,
    1STDY,NOSTEP
1381 CONTINUE
1570 ASSIGN  1560  TO NUMBER
     LOOP=1
     GO TO 1310
1580 CONTINUE
     IF(INFO3) PRINT 1586,(L,VECTOR(L,L),L=1,NOVMI)
     CALL PRINT 2
     VFIT=DEVMAX=SWT=XIR=0.0
     DO1660N=1,INDATA
     WTN=NUSE(N)*WT(N)
     WHT=WTN/AVEWHT
     YPRED = 0.0
     DO 1630  I = 1,NOIN
     LASSIE = INDEX(INDEX(I))
1630 YPRED = YPRED + COEN(I)*DATA(LASSIE,N)
     DEV=FORS(N)-FCALC(N)-YPRED
     IF(10.*WT(N))1652,1652,1651
1651 VFIT=VFIT+WTN*DEV**2
     XIR=XIR+1.0
     SWT=SWT+WT(N)
1652 FREQPRD=FCALC(N)+YPRED
     WHT=WHT*AVEWHT
     CALL PRINT 3(DATA,FORS,FCALC, WT, NUSE, NCONP1, INDATA)
     ADEV=ABSF(DEV)*SQRTF(WHT)*NUSE(N)
```

```
      IF(DEVMAX-ADEV)1610,1610,1660
 1610 NMAX=N
      DEVMAX=ADEV
 1660 CONTINUE
      VFIT=VFIT*XIR/((XIR-NOIN)*SWT)
      STDFIT=SQRTF(VFIT)
      PRINT150, VFIT, STDFIT
      IF(NDELMAX-NDEL)172,172,1624
 1624 IF(DEVMAX-XDEVMAX)172,172,1620
 1620 NUSE(NMAX)=0
      NDEL=NDEL+1
      NODATA=NODATA-1
      SUMWHT=SUMWHT-WT(NMAX)
      PRINT 9001,NMAX
      GOTO495
  172 RETURN
   15 FORMAT(*         Y*7I17,/)
   17 FORMAT(X1P7E17.6,E16.6,//)
 1116 FORMAT(I10,6I17,/)
  150 FORMAT(*0STAT FROM LINES WHTD LT 10.0*/*0VAR. =*F10.6*     STD. DE
     1V =*F7.4/*7*)
  151 FORMAT (10A8)
  152 FORMAT(*RAW SSCP MATRIX*/5I26)
  153 FORMAT(XI2,1P5E26.10)
  154 FORMAT(*  Y*1P5E26.10)
  155 FORMAT(*  Y VS Y*F15.4)
  156 FORMAT (13I1,3FXI2,10XI5,F5,2XA8)
  159 FORMAT (*-PARTIAL CORR. COEFF.*//16I8)
  160 FORMAT (I3,16F8.4)
  161 FORMAT (*  Y*16F8.4)
  162 FORMAT (*   F LEVEL OF X-*I1,E10.2,9X*STD DEV OF (O-P)*F7.4//10X*V
     1ARIABLE     COEFFICIENT         STD ERROR*/)
  163 FORMAT (I11,A9,2F17.12)
  167 FORMAT(*1LEAST SQUARES FIT OF *2A8   /* FIT *I4* DATA POINTS TO *
     1I2* VARIABLES*/* DELETES UP TO *I2* POINTS IF (O-P) IS GT *F6.3/
     2* WHT NORM * F6.2/* STD DEV OF (O-C)*F8.4/* COMPLETED *I2* STEPS*)
  168 FORMAT (*0STEP NO*I3/*   VAR. REMOVED*I3)
  169 FORMAT (*0STEP NO*I3/*   VAR. ENTERED*I3)
  701 FORMAT (4F15)
  702 FORMAT (*ABOVE NON-EIGENVALUE NOT DIAG. AFTER 10 CYCLES*)
  793 FORMAT (* ERROR RESID SQ VAR*I3* IS NEG*)
  795 FORMAT (*0VAR*I5* IS CONST*)
  850 FORMAT (X6I3,F20,F10,23XA8)
  906 FORMAT (*0ERROR, VMIN POS*)
  907 FORMAT (*0ERROR NOIN NEG*)
 1000 FORMAT (*0LINE NO*I4* DELETED*5X6I3,2F10.4)
 1004 FORMAT (*0Y SQUARE NEG STEP*I5)
 1019 FORMAT (*0ZERO DEG FREEDOM STEP*I3)
 1044 FORMAT (*SQUARE X-*I2* NEGATIVE STEP*I3)
 1395 FORMAT (*K=0 STEP*I3)
 1586 FORMAT (*0  DIAG ELEMENTS*/* VAR NO    VALUE*//(I4,F12.6))
 9000 FORMAT (2I5,F10)
 9001 FORMAT (*-LINE NO*I4* BEING DELETED FROM FIT*)
      END
```

```
7/9 RUN CARD 45 SECONDS



                TYPICAL DATA DECK

C       IDENTIFY THE ISOTOPE

15

C       THE MAXIMUM NUMBER OF CONSTANTS AND TYPICAL TOLERANCES

     9     1 1.0           2
     1     1     1 0.00001    0.0         0.0

C       VALUES OF OMEGA 1,2,3 AND A PARAMETER 0 IF NOT VARIED 1 IF VARIED

1342.5               1
747.1                0
1028.0               1

C       THE PRELIMINARY X SUB IJ VALUES WITH 1 (0) IF VARIED (NOT VARIED)

-8.8                 1
-0.4                 0
-15.6                1
-9.5                 0
-27.7                1
-2.6                 0

C       A BLANK CARD IS INSERTED HERE

C       THE FOLLOWING ARE DATA CARDS WITH THE FIRST THREE INTEGERS IDENTIFYING
C       THE UPPER STATE FOLLOWED BY THE BAND ORIGIN AND THE WEIGHT

   1   0   1 2858.7071    1.0
   2   0   1 4120.3673    1.0
   0   0   3 4655.2283    1.0
   3   0   1 5367.3149    1.0
   1   0   3 5874.9510    1.0
   0   0   1 1580.32      0.01
   1   0   0 1306.0       0.01

C       A BLANK CARD IS INSERTED HERE
```

```
      PROGRAM ROTCON
      COMMON/123/NK(30), NDELMAX, XDEVMAX
      COMMON/12/ INFO1,INFO2, INFO3,NUMCON,JUMP,CONST(30),EFIN,EFOUT,TOL
     1, IDENT(2)
      COMMON/A/ NAME(30)
      DIMENSION CON(5,30), FOBS(30),FCALC(30),WT(30),NUSE(30)
      DIMENSION NU1(30),NU2(30),NU3(30)
      READ 20, A, III
   20 FORMAT( A8, I2)
      PRINT 21, A, III
   21 FORMAT(* THE FOLLOWING ROTATIONAL CONSTANTS ARE FOR THE *A8* OF *I
     12*NO2*)
  100 NUMCON = 4
      NCONP1 = NUMCON + 1
      NAME(1) = 4HR000
      NAME(2) = 6HALPHA1
      NAME(3) = 6HALPHA2
      NAME(4) = 6HALPHA3
      READ   1, JUMP
      PRINT  1, JUMP
    1 FORMAT(I5)
      READ    2, CONST(1),CONST(2), CONST(3),CONST(4)
      PRINT   2, CONST(1),CONST(2), CONST(3),CONST(4)
    2 FORMAT(4F15,6)
      N = 0
  101 N = N+1
      READ   3, NU1(N),NU2(N),NU3(N),FOBS(N),WT(N)
      PRINT  3, NU1(N),NU2(N),NU3(N),FOBS(N),WT(N)
    3 FORMAT( 3I3,F10,6,F10,1)
      CON(1,N) = 1,0
      CON(2,N) =-NU1(N)
      CON(3,N) =-NU2(N)
      CON(4,N) =-NU3(N)
      IF(FOBS(N),NE,0) GO TO 101
      INDATA = N - 1
      PRINT 7, INDATA
    7 FORMAT(* INDATA IS * I4)
      READ   4, NK(1),NK(2),NK(3),NK(4),XDEVMAX,NDELMAX,INFO1,INFO2,
     1INFO3, TOL, EFIN, EFOUT
    4 FORMAT(4I1,5X,F10,5,4I2,2X,3F10,5)
      PRINT 10, NK(1),NK(2),NK(3),NK(4),XDEVMAX,NDELMAX,INFO1,INFO2,
     1INFO3, TOL, EFIN, EFOUT
   10 FORMAT(1X,4I1,5X,F10,5,4I2,2X,3F10,5)
      DO 120, N = 1, INDATA
      FCALC(N) = CONST(1)*CON(1,N) + CONST(2)*CON(2,N) + CONST(3)*
     1CON(3,N) + CONST(4)*CON(4,N)
      PRINT 8, NU1(N),NU2(N),NU3(N), FCALC(N)
    8 FORMAT( 3I3,F10,4)
  120 CONTINUE
      CALL STEPFIT(CON,FOBS,FCALC,NUSE,WT,NCONP1, INDATA)
      READ   5,XIDENT
    5 FORMAT(A8)
      PRINT  11,XIDENT
   11 FORMAT(1X, A8)
```

```
      IF(XIDENT.EQ.8HNEW DATA) GO TO 100
      END
      SUBROUTINE PRINTOUT(DATA,FOBS,FCALC,NUSE,WT,NCONP1,INDATA)
      COMMON/123/ NK(30),NDELMAX,XDEVMAX
      COMMON/23/NODATA,NOVMI,AVEWHT,STDY,NOSTEP, N, WTN, FREQPRD, YPRED,
     1 DEV
      COMMON/100/JJ(900), KK(900), JDEL(900), KDEL(900), NUDEL(900)
      DIMENSIONDATA(NCONP1,INDATA),FOBS(INDATA),FCALC(INDATA),WT(INDATA)
     1, NUSE(INDATA)
      ENTRY PRINT 2
      PRINT166
      RETURN
      ENTRY PRINT 3
      PRINT 165, N, KDEL(N), JDEL(N), KK(N), JJ(N), WTN, FOBS(N), FCALC(
     1N), FREQPRD, DATA(NCONP1, N), YPRED, DEV
      RETURN
165   FORMAT (I5,X, 2R1, I2, 1H., I2, 3X, F6.2, 6F11.7)
166   FORMAT (*1  NO,              WT    OBS FREQ  CALC FREQ  PRED FREQ
     1OBS-CALC  PRED-CALC  OBS-PRED*)
      END
      SUBROUTINE STEPFIT(DATA,FOBS,FCALC,NUSE, WT, NCONP1,INDATA)
      COMMON/123/ NK(30),NDELMAX,XDEVMAX
      COMMON/12/INFO1,INFO2,INFO3,NUMCON,JUMP,CONST(30),EFIN,EFOUT,TOL,
     1IDENT(2)
      COMMON/23/NODATA,NOVMI,AVEWHT,STDY,NOSTEP, N, WTN, FREQPRD, YPRED,
     1 DEV
      COMMON/A/ NAME(30)
      DIMENSION N1(30),VECTOR(31,31),INDEX(30),IDEX(30),SIGMA(30),
     1COEN(30),SIGMCO(30),NOTIN(30),XCONST(30)
      DIMENSIONDATA(NCONP1,INDATA),FOBS(INDATA),FCALC(INDATA),WT(INDATA)
     1, NUSE(INDATA)
      TYPE INTEGER SS,VV
      TYPE DOUBLE VECTOR,SIGMA,COEN,SIGMCO,SIGY,DEFR,VAR
      IF(IDENT(1)) 9100,9110
9100  IDENT(1)=8HINPUT DA
      IDENT(2) =2HTA
9110  CONTINUE
      IF(.NOT.EFOUT) EFOUT=1.E-8
      IF(.NOT.EFIN) EFIN=EFOUT*1.E-8
      IF(TOL.EQ.0.0) TOL=0.001
 175  NOVAR = 1
      DO 157 I=1,NUMCON
      IF(NK(I))158,157
 158  N1(NOVAR)=NAME(I)
      IF(JUMP) 8158,8159
8158  XCONST(NOVAR)=CONST(I)
8159  NOVAR=NOVAR+1
 157  CONTINUE
      NODATA=0
      DO254 N=1,INDATA
      IF(WT(N))252,253
 253  NUSE(N)=0
      GO TO 254
 252  NUSE(N)=1
```

```
      NODATA=NODATA+1
  254 CONTINUE
      NDEL=0
  495 NOIN=K=NOENT=NOMIN=NOMAX=VAR=FLEVEL=0.0
      LOOP=0
      NOVMI = NOVAR - 1
      NOVPL = NOVAR + 1
      DO 176 I = 1,NOVPL
      DO 176 J = 1,NOVPL
  176 VECTOR(I,J) = 0.0
      IF(NDEL)501,500
  500 SUMWHT=0.0
      IDEX(NOVAR)=NCONP1
      DO525N=1,INDATA
      NUM=0
      DO 512 I=1,NUMCON
      IF(NK(I))511,512
  511 NUM=NUM+1
      IDEX(NUM)=I
  512 CONTINUE
      DATA(NCONP1,N)=FOBS(N)-FCALC(N)
  525 SUMWHT=SUMWHT+WT(N)
  501 AVEWHT=SUMWHT/NODATA
      DO510N=1,INDATA
      IF(NUSE(N))146,510
  146 WHT=WT(N)/AVEWHT
      DO 540 I = 1, NOVAR
      VECTOR(I,NOVPL)=VECTOR(I,NOVPL)+DATA(IDEX(I),N)*WHT
      DO 540 J = I,NOVAR
  540 VECTOR(I,J)=VECTOR(I,J)+DATA(IDEX(I),N)*DATA(IDEX(J),N)*WHT
      VECTOR(NOVPL,NOVPL) = VECTOR(NOVPL,NOVPL) + WHT
  510 CONTINUE
      IF(INFO1)580,650
  580 PRINT 1115
 1115 FORMAT(*1SUM OF VAR*/)
      NOMAX=NOVMI
      IF(NOVMI.GT.7) NOMAX = 7
      PRINT 15, (I,I=1,NOMAX)
      PRINT 17, VECTOR(NOVAR,NOVPL),(VECTOR(I,NOVPL),I=1,NOMAX)
9581  IF(NOVMI.EQ.NOMAX) GO TO 581
      MOMAX = NOMAX + 1 $ NOMAX = MOMAX + 7
      IF(NOMAX.GT.NOVMI) NOMAX = NOVMI
      PRINT 1116, (I,I=MOMAX,NOMAX)
      PRINT 17, (VECTOR(I,NOVPL), I = MOMAX,NOMAX)
      GO TO 9581
  581 CONTINUE
      NOMIN = 1  $  NOMAX = NOVMI  $  NGO = 5
  602 IF(NOVMI.GT.NGO) NOMAX = NGO
  599 PRINT 152,(I,I = NOMIN, NOMAX)
      DO 180  J = NOMIN, NOVMI
      JJJ = J
      IF(JJJ.GT.NOMAX)  JJJ = NOMAX
  180 PRINT 153, J, (VECTOR(I,J), I = NOMIN, JJJ)
      PRINT 154, (VECTOR(I,NOVAR), I = NOMIN, NOMAX)
```

```
      IF(NOMAX,EQ,NOVMI) GO TO 603
      NOMIN = NOMAX + 1  $  NGO = NGO + 5  $  NOMAX = NOVMI
      GO TO 602
  603 CONTINUE
      PRINT155, VECTOR(NOVAR,NOVAR)
  650 NOSTEP = -1
      ASSIGN 1320 TO NUMBER
      DEFR   = VECTOR(NOVPL,NOVPL) - 1.0
      DO 800  I = 1,NOVAR
      IF(VECTOR(I,I)) 792,794,810
  792 PRINT  793, I
      GOTO172
  794 PRINT 795, I
      SIGMA(I) = 1.0
      GO TO 800
  810 SIGMA(I) =DSQRT  (VECTOR (I,I))
  800 VECTOR(I,I) = 1.0
      DO 830 I = 1,NOVMI
      IP1 = I + 1
      DO 830 J = IP1, NOVAR
      VECTOR(I,J) = VECTOR(I,J) /( SIGMA(I)* SIGMA(J))
  830 VECTOR(J,I) = VECTOR(I,J)
      IF(INFO2) 870,1001
  870 NOMIN = 1  $  NOMAX = NOVMI  $  NGO = 15  $  NOMINP = 2
 1602 IF(NOVMI,GT,NGO) NOMAX = NGO
      PRINT 159, (I,I = NOMIN, NOMAX)
      DO 885 I = NOMINP, NOVMI
      III = I - 1
      IF(III,GT,NOMAX) III = NOMAX
  885 PRINT 160, I,(VECTOR(I,J), J = 1, III)
      PRINT 161,(VECTOR(I,NOVAR), I = NOMIN, NOMAX)
      IF(NOMAX,EQ,NOVMI) GO TO 1001
      NOMIN = NOMAX + 1  $  NOMINP = NOMIN + 1
      NGO = NGO + 15  $  NOMAX = NOVMI
      GO TO 1602
 1001 NOSTEP = NOSTEP + 1
      IF (VECTOR( NOVAR,NOVAR)) 1002,1002,1010
 1002 NSTPM1 = NOSTEP - 1
      PRINT 1004, NSTPM1
      GO TO 1381
 1010 SIGY =  SIGMA(NOVAR) *DSQRT  (VECTOR(NOVAR,NOVAR)/ DEFR)
      DEFR =DEFR-1.0
      IF (DEFR )  1017,1017, 1020
 1017 PRINT  1019 ,NOSTEP
      GO TO 1381
 1020 VMIN=VMAX=NOIN=0
      DO 1050 I = 1,NOVMI
      IF (VECTOR(I,I)) 1042, 1050, 1060
 1042 PRINT 1044, I, NOSTEP
      GO TO 1381
 1060 IF(VECTOR(I,I)-TOL) 1050, 1080, 1080
 1080 VAR=VECTOR(I,NOVAR)*VECTOR(NOVAR,I)/VECTOR(I,I)
      IF(VAR)1100, 1050, 1110
 1100 NOIN = NOIN + 1
```

```
      INDEX(NOIN) = I
      COEN(NOIN)  = VECTOR(I,NOVAR) * SIGMA(NOVAR) / SIGMA (I)
      SIGMCO(NOIN) = (SIGY / SIGMA(I)) *DSQRT (VECTOR(I,I))
      IF (VMIN) 1160,1170,904
  904 PRINT 906
      GOTO172
 1170 VMIN = VAR
      NOMIN = I
      GO TO 1050
 1160 IF(VAR - VMIN)1050,1050,1170
 1110 IF (VAR - VMAX)1050,1050,1210
 1210 VMAX = VAR
      NOMAX = I
 1050 CONTINUE
      IF (NOIN) 903,1240,1300
  903 PRINT 907
      GO TO 172
 1240 STDY=SIGY
      GO TO 1350
 1300 IF(INFO3)1310,1320
 1310 IF (NOENT) 1311,1311,1313
 1311 PRINT168, NOSTEP, K
      GO TO 1314
 1313 PRINT169, NOSTEP, K
 1314 IF(LOOP) FLEVEL=FL
      PRINT 162,K,FLEVEL,SIGY
      DO1301J=1,NOIN
      N=INDEX(J)
 1301 PRINT163,N,N1(N),COEN(J),SIGMCO(J)
      IF(JUMP) 8302,8304
 8302 IF(LOOP) 8303,8304
 8303 PRINT 8305
 8305 FORMAT(*2FINAL CONSTANTS AFTER CORRECTIONS WERE ADDED*/)
      DO 8306 J=1,NOIN
      N=INDEX(J)
      XNEWCON=COEN(J)*XCONST(N)
 8306 PRINT 163,N,N1(N),XNEWCON,SIGMCO(J)
 8304 GO TO NUMBER,(1320,1580)
 1320 FL=FLEVEL
      FLEVEL=VMIN*DEFR/VECTOR(NOVAR,NOVAR)
      IF(EFOUT + FLEVEL) 1330, 1350, 1340
 1340 K =  NOMIN
 1345 NOENT = 0
      GO  TO  1391
 1350 FLEVEL = VMAX * DEFR / (VECTOR(NOVAR,NOVAR)-  VMAX)
      IF (EFIN - FLEVEL) 1370,1361,1380
 1361 IF (EFIN) 1380,1380,1370
 1370 K = NOMAX
      NOENT = K
 1391 IF(K) 1392,1392,1400
 1392 PRINT 1395, NOSTEP
      GOTO172
 1400 DO 1410   I = 1,NOVAR
      IF (I-K) 1430,1410,1430
```

```
1430 DO 1440   J = 1, NOVAR
     IF (J-K) 1460,1440,1460
1460 VECTOR(I,J)=VECTOR(I,J)-VECTOR(I,K)*VECTOR(K,J)/VECTOR(K,K)
1440 CONTINUE
1410 CONTINUE
     DO 1480  I = 1, NOVAR
     IF (I-K) 1500,1480,1500
1500 VECTOR (I,K)  =  -  VECTOR (I,K) / VECTOR (K,K)
1480 CONTINUE
     DO 1520 J = 1, NOVAR
     IF (J-K) 1540,1520,1540
1540 VECTOR(K,J) =   VECTOR (K,J) / VECTOR (K,K)
1520 CONTINUE
     VECTOR(K,K) =  1.0 / VECTOR(K,K)
     GOTO1001
1380 PRINT 167,IDENT(1),IDENT(2),NODATA,NOVMI,NDELMAX,XDEVMAX,AVEWHT,
    1STDY,NOSTEP
1381 CONTINUE
1570 ASSIGN  1580  TO NUMBER
     LOOP=1
     GO TO 1310
1580 CONTINUE
     IF(INFO3) PRINT 1586,(L,VECTOR(L,L),L=1,NOVMI)
     CALL PRINT 2
     VFIT=DEVMAX=SWT=XIR=0.0
     DO1660N=1,INDATA
     WTN=NUSE(N)*WT(N)
     WHT=WTN/AVEWHT
     YPRED = 0.0
     DO 1630  I = 1,NOIN
     LASSIE = IDEX(INDEX(I))
1630 YPRED = YPRED + COEN(I)*DATA(LASSIE,N)
     DEV=FOBS(N)-FCALC(N)-YPRED
     IF(10.-WT(N))1652,1652,1651
1651 VFIT=VFIT+WTN*DEV**2
     XIR=XIR+1.0
     SWT=SWT+WT(N)
1652 FREQPRD=FCALC(N)+YPRED
     WHT=WHT*AVEWHT
     CALL PRINT 3(DATA,FOBS,FCALC, WT, NUSE, NC0NP1, INDATA)
     ADEV=ABSF(DEV)*SQRTF(WHT)*NUSE(N)
     IF(DEVMAX-ADEV)1610,1610,1660
1610 NMAX=N
     DEVMAX=ADEV
1660 CONTINUE
     VFIT=VFIT*XIR/((XIR-NOIN)*SWT)
     STDFIT=SQRTF(VFIT)
     PRINT150, VFIT, STDFIT
     IF(NDELMAX-NDEL)172,172,1624
1624 IF(DEVMAX-XDEVMAX)172,172,1620
1620 NUSE(NMAX)=0
     NDEL=NDEL+1
     NODATA=NODATA-1
     SUMWHT=SUMWHT-WT(NMAX)
```

```
      PRINT 9001,NMAX
      GOTO495
  172 RETURN
   15 FORMAT(*         Y*7I17,/)
   17 FORMAT(X1P7E17.6,E16.6,//)
 1116 FORMAT(I10,6I17,/)
  150 FORMAT(*0STAT FROM LINES WHTD LT 10.0*/*0VAR. **F10.6*     STD. DE
     1V **F7.4/*7*)
  151 FORMAT (10A8)
  152 FORMAT(*RAW SSCP MATRIX*/5I26)
  153 FORMAT(X12,1P5E26.10)
  154 FORMAT(*  Y*1P5E26.10)
  155 FORMAT(*  Y VS Y*F15.4)
  156 FORMAT (13I1,35X12,10X15,F5.2XA8)
  159 FORMAT (*-PARTIAL CORR. COEFF.*//16I8)
  160 FORMAT (I3,16F8.4)
  161 FORMAT (*  Y*16F8.4)
  162 FORMAT (*   F LEVEL OF X=*I1,E10.2,9X*STD DEV OF (O-P)*F7.4//10X*V
     1ARIABLE     COEFFICIENT        STD ERROR*/)
  163 FORMAT (I11,A9,2F17.12)
  167 FORMAT(*1LEAST SQUARES FIT OF *2A8   /* FIT *I4* DATA POINTS TO *
     1I2* VARIABLES*/* DELETES UP TO *I2* POINTS IF (O-P) IS GT *F6.3/
     2* WHT NORM * F6.2/* STD DEV OF (O-C)*F8.4/* COMPLETED *I2* STEPS*)
  168 FORMAT (*0STEP NO*I3/*   VAR. REMOVED*I3)
  169 FORMAT (*0STEP NO*I3/*   VAR. ENTERED*I3)
  701 FORMAT (4F15)
  702 FORMAT (*ABOVE NON-EIGENVALUE NOT DIAG. AFTER 10 CYCLES*)
  793 FORMAT (* ERROR RESID SQ VAR*I3* IS NEG*)
  795 FORMAT (*0VAR*I5* IS CONST*)
  850 FORMAT (X6I3,F20.F10.23XA8)
  906 FORMAT (*0ERROR. VMIN POS*)
  907 FORMAT (*0ERROR NOIN NEG*)
 1000 FORMAT (*0LINE NO*I4* DELETED*5X6I3,2F10.4)
 1004 FORMAT (*0Y SQUARE NEG STEP*I5)
 1019 FORMAT (*0ZERO DEG FREEDOM STEP*I3)
 1044 FORMAT (*SQUARE X=*I2* NEGATIVE STEP*I3)
 1395 FORMAT (*K=0 STEP*I3)
 1586 FORMAT (*0  DIAG ELEMENTS*/* VAR NO    VALUE*//(I4',F12.6))
 9000 FORMAT (2I5,F10)
 9001 FORMAT (**LINE NO*I4* BEING DELETED FROM FIT*)
      END
```

7/9 RUN CARD 45 SECONDS

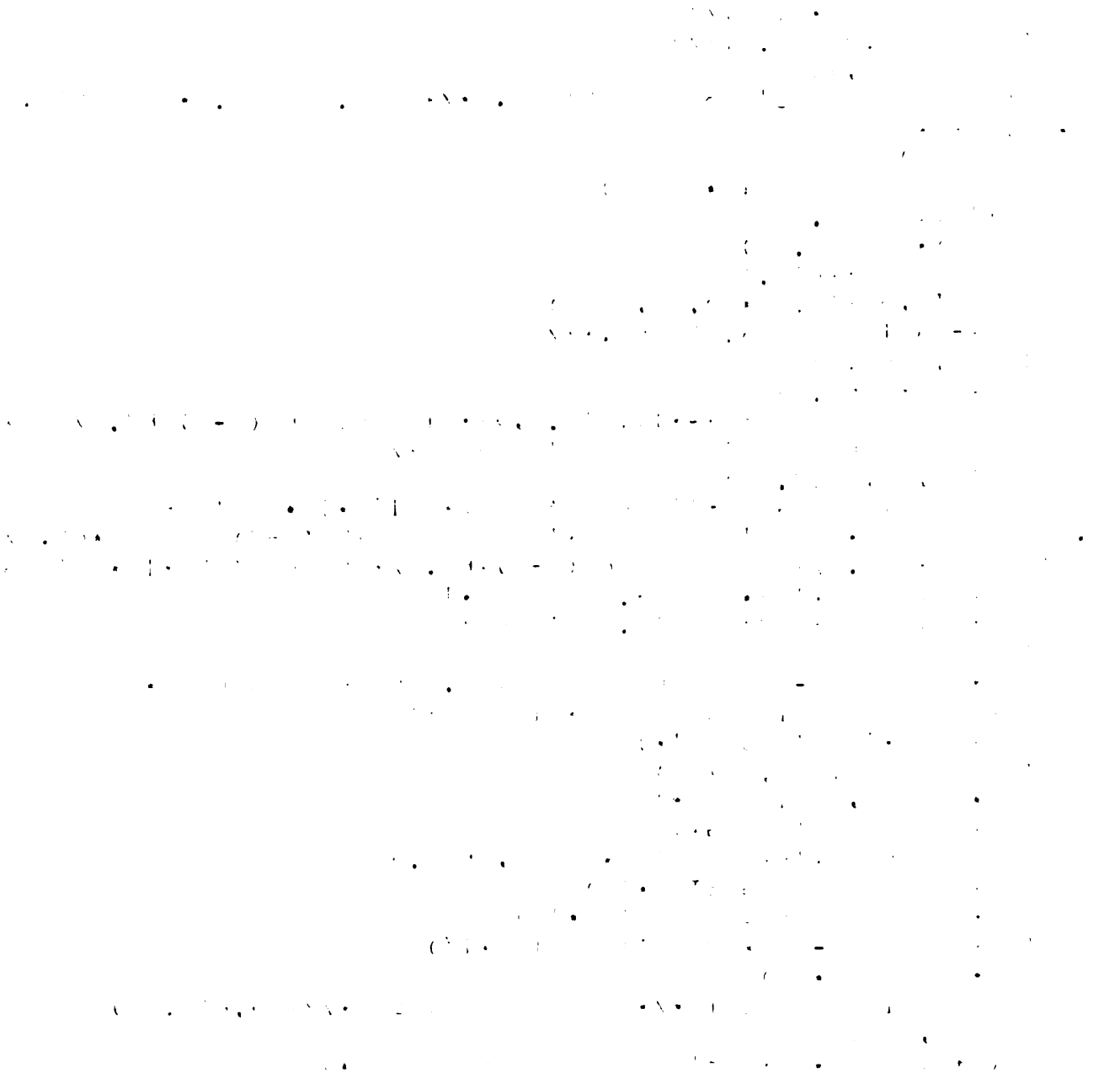

```
C       TYPICAL DATA DECK


C       THIS CARD IDENTIFIES THE ROTATIONAL CONSTANT AND ISOTOPE

    A    14

C       THIS IS A SWITCHING PARAMETER CALLED JUMP

     1

C       INPUT THE VALUE OF THE ROTATIONAL CONSTANT AND ALPHA 1,2,3

8,002509        -0,07245        0,0             0,22092

C       THE FOLLOWING ARE DATA POINTS WITH IDENTIFICATION OF THE UPPER
C       STATE AND THE WEIGHT ASSIGNED TO THE POINT

   1   0   1 7,85404   1,0
   2   0   1 7,92649   1,0
   3   0   1 8,01300   1,0
   0   0   3 7,3427    1,0
   1   0   3 7,4140    1,0

C       INSERT A BLANK CARD HERE

C       THE FIRST FOUR COLUMNS CAUSE VARIATION OF THE CONSTANTS A SUB ZERO,
C       ALPHA 1,2, AND 3 RESPECTIVELY   THE REMAINING PARAMETERS ARE USED
C       INTERNALLY AND ARE SET TO TYPICAL VALUES

0101        0,0002    2 1 1 1   0,0001    0,0         0,0

C       INSERT A BLANK CARD HERE
```

APPENDIX II

FREQUENCIES FOR THE (0,0,3) BAND OF $^{14}N^{16}O_2$

	K	N	OBS	O-P	WT		K	N	OBS	O-P	WT
P	0	48	4696,486	-0,004	0,5	P	0	46	4699,587	-0,002	0,3
P	0	44	4702,628	0,000	0,5	P	0	42	4705,616	0,011	0,0
P	0	40	4708,529	0,005	0,5	P	0	38	4711,385	0,004	0,8
P	0	36	4714,184	0,004	0,8	P	0	34	4716,913	-0,004	0,8
P	0	32	4719,597	0,003	1,0	P	0	30	4722,212	0,000	1,0
P	0	28	4724,769	0,001	1,0	P	0	26	4727,268	0,003	1,0
P	0	24	4729,699	-0,002	0,5	P	0	22	4732,084	0,007	1,0
P	0	20	4734,396	0,004	1,0	P	0	18	4736,654	0,005	0,5
P	0	16	4738,843	-0,001	0,5	P	0	14	4740,980	0,002	1,0
P	0	12	4743,055	0,002	1,0	P	0	10	4745,067	0,001	1,0
P	0	8	4747,020	0,001	0,8	P	0	6	4748,913	0,004	0,5
P	0	4	4750,737	-0,001	0,8	P	0	2	4752,505	-0,000	0,8
P	1	48	4694,569	0,018	0,5	P	1	47	4697,915	-0,000	0,3
P	1	46	4697,752	0,011	0,5	P	1	45	4700,997	0,028	0,0
P	1	44	4700,893	0,026	0,0	P	1	43	4703,948	-0,012	0,3
P	1	42	4703,948	0,019	0,5	P	1	41	4706,889	-0,003	0,3
P	1	40	4706,933	0,006	0,5	P	1	39	4709,761	-0,001	0,8
P	1	37	4712,576	0,006	0,5	P	1	36	4712,736	0,004	0,5
P	1	35	4715,318	-0,001	1,0	P	1	34	4715,527	-0,011	0,0
P	1	33	4718,009	0,004	0,5	P	1	32	4718,294	0,013	0,5
P	1	31	4720,630	-0,002	0,8	P	1	30	4720,964	0,003	1,0
P	1	29	4723,202	0,004	1,0	P	1	28	4723,574	-0,004	1,0
P	1	27	4725,705	0,002	1,0	P	1	26	4726,134	0,004	0,8
P	1	25	4728,148	0,001	1,0	P	1	24	4728,619	-0,001	1,0
P	1	23	4730,539	0,009	0,8	P	1	22	4731,043	-0,004	0,8
P	1	21	4732,861	0,008	0,5	P	1	20	4733,411	0,000	0,8
P	1	19	4735,121	0,006	0,5	P	1	18	4735,713	0,002	1,0
P	1	17	4737,307	-0,009	0,5	P	1	16	4737,947	-0,001	1,0
P	1	15	4739,456	0,000	0,8	P	1	14	4740,123	0,002	1,0
P	1	13	4741,534	-0,001	1,0	P	1	12	4742,230	-0,002	1,0
P	1	11	4743,554	0,002	0,5	P	1	10	4744,280	0,001	1,0
P	1	9	4745,510	0,000	1,0	P	1	8	4746,265	0,003	0,5
P	1	7	4747,406	-0,000	0,8	P	1	6	4748,182	-0,000	0,8
P	1	5	4749,238	-0,002	1,0	P	1	4	4750,040	0,002	1,0
P	1	3	4751,009	-0,004	1,0	P	2	48	4692,965	0,003	0,0
P	2	46	4696,168	0,011	0,5	P	2	45	4698,195	-0,003	0,5
P	2	44	4699,301	0,016	0,5	P	2	43	4701,230	-0,012	0,3
P	2	42	4702,352	0,005	0,0	P	2	41	4704,231	0,008	0,0
P	2	40	4705,337	-0,005	0,5	P	2	39	4707,137	-0,005	0,5
P	2	38	4708,267	-0,003	0,5	P	2	37	4709,996	-0,001	0,8
P	2	36	4711,135	0,002	0,5	P	2	35	4712,781	-0,009	0,8
P	2	34	4713,925	-0,005	0,8	P	2	33	4715,527	0,006	0,5

P	2	32	4716,660	-0,003	1,0	P	2	31	4718,184	-0,005	0,8
P	2	30	4719,336	0,006	0,8	P	2	29	4720,791	-0,005	1,0
P	2	28	4721,927	-0,006	1,0	P	2	27	4723,338	-0,002	1,0
P	2	26	4724,469	-0,002	1,0	P	2	25	4725,819	-0,003	1,0
P	2	24	4726,942	-0,003	0,8	P	2	23	4728,237	-0,005	1,0
P	2	22	4729,352	-0,001	1,0	P	2	21	4730,598	-0,002	0,8
P	2	20	4731,694	-0,003	1,0	P	2	19	4732,891	-0,004	0,5
P	2	18	4733,974	-0,003	1,0	P	2	17	4735,121	-0,009	1,0
P	2	16	4736,185	-0,007	0,5	P	2	15	4737,307	0,005	0,3
P	2	14	4738,340	-0,003	1,0	P	2	13	4739,415	0,003	0,5
P	2	12	4740,427	-0,003	1,0	P	2	11	4741,460	0,001	1,0
P	2	10	4742,450	-0,001	1,0	P	2	9	4743,440	-0,004	1,0
P	2	8	4744,410	0,000	0,8	P	2	7	4745,366	-0,001	1,0
P	2	6	4746,299	-0,005	0,5	P	2	5	4747,226	-0,002	1,0
P	2	4	4748,140	0,006	0,0	P	2	3	4749,042	0,016	0,0
P	3	48	4690,169	-0,016	0,0	P	3	47	4691,800	-0,012	0,3
P	3	46	4693,324	-0,013	0,5	P	3	45	4694,913	-0,012	0,3
P	3	44	4696,403	-0,021	0,5	P	3	43	4697,989	0,014	0,0
P	3	42	4699,434	-0,013	0,5	P	3	41	4700,944	-0,018	0,3
P	3	40	4702,393	-0,013	0,0	P	3	39	4703,872	-0,012	0,3
P	3	38	4705,290	-0,012	0,5	P	3	37	4706,734	-0,009	0,5
P	3	36	4708,122	-0,011	0,5	P	3	35	4709,530	-0,010	0,8
P	3	34	4710,892	-0,009	0,8	P	3	33	4712,267	-0,006	0,8
P	3	32	4713,599	-0,007	1,0	P	3	31	4714,934	-0,010	1,0
P	3	30	4716,238	-0,010	1,0	P	3	29	4717,546	-0,006	1,0
P	3	28	4718,821	-0,006	1,0	P	3	27	4720,095	-0,003	0,8
P	3	26	4721,337	-0,007	1,0	P	3	25	4722,579	-0,003	0,8
P	3	24	4723,794	-0,004	0,8	P	3	23	4724,996	-0,007	1,0
P	3	22	4726,185	-0,004	0,8	P	3	21	4727,362	-0,001	1,0
P	3	20	4728,514	-0,004	1,0	P	3	19	4729,658	-0,001	0,8
P	3	18	4730,782	-0,001	1,0	P	3	17	4731,894	0,001	1,0
P	3	16	4732,983	-0,004	0,8	P	3	15	4734,060	-0,006	1,0
P	3	14	4735,121	-0,008	0,0	P	3	13	4736,185	0,009	1,0
P	3	12	4737,207	0,000	0,8	P	3	11	4738,222	-0,001	1,0
P	3	10	4739,223	-0,001	1,0	P	3	9	4740,205	-0,004	0,5
P	3	8	4741,178	-0,000	1,0	P	3	7	4742,132	0,000	0,8
P	3	6	4743,055	-0,015	0,0	P	3	5	4743,985	-0,007	0,5
P	3	4	4744,883	-0,016	0,0	P	4	46	4689,063	0,034	0,3
P	4	45	4690,605	0,034	0,5	P	4	44	4692,124	0,028	0,5
P	4	43	4693,633	0,026	0,0	P	4	42	4695,130	0,030	0,0
P	4	41	4696,590	0,010	0,0	P	4	40	4698,062	0,020	0,3
P	4	39	4699,511	0,021	0,5	P	4	38	4700,944	0,022	0,3
P	4	37	4702,352	0,013	0,0	P	4	36	4703,757	0,019	0,5
P	4	35	4705,141	0,017	0,5	P	4	34	4706,509	0,016	0,5
P	4	33	4707,867	0,020	0,5	P	4	32	4709,198	0,012	0,0
P	4	31	4710,522	0,013	0,8	P	4	30	4711,831	0,015	0,8
P	4	29	4713,119	0,011	0,5	P	4	28	4714,398	0,012	1,0
P	4	27	4715,656	0,010	1,0	P	4	26	4716,913	0,021	0,5
P	4	25	4718,135	0,012	0,8	P	4	24	4719,336	-0,002	0,3
P	4	22	4721,731	0,009	0,5	P	4	21	4722,895	0,004	1,0
P	4	20	4724,056	0,012	0,5	P	4	19	4725,192	0,010	1,0
P	4	18	4726,311	0,007	1,0	P	4	17	4727,416	0,005	0,8
P	4	16	4728,514	0,011	1,0	P	4	15	4729,588	0,009	0,5
P	4	14	4730,644	0,004	0,5	P	4	13	4731,694	0,008	1,0

P	4	12	4732,721	0,006	1,0	P	4	11	4733,737	0,007	1,0
P	4	10	4734,735	0,006	0,8	P	4	9	4735,713	-0,000	1,0
P	4	8	4736,685	0,004	0,5	P	4	7	4737,635	0,001	1,0
P	4	6	4738,582	0,010	0,5	P	4	5	4739,499	0,005	0,0
P	5	42	4689,349	-0,165	0,0	P	5	41	4690,820	-0,166	0,0
P	5	40	4692,284	-0,158	0,0	P	5	39	4693,729	-0,153	0,0
P	5	38	4695,168	-0,139	0,0	P	5	37	4696,590	-0,126	0,0
P	5	36	4697,989	-0,122	0,0	P	5	35	4699,369	-0,121	0,0
P	5	34	4700,734	-0,120	0,0	P	5	33	4702,090	-0,112	0,0
P	5	32	4703,436	-0,099	0,0	P	5	31	4704,754	-0,099	0,0
P	5	30	4706,064	-0,091	0,0	P	5	29	4707,358	-0,085	0,0
P	5	28	4708,634	-0,081	0,0	P	5	27	4709,892	-0,080	0,0
P	5	26	4711,135	-0,079	0,0	P	5	25	4712,380	-0,060	0,0
P	5	24	4713,599	-0,053	0,0	P	5	23	4714,804	-0,043	0,0
P	5	22	4715,978	-0,050	0,0	P	5	21	4717,153	-0,041	0,0
P	5	20	4718,294	-0,049	0,0	P	5	19	4719,446	-0,032	0,8
P	5	18	4720,563	-0,036	0,0	P	5	17	4721,689	-0,014	0,5
P	5	16	4722,771	-0,022	0,5	P	5	15	4723,851	-0,016	0,8
P	5	14	4724,919	-0,006	0,8	P	5	13	4725,965	-0,004	1,0
P	5	12	4726,990	-0,008	0,8	P	5	11	4728,010	-0,000	1,0
P	5	10	4729,011	0,002	1,0	P	5	9	4729,999	0,008	0,5
P	5	8	4730,970	0,012	0,5	P	6	42	4682,738	-0,015	0,3
P	6	41	4684,169	-0,048	0,0	P	6	40	4685,623	-0,042	0,0
P	6	39	4687,074	-0,025	0,5	P	6	38	4688,485	-0,032	0,3
P	6	37	4689,897	-0,023	0,5	P	6	36	4691,289	-0,019	0,0
P	6	35	4692,661	-0,020	0,5	P	6	34	4694,018	-0,022	0,3
P	6	33	4695,362	-0,020	0,5	P	6	32	4696,694	-0,015	0,0
P	6	31	4697,989	-0,033	0,5	P	6	30	4699,301	-0,018	0,0
P	6	29	4700,593	-0,009	0,5	P	6	28	4701,865	-0,005	0,3
P	6	27	4703,115	-0,007	0,5	P	6	26	4704,358	-0,002	0,5
P	6	25	4705,582	-0,000	0,5	P	6	24	4706,794	0,005	0,5
P	6	23	4707,976	-0,006	0,0	P	6	22	4709,174	0,015	0,0
P	6	21	4710,324	0,003	0,8	P	6	20	4711,468	-0,000	0,8
P	6	19	4712,602	0,001	0,0	P	6	18	4713,718	-0,000	0,5
P	6	17	4714,827	0,006	0,0	P	6	16	4715,918	0,010	0,5
P	6	15	4716,977	-0,003	0,5	P	6	14	4718,041	0,005	0,5
P	6	13	4719,084	0,006	0,5	P	6	11	4721,123	0,006	0,5
P	6	10	4722,119	0,006	0,5	P	6	9	4723,109	0,014	0,3
P	6	8	4724,101	0,040	0,0	P	6	7	4725,046	0,034	0,0
P	7	37	4682,044	0,033	0,0	P	7	36	4683,419	0,026	0,0
P	7	35	4684,793	0,032	0,5	P	7	34	4686,145	0,032	0,0
P	7	33	4687,479	0,028	0,0	P	7	32	4688,773	-0,001	0,3
P	7	31	4690,104	0,023	0,5	P	7	30	4691,395	0,021	0,3
P	7	29	4692,661	0,009	0,0	P	7	28	4693,924	0,008	0,3
P	7	27	4695,167	0,003	0,5	P	7	26	4696,403	0,006	0,5
P	7	25	4697,621	0,005	0,5	P	7	24	4698,819	-0,002	0,5
P	7	23	4700,014	0,004	0,5	P	7	22	4701,182	-0,002	0,3
P	7	21	4702,352	0,008	0,0	P	7	20	4703,480	-0,008	0,3
P	7	19	4704,598	-0,019	0,0	P	7	18	4705,732	0,000	0,3
P	7	17	4706,830	-0,002	0,0	P	7	16	4707,906	-0,010	0,0
P	7	15	4708,973	-0,013	0,0	P	7	14	4710,037	-0,005	0,0
P	7	13	4711,071	-0,011	0,0	P	7	12	4712,088	-0,019	0,5
P	7	11	4713,119	0,002	0,0	P	7	10	4714,093	-0,020	0,0
C	1	13	4754,215	0,008	0,5	Q	1	1	4753,565	0,001	0,3

Q	2	15	4749,862	0,009	0,0		Q	2	14	4749,862	0,002	0,0
Q	2	13	4750,252	-0,001	0,5		Q	2	11	4750,613	0,002	0,3
Q	2	10	4750,702	-0,014	0,0		Q	2	9	4750,918	-0,001	0,5
Q	2	7	4751,180	0,005	0,5		Q	2	6	4751,273	-0,000	0,0
Q	2	4	4751,449	0,000	0,0		Q	2	3	4751,515	0,002	0,0
Q	2	2	4751,582	0,023	0,0		Q	3	10	4747,507	-0,006	0,0
Q	3	8	4747,799	-0,010	0,0		Q	3	7	4747,921	-0,014	0,0
Q	3	6	4748,047	0,004	0,0		Q	3	5	4748,140	0,004	0,0
Q	4	11	4742,846	-0,006	0,5		Q	5	14	4736,510	-0,030	0,0
Q	5	13	4736,728	-0,027	0,0		Q	5	11	4737,119	-0,018	0,0
Q	5	10	4737,307	0,001	0,0		Q	5	8	4737,580	-0,017	0,0
Q	5	7	4737,691	-0,028	0,0		Q	5	6	4737,796	-0,030	0,0
Q	5	5	4737,890	-0,028	0,0		Q	6	6	4730,889	-0,041	0,0
R	0	46	4775,202	-0,004	0,5		R	0	44	4775,049	-0,005	0,5
R	0	42	4774,865	0,024	0,0		R	0	40	4774,573	0,008	0,5
R	0	38	4774,227	0,003	0,8		R	0	36	4773,823	0,004	1,0
R	0	34	4773,348	-0,002	0,8		R	0	32	4772,818	0,003	1,0
R	0	30	4772,218	0,006	0,8		R	0	28	4771,548	0,004	0,8
R	0	26	4770,817	0,011	0,8		R	0	24	4770,004	0,004	0,8
R	0	22	4769,130	0,005	1,0		R	0	20	4768,184	0,003	1,0
R	0	18	4767,168	-0,001	0,8		R	0	16	4766,087	-0,000	1,0
R	0	14	4764,938	-0,000	1,0		R	0	12	4763,722	0,001	0,8
R	0	10	4762,418	-0,020	0,0		R	0	8	4761,087	-0,001	1,0
R	0	6	4759,667	-0,005	1,0		R	0	4	4758,204	0,013	0,3
R	0	2	4756,635	-0,012	0,5		R	0	0	4755,041	0,004	0,0
R	1	45	4774,813	-0,004	0,5		R	1	44	4774,865	0,012	0,3
R	1	42	4774,668	0,010	0,5		R	1	41	4774,305	-0,007	0,3
R	1	40	4774,401	0,012	0,5		R	1	39	4773,962	-0,001	0,8
R	1	38	4774,052	0,005	0,8		R	1	37	4773,549	-0,001	0,8
R	1	36	4773,635	0,002	0,5		R	1	35	4773,074	0,003	0,8
R	1	34	4773,149	0,003	1,0		R	1	33	4772,540	0,011	0,0
R	1	32	4772,587	-0,001	0,5		R	1	31	4771,929	0,007	0,5
R	1	30	4771,960	0,002	0,5		R	1	29	4771,257	0,007	0,8
R	1	28	4771,257	-0,003	0,8		R	1	27	4770,505	-0,010	0,0
R	1	26	4770,505	0,014	0,0		R	1	25	4769,715	-0,000	1,0
R	1	24	4769,656	0,002	0,8		R	1	23	4768,847	-0,005	0,8
R	1	22	4768,755	0,006	0,8		R	1	21	4767,931	0,006	1,0
R	1	20	4767,771	-0,003	0,8		R	1	19	4766,937	0,003	1,0
R	1	18	4766,739	0,005	0,5		R	1	17	4765,880	0,000	1,0
R	1	16	4765,631	0,005	0,8		R	1	15	4764,761	-0,001	0,8
R	1	14	4764,451	-0,001	0,5		R	1	13	4763,585	0,004	0,5
R	1	12	4763,211	-0,001	1,0		R	1	11	4762,345	0,008	0,5
R	1	10	4761,911	0,005	0,8		R	1	9	4761,034	0,004	0,8
R	1	8	4760,515	-0,019	0,0		R	1	7	4759,667	0,007	0,8
R	1	6	4759,098	0,001	0,8		R	1	5	4758,224	-0,003	0,3
R	1	4	4757,594	-0,001	0,8		R	1	3	4756,723	-0,010	0,5
R	1	2	4756,021	-0,008	0,5		R	1	1	4755,151	-0,025	0,0
R	2	47	4773,232	0,003	0,0		R	2	45	4773,074	-0,015	0,5
R	2	44	4773,635	0,016	0,5		R	2	43	4772,878	-0,005	0,3
R	2	42	4773,348	0,011	0,0		R	2	41	4772,587	-0,020	0,0
R	2	40	4772,982	-0,001	0,5		R	2	39	4772,260	-0,004	0,3
R	2	38	4772,540	-0,018	0,0		R	2	37	4771,852	-0,001	0,3
R	2	36	4772,053	-0,010	0,5		R	2	35	4771,372	-0,003	0,5
R	2	34	4771,503	0,001	0,5		R	2	33	4770,817	-0,014	0,8

R	2	32	4770,860	-0,013	0,5	R	2	31	4770,214	-0,006	0,3
R	2	30	4770,180	0,000	0,5	R	2	29	4769,541	-0,001	1,0
R	2	28	4769.422	0,000	1,0	R	2	27	4768,801	0,002	0,5
R	2	26	4768,600	-0,003	1,0	R	2	25	4767,984	-0,006	0,8
R	2	24	4767,724	0,002	0,5	R	2	23	4767,125	0,010	0,5
R	2	22	4766,777	-0,003	0,8	R	2	21	4766,173	-0,003	0,8
R	2	20	4765.772	-0,006	1,0	R	2	19	4765,168	-0,003	1,0
R	2	18	4764,720	0,004	0,5	R	2	17	4764,099	-0,003	1,0
R	2	16	4763,585	-0,009	0,5	R	2	15	4762,980	0,011	0,5
R	2	14	4762,418	0,006	0,5	R	2	13	4761,770	-0,001	1,0
R	2	12	4761,167	-0,003	1,0	R	2	11	4760,515	0,005	0,5
R	2	10	4759,865	-0,003	1,0	R	2	9	4759,172	-0,012	0,0
R	2	8	4758,511	0,007	0,5	R	2	7	4757,795	0,000	1,0
R	2	6	4757,069	-0,010	0,5	R	2	5	4756,346	0,004	0,3
R	2	4	4755,592	-0,001	0,5	R	2	3	4754,821	-0,007	0,5
R	2	2	4754,055	0,009	0,5	R	3	45	4770,180	-0,032	0,3
R	3	44	4770,260	-0,021	0,5	R	3	43	4769,970	-0,002	0,3
R	3	42	4769,970	-0,003	0,5	R	3	41	4769,656	-0,009	0,8
R	3	40	4769,593	-0,009	0,5	R	3	39	4769,279	-0,013	0,3
R	3	38	4769,178	0,008	0,0	R	3	37	4768,847	-0,004	0,8
R	3	36	4768,658	-0,018	0,5	R	3	35	4768,336	-0,009	0,8
R	3	34	4768,111	-0,010	0,5	R	3	33	4767,771	-0,003	0,5
R	3	32	4767,490	-0,014	1,0	R	3	31	4767,125	-0,014	0,5
R	3	30	4766,814	-0,011	0,5	R	3	29	4766,429	-0,010	1,0
R	3	28	4766,087	0,002	0,5	R	3	27	4765,665	-0,010	0,3
R	3	26	4765,273	-0,010	1,0	R	3	25	4764,836	-0,011	0,8
R	3	24	4764,421	0,002	0,5	R	3	23	4763,952	-0,004	1,0
R	3	22	4763,488	-0,005	1,0	R	3	21	4762,980	-0,022	0,0
R	3	20	4762,496	-0,009	0,5	R	3	19	4761,984	-0,000	0,8
R	3	18	4761,451	-0,004	1,0	R	3	17	4760,901	-0,003	1,0
R	3	16	4760.344	0,001	0,8	R	3	15	4759,755	-0,007	1,0
R	3	14	4759,172	0,004	1,0	R	3	13	4758,547	-0,009	0,3
R	3	12	4757,927	-0,003	0,8	R	3	11	4757,292	0,003	0,5
R	3	10	4756,635	0,003	0,8	R	3	9	4755,963	0,005	0,5
R	3	8	4755,267	-0,003	0,0	R	3	7	4754,570	0,004	0,5
R	3	6	4753,844	-0,001	0,5	R	3	5	4753,112	0,001	0,8
R	3	4	4752,354	-0,005	0,5	R	4	45	4765,928	0,023	0,0
R	4	43	4765,665	0,022	0,0	R	4	42	4765,530	0,033	0,3
R	4	41	4765.333	0,017	0,5	R	4	39	4764,938	0,014	0,0
R	4	38	4764.720	0,012	0,0	R	4	37	4764,489	0,021	0,0
R	4	36	4764,238	0,020	0,5	R	4	35	4763,952	0,005	0,8
R	4	34	4763,688	0,023	0,5	R	4	33	4763,382	0,019	0,5
R	4	32	4763,053	0,003	0,5	R	4	31	4762,732	0,015	0,8
R	4	29	4762,019	0,012	0,0	R	4	28	4761,641	0,013	1,0
R	4	27	4761,238	0,004	0,5	R	4	26	4760,844	0,020	0,3
R	4	25	4760,407	0,008	0,8	R	4	24	4759,964	0,006	0,8
R	4	23	4759,510	0,010	1,0	R	4	22	4759,046	0,018	0,3
R	4	21	4758,547	0,008	0,5	R	4	20	4758,043	0,007	1,0
R	4	19	4757,531	0,015	0,5	R	4	18	4756,986	0,004	0,8
R	4	17	4756,434	0,003	0,8	R	4	16	4755,882	0,017	0,0
R	4	15	4755,283	-0,001	0,5	R	4	14	4754,679	-0,008	0,0
R	4	13	4754,076	0,001	0,0	R	4	12	4753,445	-0,002	0,0
R	4	11	4752,799	-0,004	0,0	R	4	10	4752,132	-0,012	0,0
R	4	9	4751,449	-0,020	0,0	R	4	8	4750,779	-0,000	0,3

R	4	7	4750,079	0,005	1,0	R	4	6	4749,352	-0,001	0,3
R	4	5	4748,619	0,002	0,5	R	5	31	4756,986	-0,091	0,0
R	5	30	4756,635	-0,091	0,0	R	5	29	4756,267	-0,091	0,0
R	5	28	4755,882	-0,092	0,0	R	5	27	4755,490	-0,086	0,0
R	5	26	4755,084	-0,078	0,0	R	5	25	4754,679	-0,054	0,0
R	5	24	4754,215	-0,072	0,0	R	5	23	4753,770	-0,056	0,0
R	5	22	4753,300	-0,051	0,0	R	5	21	4752,828	-0,031	0,0
R	5	20	4752,313	-0,039	0,0	R	5	19	4751,804	-0,025	0,3
R	5	16	4750,147	-0,021	0,5	R	5	15	4749,563	-0,021	0,5
R	5	14	4748,971	-0,014	0,5	R	5	13	4748,350	-0,019	0,8
R	5	12	4747,735	-0,005	0,5	R	5	11	4747,091	-0,002	0,3
R	5	10	4746,429	-0,004	0,5	R	5	9	4745,756	0,000	0,5
R	5	8	4745,057	-0,007	0,5	R	5	7	4744,338	-0,019	0,0
R	5	6	4743,614	-0,020	0,5	R	6	22	4746,496	-0,005	0,5
R	6	21	4746,014	0,008	0,5	R	6	17	4743,878	0,008	0,5
R	6	16	4743,311	0,013	0,5	R	6	15	4742,719	0,007	0,5
R	6	12	4740,879	0,021	0,5						

APPENDIX III

FREQUENCIES FOR THE (0,0,3) BAND OF 15N02

	K	N	OBS	O-P	WT		K	N	OBS	O-P	WT
P	0	38	4612.866	0.004	0.8	P	0	36	4615.619	0.006	1.0
P	0	34	4618.317	0.009	0.0	P	0	32	4620.944	0.000	1.0
P	0	30	4623.526	0.004	1.0	P	0	28	4626.036	-0.007	0.8
P	0	26	4628.509	0.003	1.0	P	0	24	4630.915	0.005	0.5
P	0	22	4633.260	0.002	1.0	P	0	20	4635.562	0.016	0.0
P	0	18	4637.783	0.006	1.0	P	0	16	4639.960	0.009	0.8
P	0	14	4642.067	0.002	1.0	P	0	12	4644.126	0.003	1.0
P	0	10	4646.131	0.009	1.0	P	0	8	4648.064	0.002	0.8
P	0	6	4649.946	0.003	0.8	P	0	4	4651.778	0.013	0.3
P	0	2	4653.541	0.014	0.0	P	1	39	4611.313	0.009	0.0
P	1	38	4611.339	0.009	0.0	P	1	37	4614.071	0.003	0.0
P	1	36	4614.164	0.005	0.8	P	1	35	4616.772	-0.002	1.0
P	1	34	4616.920	*0.007	0.8	P	1	33	4619.421	-0.001	1.0
P	1	32	4619.647	0.014	0.0	P	1	31	4622.010	-0.000	1.0
P	1	30	4622.274	*0.005	0.0	P	1	29	4624.543	0.003	1.0
P	1	28	4624.852	*0.013	0.5	P	1	27	4627.015	0.003	1.0
P	1	26	4627.389	0.001	1.0	P	1	25	4629.429	0.004	0.3
P	1	24	4629.850	*0.001	1.0	P	1	23	4631.779	-0.000	1.0
P	1	22	4632.251	*0.001	0.0	P	1	21	4634.076	0.002	0.8
P	1	20	4634.585	*0.008	0.0	P	1	19	4636.313	0.002	1.0
P	1	18	4636.873	0.001	1.0	P	1	17	4638.488	-0.001	0.5
P	1	16	4639.091	0.000	1.0	P	1	15	4640.611	0.002	0.8
P	1	14	4641.250	0.002	1.0	P	1	13	4642.669	-0.000	0.3
P	1	12	4643.351	0.008	0.3	P	1	11	4644.685	0.014	0.0
P	1	10	4645.384	0.006	0.5	P	1	9	4646.612	-0.002	0.3
P	1	8	4647.351	0.000	1.0	P	1	7	4648.497	-0.001	0.5
P	1	6	4649.274	0.012	0.3	P	1	5	4650.324	0.000	0.5
P	1	4	4651.111	*0.001	0.5	P	1	3	4652.088	-0.002	0.3
P	1	2	4652.908	0.007	0.0	P	2	37	4611.604	-0.003	0.8
P	2	36	4612.671	*0.007	0.3	P	2	35	4614.363	0.003	0.3
P	2	34	4615.434	*0.008	0.0	P	2	33	4617.049	-0.004	1.0
P	2	32	4618.142	*0.001	1.0	P	2	31	4619.675	-0.011	0.0
P	2	30	4620.785	0.003	0.5	P	2	29	4622.251	-0.008	0.0
P	2	28	4623.354	*0.003	1.0	P	2	27	4624.771	-0.001	0.5
P	2	26	4625.865	*0.004	0.5	P	2	25	4627.228	-0.005	0.0
P	2	24	4628.315	*0.003	1.0	P	2	23	4629.611	-0.007	0.8
P	2	22	4630.703	*0.002	1.0	P	2	21	4631.946	-0.006	0.5
P	2	20	4633.022	*0.006	0.5	P	2	19	4634.222	-0.003	0.8
P	2	18	4635.286	*0.003	1.0	P	2	17	4636.436	-0.003	1.0
P	2	16	4637.485	*0.002	0.5	P	2	15	4638.589	-0.003	1.0
P	2	14	4639.617	*0.005	1.0	P	2	13	4640.690	0.004	0.0
P	2	12	4641.694	0.000	0.5	P	2	11	4642.711	-0.008	0.3

P	2	10	4643.702	0.002	0.8	P	2	9	4644.685	-0.007	0.3
P	2	8	4645.648	0.003	1.0	P	2	7	4646.612	0.006	0.3
P	2	6	4647.532	0.005	1.0	P	2	5	4648.461	0.003	0.3
P	2	4	4649.362	0.000	0.0	P	2	3	4650.255	0.005	0.0
P	3	35	4611.339	0.011	0.0	P	3	34	4612.671	0.004	0.0
P	3	33	4614.047	0.021	0.5	P	3	32	4615.345	0.006	0.5
P	3	31	4616.671	0.006	1.0	P	3	30	4617.955	0.005	1.0
P	3	29	4619.246	0.004	1.0	P	3	28	4620.505	0.005	0.5
P	3	27	4621.763	0.004	0.8	P	3	26	4622.990	0.001	1.0
P	3	25	4624.219	0.002	0.8	P	3	24	4625.418	0.000	1.0
P	3	23	4626.612	0.001	1.0	P	3	22	4627.785	-0.001	1.0
P	3	21	4628.951	0.001	1.0	P	3	20	4630.090	-0.003	1.0
P	3	19	4631.229	0.004	0.3	P	3	18	4632.334	-0.005	0.0
P	3	17	4633.439	0.002	0.5	P	3	16	4634.524	-0.001	0.0
P	3	15	4635.583	0.012	0.0	P	3	14	4636.645	-0.006	1.0
P	3	13	4637.683	0.007	1.0	P	3	12	4638.708	-0.007	1.0
P	3	11	4639.717	0.007	1.0	P	3	10	4640.707	-0.013	0.0
P	3	9	4641.694	0.005	0.5	P	3	8	4642.669	0.006	0.3
P	3	7	4643.607	0.005	0.3	P	3	6	4644.531	-0.015	0.0
P	3	5	4645.464	0.001	0.3	P	3	4	4646.357	-0.012	0.3
P	4	32	4611.374	0.134	0.0	P	4	31	4612.671	0.123	0.0
P	4	30	4613.956	0.116	0.0	P	4	29	4615.220	0.102	0.0
P	4	28	4616.486	0.106	0.0	P	4	27	4617.716	0.087	0.0
P	4	26	4618.939	0.078	0.0	P	4	25	4620.152	0.072	0.0
P	4	24	4621.347	0.064	0.0	P	4	23	4622.533	0.063	0.0
P	4	22	4623.697	0.054	0.0	P	4	21	4624.852	0.050	0.0
P	4	20	4625.987	0.042	0.3	P	4	19	4627.113	0.039	0.8
P	4	18	4628.218	0.032	0.8	P	4	17	4629.311	0.026	0.8
P	4	16	4630.390	0.021	0.8	P	4	15	4631.454	0.017	1.0
P	4	14	4632.506	0.016	1.0	P	4	13	4633.542	0.013	0.5
P	4	12	4634.567	0.014	0.0	P	4	11	4635.562	0.001	0.0
P	4	10	4636.559	0.004	1.0	P	4	9	4637.527	-0.006	0.5
P	4	8	4638.488	0.010	0.0	P	4	7	4639.440	-0.006	0.5
P	4	6	4640.371	0.009	0.3	P	4	5	4641.273	-0.025	0.0
P	5	28	4611.074	0.039	0.0	P	5	27	4612.328	-0.030	0.5
P	5	26	4613.569	0.018	0.8	P	5	25	4614.779	-0.022	1.0
P	5	24	4615.979	0.022	0.5	P	5	23	4617.173	-0.013	1.0
P	5	22	4618.344	0.012	0.0	P	5	21	4619.497	-0.015	0.8
P	5	20	4620.642	0.011	1.0	P	5	19	4621.763	-0.016	0.3
P	5	18	4622.872	0.018	0.0	P	5	17	4623.975	-0.012	0.5
P	5	16	4625.062	0.006	1.0	P	5	15	4626.133	-0.002	0.5
P	5	14	4627.193	0.006	0.0	P	5	13	4628.218	-0.007	0.3
P	5	12	4629.246	0.002	0.5	P	5	11	4630.252	-0.003	0.8
P	5	10	4631.229	0.019	0.0	P	5	9	4632.222	-0.004	0.0
P	5	8	4633.185	0.004	0.5	P	5	7	4634.123	-0.014	0.3
P	5	6	4635.070	0.001	0.5	P	6	22	4612.003	0.023	0.3
P	6	21	4613.142	0.010	0.5	P	6	20	4614.288	0.017	0.5
P	6	19	4615.401	0.006	0.0	P	6	18	4616.514	0.010	0.0
P	6	17	4617.606	0.008	0.5	P	6	16	4618.686	0.008	0.5
P	6	15	4619.742	0.002	0.3	P	6	14	4620.785	-0.010	0.0
P	6	13	4621.822	0.009	0.0	P	6	12	4622.842	-0.011	0.0
P	6	11	4623.859	0.001	0.5	P	6	10	4624.852	0.001	0.0
P	6	9	4625.821	0.008	0.0	P	6	8	4626.785	-0.007	0.3
P	7	15	4612.301	0.046	0.0	P	7	14	4613.358	-0.038	0.3

P	7	12	4615.401	*0.051	0.0		P	7	11	4616.416	-0.041	0.0
P	7	10	4617.433	*0.015	0.3		Q	1	1	4654.652	0.016	0.0
Q	1	3	4654.687	0.007	0.0		Q	1	4	4654.229	-0.006	0.5
Q	1	5	4654.760	0.001	0.3		Q	1	8	4653.205	-0.012	0.0
Q	2	2	4652.776	*0.005	0.0		Q	2	3	4652.732	-0.004	0.0
Q	2	4	4652.671	*0.003	0.3		Q	2	5	4652.618	0.017	0.0
Q	2	6	4652.498	*0.005	0.3		Q	2	7	4652.407	-0.002	0.0
Q	2	8	4652.258	*0.010	0.5		Q	2	9	4652.147	-0.018	0.0
Q	2	10	4651.952	*0.010	0.0		Q	2	13	4651.527	-0.005	0.0
Q	3	3	4649.727	*0.016	0.5		Q	3	4	4649.688	0.005	0.5
Q	3	5	4649.601	*0.006	0.3		Q	3	6	4649.511	-0.006	0.5
Q	3	7	4649.397	*0.014	0.0		Q	3	9	4649.144	-0.010	0.8
Q	3	10	4648.999	*0.005	0.5		Q	3	11	4648.829	-0.009	0.3
Q	4	4	4645.502	*0.015	0.0		Q	4	5	4645.445	0.003	0.0
Q	4	6	4645.352	*0.000	0.0		Q	4	7	4645.247	-0.001	0.0
Q	4	8	4645.131	0.004	0.0		Q	4	9	4644.996	0.004	0.0
Q	4	10	4644.836	*0.006	0.0		Q	4	12	4644.495	-0.002	0.0
Q	4	13	4644.315	0.013	0.0		Q	4	15	4643.878	0.012	0.3
Q	5	5	4640.144	0.009	0.5		Q	5	6	4640.036	-0.009	0.3
Q	5	8	4639.812	*0.010	0.5		Q	5	9	4639.683	-0.005	0.0
Q	5	11	4639.376	0.000	0.0		Q	5	12	4639.203	0.007	0.3
Q	6	6	4633.647	*0.003	0.5		Q	6	7	4633.551	0.004	0.5
Q	6	8	4633.430	0.001	0.0		Q	6	9	4633.287	-0.008	0.0
Q	6	10	4633.143	*0.005	0.0		R	0	44	4676.562	0.008	0.3
R	0	42	4676.287	*0.004	0.3		R	0	40	4675.956	-0.013	0.5
R	0	38	4675.591	0.004	1.0		R	0	36	4675.149	0.004	1.0
R	0	34	4674.635	*0.005	0.8		R	0	32	4674.074	0.002	1.0
R	0	30	4673.436	*0.006	0.0		R	0	28	4672.750	0.005	1.0
R	0	26	4671.980	*0.003	0.0		R	0	24	4671.151	-0.003	1.0
R	0	22	4670.260	0.001	1.0		R	0	20	4669.295	-0.002	0.8
R	0	18	4668.271	0.005	1.0		R	0	16	4667.178	0.000	1.0
R	0	14	4666.017	0.011	0.0		R	0	12	4664.779	0.002	1.0
R	0	10	4663.490	0.008	0.5		R	0	8	4662.123	-0.000	0.3
R	0	6	4660.683	*0.018	0.0		R	0	4	4659.220	0.005	1.0
R	0	2	4657.670	0.003	0.5		R	0	0	4656.061	0.004	0.3
R	1	45	4676.390	*0.007	0.3		R	1	44	4676.390	-0.005	0.3
R	1	43	4676.120	*0.009	0.3		R	1	42	4676.162	0.003	0.3
R	1	41	4675.787	*0.012	0.5		R	1	40	4675.853	0.002	0.5
R	1	39	4675.402	*0.005	0.5		R	1	38	4675.477	0.003	0.8
R	1	37	4674.955	*0.001	0.5		R	1	36	4675.026	0.001	0.3
R	1	35	4674.437	*0.004	0.8		R	1	34	4674.505	-0.001	0.8
R	1	33	4673.866	0.002	0.3		R	1	32	4673.914	-0.003	0.5
R	1	31	4673.225	*0.000	0.0		R	1	30	4673.249	-0.011	0.0
R	1	29	4672.528	0.003	1.0		R	1	28	4672.528	-0.005	1.0
R	1	27	4671.749	*0.013	0.0		R	1	26	4671.749	0.010	0.0
R	1	25	4670.937	*0.001	0.3		R	1	24	4670.866	-0.011	0.5
R	1	23	4670.048	*0.002	0.5		R	1	22	4669.948	-0.001	0.8
R	1	21	4669.102	0.001	1.0		R	1	20	4668.956	0.001	1.0
R	1	19	4668.109	0.019	0.0		R	1	18	4667.887	-0.007	1.0
R	1	17	4667.018	0.000	1.0		R	1	16	4666.771	0.002	0.0
R	1	15	4665.885	0.001	0.5		R	1	14	4665.572	-0.006	0.0
R	1	13	4664.691	0.002	1.0		R	1	12	4664.323	-0.001	1.0
R	1	11	4663.439	0.006	0.5		R	1	10	4663.008	0.002	0.0
R	1	9	4662.123	0.007	0.3		R	1	8	4661.627	0.003	1.0

R	1	7	4660.736	*0.002	0.0	R	1	6	4660.182	0.003	0.8
R	1	5	4659.300	*0.001	1.0	R	1	4	4658.680	0.010	0.3
R	1	3	4657.798	*0.004	0.3	R	1	2	4657.106	0.006	0.0
R	1	1	4656.247	0.003	0.8	R	2	45	4674.813	-0.007	0.3
R	2	44	4675.355	0.004	0.0	R	2	43	4674.560	-0.004	0.3
R	2	42	4675.026	0.001	0.0	R	2	41	4674.240	-0.003	0.5
R	2	40	4674.635	0.005	0.0	R	2	39	4673.866	0.007	0.5
R	2	38	4674.163	*0.003	0.5	R	2	37	4673.404	-0.005	0.0
R	2	36	4673.632	*0.002	1.0	R	2	35	4672.893	-0.002	1.0
R	2	34	4673.031	*0.005	1.0	R	2	33	4672.317	0.000	0.5
R	2	32	4672.367	*0.006	0.5	R	2	31	4671.662	-0.012	0.0
R	2	30	4671.640	*0.007	0.0	R	2	29	4670.961	-0.007	0.0
R	2	28	4670.866	0.007	0.3	R	2	27	4670.198	0.000	0.8
R	2	26	4670.006	*0.004	0.5	R	2	25	4669.350	-0.013	0.8
R	2	24	4669.102	0.001	0.5	R	2	23	4668.461	-0.004	0.8
R	2	22	4668.133	*0.001	0.0	R	2	21	4667.503	-0.001	1.0
R	2	20	4667.099	*0.008	0.8	R	2	19	4666.470	-0.010	0.0
R	2	18	4666.017	*0.007	0.0	R	2	17	4665.388	-0.005	1.0
R	2	16	4664.875	*0.008	0.5	R	2	15	4664.238	-0.006	1.0
R	2	14	4663.687	0.002	0.0	R	2	12	4662.428	0.000	0.3
R	2	11	4661.757	*0.002	1.0	R	2	10	4661.107	-0.006	1.0
R	2	9	4660.423	0.000	0.3	R	2	8	4659.739	-0.001	0.5
R	2	7	4659.026	0.001	0.8	R	2	6	4658.316	0.008	0.0
R	2	5	4657.572	0.005	0.8	R	2	4	4656.808	-0.008	0.3
R	2	3	4656.042	*0.006	0.3	R	2	2	4655.264	-0.002	0.0
R	3	45	4672.196	0.005	0.3	R	3	44	4672.274	0.005	0.0
R	3	43	4671.914	0.013	0.3	R	3	42	4671.914	0.008	0.3
R	3	41	4671.561	0.014	0.3	R	3	40	4671.493	0.008	0.3
R	3	39	4671.151	0.021	0.0	R	3	38	4671.005	-0.002	0.0
R	3	37	4670.660	0.010	0.8	R	3	36	4670.478	0.008	0.8
R	3	35	4670.112	0.005	0.3	R	3	34	4669.885	0.009	0.5
R	3	33	4669.503	0.001	1.0	R	3	32	4669.232	0.009	0.5
R	3	31	4668.839	0.005	1.0	R	3	30	4668.512	0.000	0.5
R	3	29	4668.133	0.028	0.0	R	3	28	4667.739	-0.002	0.8
R	3	27	4667.318	0.005	1.0	R	3	26	4666.913	0.002	1.0
R	3	25	4666.470	0.010	0.0	R	3	24	4666.017	-0.005	0.0
R	3	23	4665.541	*0.004	0.0	R	3	22	4665.073	0.001	1.0
R	3	21	4664.573	0.003	1.0	R	3	20	4664.061	-0.003	0.5
R	3	19	4663.526	*0.007	0.3	R	3	18	4663.008	0.013	0.0
R	3	17	4662.428	*0.007	0.0	R	3	16	4661.860	-0.006	1.0
R	3	15	4661.272	*0.005	0.8	R	3	14	4660.683	0.007	0.0
R	3	13	4660.054	*0.005	1.0	R	3	12	4659.425	-0.002	0.5
R	3	11	4658.769	*0.010	0.8	R	3	10	4658.112	-0.004	1.0
R	3	9	4657.439	0.000	0.0	R	3	8	4656.749	0.003	0.0
R	3	7	4656.037	*0.002	0.5	R	3	6	4655.310	-0.006	0.3
R	3	5	4654.570	*0.008	0.5	R	3	4	4653.817	-0.008	0.8
R	3	3	4653.066	0.009	0.0	R	4	37	4666.771	0.187	0.0
R	4	36	4666.513	0.196	0.0	R	4	35	4666.215	0.189	0.0
R	4	34	4665.885	0.158	0.0	R	4	32	4665.229	0.151	0.0
R	4	31	4664.875	0.147	0.0	R	4	30	4664.506	0.138	0.0
R	4	29	4664.104	0.115	0.0	R	4	28	4663.687	0.089	0.0
R	4	27	4663.294	0.104	0.0	R	4	26	4662.862	0.094	0.0
R	4	25	4662.428	0.098	0.0	R	4	24	4661.954	0.077	0.0
R	4	23	4661.481	0.072	0.0	R	4	22	4660.991	0.064	0.0

R	4	21	4660.480	0.051	0.0	R	4	20	4659.978	0.054	0.0
R	4	19	4659.425	0.037	0.0	R	4	18	4658.885	0.040	1.0
R	4	17	4658.316	0.029	0.0	R	4	16	4657.738	0.024	0.0
R	4	15	4657.140	0.015	0.3	R	4	14	4656.551	0.029	0.0
R	4	13	4655.921	0.017	0.8	R	4	12	4655.286	0.016	0.0
R	4	11	4654.626	0.004	0.0	R	4	10	4653.963	0.005	0.8
R	4	9	4653.284	0.005	1.0	R	4	8	4652.588	0.002	0.8
R	4	7	4651.873	-0.004	0.5	R	4	6	4651.151	-0.003	0.5
R	4	5	4650.419	0.004	0.5	R	4	4	4649.665	0.004	0.5
R	5	33	4660.126	-0.052	0.3	R	5	32	4659.785	-0.056	0.0
R	5	30	4659.077	-0.046	0.0	R	5	28	4658.316	-0.029	0.0
R	5	27	4657.899	-0.035	0.8	R	5	26	4657.485	-0.023	0.0
R	5	25	4657.044	-0.023	0.0	R	5	24	4656.593	-0.018	0.0
R	5	23	4656.104	-0.036	0.0	R	5	22	4655.636	-0.018	0.8
R	5	21	4655.131	-0.023	0.3	R	5	20	4654.626	-0.012	0.0
R	5	19	4654.106	-0.001	0.3	R	5	18	4653.541	-0.021	0.0
R	5	17	4652.997	-0.004	0.5	R	5	16	4652.420	-0.006	0.3
R	5	14	4651.220	-0.010	0.3	R	5	13	4650.605	-0.005	1.0
R	5	12	4649.967	-0.007	0.3	R	5	10	4648.661	0.001	0.5
R	5	9	4647.976	-0.003	0.8	R	5	8	4647.283	-0.002	0.8
R	5	6	4645.852	0.002	0.3	R	6	27	4651.615	0.017	0.3
R	6	25	4650.741	0.019	0.8	R	6	23	4649.794	0.007	0.3
R	6	21	4648.808	0.014	0.5	R	6	20	4648.291	0.016	0.5
R	6	19	4647.756	0.015	0.5	R	6	18	4647.211	0.018	0.8
R	6	16	4646.069	0.017	0.5	R	6	15	4645.441	-0.018	0.0
R	6	14	4644.831	-0.021	0.3	R	6	13	4644.221	-0.008	0.3
R	6	12	4643.599	0.007	0.0	R	6	11	4642.939	-0.001	0.3
R	6	10	4642.275	0.002	0.8	R	6	8	4640.895	-0.001	0.3
R	6	7	4640.181	-0.003	0.3	R	6	6	4639.457	-0.001	0.0

APPENDIX IV

FREQUENCIES FOR THE (1,0,3) BAND OF 14NO2

	K	N	OBS	O-P	WT		K	N	OBS	O-P	WT
P	0	46	5923,372	0,010	0,0	P	0	42	5930,554	-0,004	0,0
P	0	40	5934,026	0,003	0,5	P	0	38	5937,387	-0,013	0,3
P	0	36	5940,689	0,002	0,3	P	0	34	5943,883	-0,002	0,5
P	0	32	5946,983	-0,009	0,5	P	0	30	5950,010	0,001	1,0
P	0	28	5952,927	-0,009	0,5	P	0	26	5955,773	0,000	0,8
P	0	24	5958,533	0,012	0,5	P	0	22	5961,179	-0,001	1,0
P	0	20	5963,749	-0,002	1,0	P	0	18	5966,248	0,015	0,0
P	0	16	5968,620	-0,009	0,8	P	0	14	5970,936	-0,003	1,0
P	0	12	5973,157	-0,005	1,0	P	0	10	5975,305	0,006	1,0
P	0	8	5977,356	0,005	1,0	P	0	6	5979,326	0,008	0,5
P	0	4	5981,203	0,003	1,0	P	0	2	5982,988	-0,008	0,3
P	1	46	5922,620	-0,032	0,0	P	1	45	5924,938	-0,019	0,0
P	1	44	5926,296	0,006	0,0	P	1	43	5928,533	-0,001	0,3
P	1	42	5929,833	-0,005	0,0	P	1	41	5932,020	-0,004	0,0
P	1	40	5933,288	-0,006	0,3	P	1	39	5935,411	-0,013	0,5
P	1	38	5936,656	-0,003	0,3	P	1	37	5938,734	-0,003	0,8
P	1	36	5939,935	-0,001	0,5	P	1	35	5941,963	0,002	0,5
P	1	34	5943,133	0,010	0,0	P	1	33	5945,097	0,000	0,8
P	1	32	5946,224	0,002	1,0	P	1	31	5948,157	0,014	0,0
P	1	30	5949,240	0,006	0,5	P	1	29	5951,099	-0,003	1,0
P	1	28	5952,151	-0,006	0,8	P	1	27	5953,973	0,001	1,0
P	1	26	5954,991	-0,004	1,0	P	1	25	5956,750	-0,003	1,0
P	1	24	5957,747	0,001	0,8	P	1	23	5959,446	-0,001	1,0
P	1	22	5960,411	-0,000	1,0	P	1	21	5962,044	-0,009	1,0
P	1	20	5962,999	0,008	0,5	P	1	19	5964,577	0,006	0,8
P	1	18	5965,486	0,000	1,0	P	1	17	5966,998	-0,003	1,0
P	1	16	5967,900	0,005	0,3	P	1	15	5969,341	-0,002	1,0
P	1	14	5970,216	-0,005	1,0	P	1	13	5971,601	0,002	1,0
P	1	12	5972,467	0,006	1,0	P	1	11	5973,766	-0,000	1,0
P	1	10	5974,618	0,002	1,0	P	1	9	5975,845	-0,002	1,0
P	1	8	5976,690	0,002	1,0	P	1	7	5977,841	0,001	1,0
P	1	6	5978,677	0,002	0,8	P	1	5	5979,751	0,005	0,5
P	1	4	5980,567	-0,009	0,3	P	1	3	5981,564	0,000	0,5
P	2	46	5921,505	0,035	0,0	P	2	44	5925,043	-0,006	0,0
P	2	43	5926,665	0,028	0,0	P	2	42	5928,533	-0,008	0,3
P	2	41	5930,148	0,027	0,0	P	2	40	5931,954	0,006	0,0
P	2	39	5933,529	0,011	0,0	P	2	38	5935,272	0,002	0,3
P	2	37	5936,837	0,010	0,3	P	2	36	5938,517	0,010	0,0
P	2	35	5940,053	0,005	0,3	P	2	34	5941,663	0,002	0,5
P	2	33	5943,180	-0,001	0,5	P	2	32	5944,735	0,004	0,5
P	2	31	5946,224	-0,003	0,5	P	2	30	5947,702	-0,017	0,0
P	2	29	5949,212	0,026	0,0	P	2	28	5950,618	-0,005	0,5

P	2	27	5952,055	-0,003	0,5	P	2	26	5953,439	-0,005	1,0
P	2	25	5954,843	-0,000	1,0	P	2	24	5956,180	-0,001	1,0
P	2	23	5957,544	0,002	1,0	P	2	22	5958,837	0,002	1,0
P	2	21	5960,156	0,001	0,8	P	2	20	5961,403	-0,002	0,5
P	2	19	5962,680	-0,001	1,0	P	2	18	5963,885	-0,005	1,0
P	2	17	5965,118	-0,002	0,8	P	2	16	5966,284	-0,007	0,0
P	2	15	5967,477	0,002	1,0	P	2	14	5968,620	0,014	0,8
P	2	13	5969,745	0,003	1,0	P	2	12	5970,832	-0,002	1,0
P	2	11	5971,923	-0,002	1,0	P	2	10	5972,975	-0,003	1,0
P	2	9	5974,023	0,002	1,0	P	2	8	5975,042	0,009	0,5
P	2	7	5976,029	-0,003	1,0	P	2	6	5976,999	-0,004	0,5
P	2	5	5977,946	-0,011	0,5	P	2	4	5978,893	0,006	0,5
P	3	46	5918,669	0,008	0,0	P	3	45	5920,379	0,022	0,0
P	3	44	5922,226	0,003	0,0	P	3	43	5923,904	0,000	0,0
P	3	42	5925,701	-0,004	0,0	P	3	41	5927,388	0,023	0,0
P	3	40	5929,100	-0,006	0,5	P	3	39	5930,736	-0,004	0,0
P	3	38	5932,433	0,006	0,5	P	3	37	5934,026	-0,005	0,5
P	3	36	5935,670	0,006	0,5	P	3	35	5937,245	0,010	0,3
P	3	34	5938,814	-0,005	0,5	P	3	33	5940,357	0,001	0,5
P	3	32	5941,897	0,007	0,0	P	3	31	5943,395	0,006	0,5
P	3	30	5944,893	0,015	0,0	P	3	29	5946,330	-0,008	0,8
P	3	28	5947,791	0,008	0,5	P	3	27	5949,212	0,010	0,5
P	3	26	5950,618	0,015	0,5	P	3	25	5951,979	-0,001	0,3
P	3	24	5953,341	0,004	0,8	P	3	23	5954,672	-0,002	1,0
P	3	22	5955,988	0,000	1,0	P	3	21	5957,281	-0,001	1,0
P	3	20	5958,536	-0,017	1,0	P	3	19	5959,805	0,001	1,0
P	3	18	5961,025	-0,009	0,5	P	3	17	5962,244	0,003	1,0
P	3	16	5963,427	-0,001	1,0	P	3	15	5964,609	0,015	0,5
P	3	14	5965,740	0,003	1,0	P	3	13	5966,858	-0,002	1,0
P	3	12	5967,954	-0,007	0,5	P	3	11	5969,045	0,004	1,0
P	3	10	5970,106	0,007	1,0	P	3	9	5971,133	-0,004	1,0
P	3	8	5972,157	0,005	0,8	P	3	7	5973,157	0,010	0,5
P	3	6	5974,108	-0,012	0,5	P	3	5	5975,073	0,002	0,0
P	3	4	5975,992	-0,010	0,0	P	4	43	5919,608	-0,469	0,0
P	4	42	5921,350	-0,463	0,0	P	4	41	5923,044	-0,476	0,0
P	4	40	5924,737	-0,475	0,0	P	4	39	5926,419	-0,459	0,0
P	4	37	5929,694	-0,459	0,0	P	4	36	5931,293	-0,467	0,0
P	4	35	5932,892	-0,452	0,0	P	4	34	5934,433	-0,475	0,0
P	4	33	5935,997	-0,453	0,0	P	4	32	5937,510	-0,461	0,0
P	4	31	5939,026	-0,446	0,0	P	4	30	5940,507	-0,445	0,0
P	4	29	5941,963	-0,447	0,0	P	4	28	5943,395	-0,452	0,0
P	4	27	5944,820	-0,443	0,0	P	4	26	5946,224	-0,434	0,0
P	4	25	5947,597	-0,434	0,0	P	4	24	5948,956	-0,429	0,0
P	4	23	5950,288	-0,428	0,0	P	4	22	5951,582	-0,445	0,0
P	4	21	5952,868	-0,449	0,0	P	4	20	5954,158	-0,426	0,0
P	4	19	5955,417	-0,415	0,0	P	4	18	5956,627	-0,431	0,0
P	4	17	5957,814	-0,448	0,0	P	4	16	5958,999	-0,447	0,0
P	4	14	5961,265	-0,485	0,0	P	5	30	5935,863	-0,202	0,0
P	5	29	5937,307	-0,207	0,0	P	5	28	5938,734	-0,209	0,0
P	5	27	5940,136	-0,214	0,0	P	5	26	5941,535	-0,203	0,0
P	5	25	5942,903	-0,200	0,0	P	5	24	5944,252	-0,197	0,0
P	5	23	5945,592	-0,181	0,0	P	5	22	5946,904	-0,172	0,0
P	5	20	5949,456	-0,165	0,0	P	5	19	5950,693	-0,169	0,0
P	5	18	5951,918	-0,165	0,0	P	5	17	5953,129	-0,152	0,0

P	5	16	5954,316	-0,144	0,0	P	5	15	5955,477	-0,141	0,0
P	5	14	5956,627	-0,128	0,0	Q	1	3	5984,133	-0,006	0,0
Q	2	2	5982,317	-0,012	0,0	Q	2	3	5982,268	0,004	0,3
Q	2	4	5982,175	-0,002	0,0	Q	2	7	5981,792	-0,007	0,0
Q	3	4	5979,287	-0,007	0,0	Q	3	5	5979,187	-0,000	0,3
Q	3	6	5979,069	0,010	0,5	Q	3	7	5978,893	-0,016	0,0
Q	3	8	5978,751	0,014	0,0	Q	3	9	5978,542	-0,003	0,0
Q	3	10	5978,322	-0,009	0,5	R	0	44	5998,842	0,015	0,0
R	0	42	5999,211	-0,007	0,0	R	0	40	5999,534	0,018	0,3
R	0	38	5999,715	-0,009	0,0	R	0	36	5999,856	0,018	0,3
R	0	34	5999,856	-0,001	0,5	R	0	32	5999,790	0,008	0,0
R	0	30	5999,603	-0,008	0,5	R	0	28	5999,342	0,001	0,0
R	0	26	5998,987	0,014	0,5	R	0	24	5998,511	0,003	1,0
R	0	22	5997,955	0,010	0,5	R	0	20	5997,287	0,003	0,8
R	0	18	5996,527	0,001	1,0	R	0	16	5995,669	-0,003	1,0
R	0	14	5994,722	-0,002	0,8	R	0	12	5993,681	-0,000	0,8
R	0	10	5992,530	-0,016	0,5	R	0	8	5991,319	-0,002	0,8
R	0	6	5990,003	-0,002	0,8	R	0	4	5988,599	-0,002	0,0
R	0	2	5987,093	-0,014	0,5	R	0	0	5985,522	-0,006	0,0
R	1	45	5998,212	0,019	0,0	R	1	43	5998,594	0,008	0,0
R	1	42	6000,082	0,001	0,0	R	1	40	6000,309	0,012	0,0
R	1	38	6000,418	0,004	0,5	R	1	37	5999,211	-0,002	0,0
R	1	36	6000,442	0,011	0,0	R	1	35	5999,243	0,005	0,0
R	1	34	6000,357	0,006	0,0	R	1	33	5999,178	0,006	0,5
R	1	32	6000,173	0,000	0,5	R	1	30	5999,894	-0,005	0,0
R	1	29	5998,759	-0,002	0,5	R	1	28	5999,534	0,002	0,5
R	1	27	5998,425	0,006	0,5	R	1	26	5999,071	-0,000	0,8
R	1	25	5997,983	-0,002	0,0	R	1	24	5998,512	-0,007	0,8
R	1	23	5997,457	-0,003	1,0	R	1	22	5997,878	0,005	0,5
R	1	21	5996,841	-0,002	1,0	R	1	20	5997,150	0,011	0,3
R	1	19	5996,140	0,006	0,8	R	1	18	5996,318	0,004	1,0
R	1	17	5995,342	0,006	0,5	R	1	16	5995,407	0,006	0,5
R	1	15	5994,432	-0,016	0,0	R	1	14	5994,380	-0,019	0,0
R	1	13	5993,483	0,014	0,8	R	1	12	5993,326	0,016	0,8
R	1	11	5992,398	-0,002	1,0	R	1	10	5992,134	-0,000	1,0
R	1	9	5991,244	0,001	0,5	R	1	8	5990,858	-0,013	0,8
R	1	7	5990,003	0,007	0,8	R	1	6	5989,528	0,005	0,0
R	1	5	5988,666	0,005	0,0	R	1	4	5988,094	0,006	0,8
R	1	3	5987,235	-0,003	0,5	R	1	2	5986,552	-0,015	0,8
R	1	1	5985,724	-0,002	0,0	R	2	40	5999,178	-0,001	0,5
R	2	39	5998,176	0,014	0,0	R	2	37	5998,241	0,011	0,8
R	2	36	5999,071	0,007	0,0	R	2	35	5998,212	0,007	0,0
R	2	34	5998,870	-0,006	0,5	R	2	33	5998,085	-0,003	0,0
R	2	32	5998,594	-0,009	0,5	R	2	31	5997,878	-0,001	0,5
R	2	30	5998,240	-0,007	0,5	R	2	29	5997,579	-0,002	0,5
R	2	28	5997,806	-0,004	0,0	R	2	27	5997,194	0,005	0,0
R	2	26	5997,287	-0,005	0,5	R	2	25	5996,702	-0,006	1,0
R	2	24	5996,702	0,009	1,0	R	2	23	5996,140	0,003	0,5
R	2	22	5996,021	0,005	1,0	R	2	20	5995,256	-0,004	0,5
R	2	19	5994,722	-0,004	0,8	R	2	18	5994,432	0,008	0,0
R	2	17	5993,894	0,007	0,5	R	2	16	5993,483	-0,025	0,5
R	2	15	5992,965	0,005	0,5	R	2	14	5992,531	0,019	0,5
R	2	13	5991,931	-0,013	0,5	R	2	12	5991,423	-0,011	0,3
R	2	11	5990,858	0,018	0,5	R	2	10	5990,280	0,006	0,3

R	2	9	5989,651	0,002	0,0	R	2	8	5989,032	0,002	0,3
R	2	7	5988,366	-0,005	0,8	R	2	6	5987,699	-0,005	1,0
R	2	5	5987,020	0,014	0,0	R	2	4	5986,288	-0,006	0,3
R	2	3	5985,543	-0,012	0,0	R	2	2	5984,789	-0,009	0,0
R	3	45	5995,114	-0,010	0,5	R	3	43	5995,407	0,003	0,5
R	3	42	5995,753	-0,019	0,0	R	3	40	5995,863	0,003	0,0
R	3	39	5995,696	0,000	0,0	R	3	38	5995,863	-0,007	0,0
R	3	37	5995,706	-0,003	0,0	R	3	36	5995,787	-0,014	0,0
R	3	35	5995,623	-0,010	0,0	R	3	34	5995,641	-0,011	0,0
R	3	33	5995,466	-0,005	0,5	R	3	32	5995,407	-0,015	0,5
R	3	31	5995,212	-0,010	0,0	R	3	30	5995,114	0,004	0,8
R	3	29	5994,881	-0,003	0,5	R	3	28	5994,722	0,006	0,5
R	3	26	5994,240	0,001	0,8	R	3	25	5993,949	-0,002	0,3
R	3	24	5993,681	0,003	0,8	R	3	23	5993,365	0,011	0,0
R	3	22	5993,029	-0,004	0,5	R	3	21	5992,669	-0,003	0,8
R	3	20	5992,307	0,003	0,8	R	3	19	5991,931	0,027	0,0
R	3	18	5991,480	-0,011	0,0	R	3	17	5991,044	-0,005	1,0
R	3	16	5990,591	-0,001	0,5	R	3	15	5990,099	-0,010	0,8
R	3	14	5989,615	0,006	0,5	R	3	13	5989,063	-0,021	0,0
R	3	12	5988,632	0,093	0,0	R	3	11	5987,970	-0,003	0,3
R	3	10	5987,384	-0,002	1,0	R	3	9	5986,773	-0,003	0,8
R	3	8	5986,166	0,021	0,5	R	3	6	5984,819	-0,002	0,3
R	4	33	5991,123	-0,461	0,0	R	4	32	5991,014	-0,450	0,0
R	4	31	5990,891	-0,428	0,0	R	4	30	5990,700	-0,457	0,0
R	4	29	5990,525	-0,445	0,0	R	4	28	5990,326	-0,438	0,0
R	4	27	5990,099	-0,436	0,0	R	4	26	5989,847	-0,439	0,0
R	4	25	5989,615	-0,400	0,0	R	4	24	5989,286	-0,437	0,0
R	4	23	5989,032	-0,377	0,0	R	4	22	5988,632	-0,443	0,0
R	4	21	5988,295	-0,423	0,0	R	4	20	5987,922	-0,419	0,0
R	4	19	5987,506	-0,437	0,0	R	4	18	5987,093	-0,430	0,0
R	4	17	5986,639	-0,443	0,0	R	4	16	5986,166	-0,453	0,0
R	4	15	5985,695	-0,441	0,0	R	4	14	5985,190	-0,441	0,0
R	4	13	5984,666	-0,439	0,0	R	4	12	5984,117	-0,439	0,0
R	4	11	5983,554	-0,434	0,0	R	5	29	5985,903	-0,197	0,0
R	5	26	5985,190	-0,200	0,0	R	5	24	5984,621	-0,190	0,0
R	5	23	5984,282	-0,207	0,0	R	5	22	5983,963	-0,185	0,0
R	5	21	5983,581	-0,203	0,0	R	5	20	5983,217	-0,183	0,0
R	5	19	5982,820	-0,175	0,0	R	5	18	5982,386	-0,182	0,0
R	5	17	5981,955	-0,166	0,0	R	5	15	5981,007	-0,156	0,0
R	5	14	5980,471	-0,182	0,0	R	5	13	5979,967	-0,155	0,0
R	5	12	5979,402	-0,167	0,0	R	5	10	5978,227	-0,174	0,0

APPENDIX V

FREQUENCIES FOR THE (1,0,3) BAND OF 15NO2

	K	N	OBS	O-P	WT		K	N	OBS	O-P	WT
P	0	40	5824.847	0.006	0.0	P	0	38	5828.163	-0.007	0.3
P	0	36	5831.387	-0.023	0.0	P	0	34	5834.548	-0.012	0.5
P	0	32	5837.575	-0.046	0.5	P	0	30	5840.612	0.018	0.0
P	0	28	5843.508	0.029	0.5	P	0	26	5846.257	-0.020	0.0
P	0	24	5848.972	-0.015	0.8	P	0	22	5851.610	-0.002	0.8
P	0	20	5854.137	-0.014	0.3	P	0	18	5856.605	0.001	1.0
P	0	16	5858.977	0.003	0.3	P	0	14	5861.267	0.006	0.5
P	0	12	5863.464	-0.000	0.5	P	0	10	5865.601	0.015	0.5
P	0	8	5867.629	0.005	1.0	P	0	6	5869.595	0.015	0.8
P	0	4	5871.464	0.011	0.8	P	0	2	5873.255	0.012	0.0
P	1	39	5826.289	0.015	0.3	P	1	37	5829.543	0.004	0.3
P	1	36	5830.626	-0.005	0.3	P	1	35	5832.710	-0.005	0.3
P	1	34	5833.768	-0.009	0.3	P	1	33	5835.794	-0.009	0.3
P	1	32	5836.794	-0.041	0.0	P	1	31	5838.799	-0.006	0.8
P	1	30	5839.789	-0.019	0.3	P	1	29	5841.723	0.004	0.8
P	1	28	5842.658	-0.037	0.0	P	1	27	5844.540	-0.007	0.5
P	1	26	5845.469	-0.028	0.0	P	1	25	5847.287	-0.002	0.8
P	1	24	5848.203	-0.013	0.5	P	1	23	5849.957	0.011	0.3
P	1	22	5850.847	-0.003	0.8	P	1	21	5852.530	0.013	0.0
P	1	20	5853.403	-0.000	0.8	P	1	19	5855.006	0.002	1.0
P	1	18	5855.867	-0.006	1.0	P	1	17	5857.416	0.010	0.3
P	1	16	5858.264	0.004	1.0	P	1	15	5859.714	-0.009	0.3
P	1	14	5860.569	0.003	1.0	P	1	13	5861.956	0.001	1.0
P	1	12	5862.776	-0.014	0.0	P	1	11	5864.101	-0.003	1.0
P	1	10	5864.929	-0.002	1.0	P	1	9	5866.163	-0.005	0.8
P	1	8	5866.990	-0.001	0.8	P	1	7	5868.161	0.013	0.3
P	1	6	5868.963	-0.006	0.3	P	1	5	5870.037	-0.006	0.3
P	1	4	5870.867	0.002	1.0	P	1	3	5871.864	0.012	0.5
P	1	2	5872.676	-0.002	0.3	P	2	37	5827.699	-0.000	0.3
P	2	36	5829.327	0.006	0.3	P	2	35	5830.857	-0.015	0.3
P	2	34	5832.414	-0.019	0.3	P	2	33	5833.962	0.002	0.5
P	2	32	5835.457	-0.005	0.3	P	2	31	5836.946	-0.016	0.3
P	2	30	5838.414	0.005	1.0	P	2	29	5839.865	-0.013	0.3
P	2	28	5841.263	-0.013	0.8	P	2	27	5842.696	-0.014	0.0
P	2	26	5844.065	0.003	0.3	P	2	25	5845.469	0.010	0.0
P	2	23	5848.118	-0.005	0.5	P	2	22	5849.381	-0.009	0.8
P	2	21	5850.701	-0.003	1.0	P	2	20	5851.926	-0.007	1.0
P	2	19	5853.197	-0.005	0.5	P	2	18	5854.381	-0.012	1.0
P	2	17	5855.617	0.001	1.0	P	2	16	5856.762	-0.008	0.8
P	2	15	5857.944	-0.003	0.5	P	2	14	5859.049	-0.017	0.3
P	2	13	5860.188	-0.008	1.0	P	2	12	5861.267	-0.011	0.0
P	2	11	5862.359	-0.002	1.0	P	2	9	5864.437	-0.007	0.8

P	2	8	5865.446	*0.003	0.8	P	2	7	5866.429	-0.014	0.8
P	2	6	5867.402	*0.008	0.5	P	2	5	5868.348	-0.011	0.5
P	2	4	5869.314	0.029	0.0	P	3	36	5826.713	0.047	0.0
P	3	35	5828.272	0.058	0.3	P	3	34	5829.813	0.041	0.3
P	3	33	5831.308	0.022	0.0	P	3	32	5832.844	0.047	0.0
P	3	31	5834.326	0.050	0.5	P	3	30	5835.794	0.052	0.3
P	3	29	5837.221	0.038	0.3	P	3	28	5838.650	0.043	0.5
P	3	27	5840.047	0.039	1.0	P	3	26	5841.426	0.037	0.8
P	3	25	5842.771	0.020	0.3	P	3	24	5844.112	0.021	0.3
P	3	23	5845.469	0.057	0.0	P	3	22	5846.739	0.029	0.0
P	3	21	5848.812	0.022	0.5	P	3	20	5849.265	0.017	0.8
P	3	19	5850.506	0.020	1.0	P	3	18	5851.714	0.010	0.8
P	3	17	5852.912	0.011	0.5	P	3	16	5854.100	0.023	0.0
P	3	15	5855.244	0.011	0.8	P	3	14	5856.372	0.005	0.8
P	3	13	5857.476	*0.006	0.3	P	3	12	5858.573	-0.002	1.0
P	3	11	5859.655	0.007	0.3	P	3	10	5860.698	-0.002	0.5
P	3	9	5861.733	0.002	1.0	P	3	8	5862.776	0.034	0.0
P	3	7	5863.728	*0.003	0.3	P	3	6	5864.693	-0.007	0.5
P	3	5	5865.645	*0.003	0.0	P	4	36	5822.897	-0.028	0.0
P	4	35	5824.454	*0.030	0.0	P	4	33	5827.488	-0.056	0.3
P	4	32	5829.003	*0.042	0.3	P	4	31	5830.455	-0.069	0.3
P	4	29	5833.370	*0.054	0.5	P	4	28	5834.794	-0.049	0.5
P	4	27	5836.189	*0.053	0.3	P	4	26	5837.575	-0.046	0.0
P	4	25	5838.946	*0.034	0.5	P	4	24	5840.285	-0.034	0.8
P	4	23	5841.600	*0.036	0.5	P	4	22	5842.897	-0.038	0.5
P	4	21	5844.208	*0.005	0.0	P	4	20	5845.469	-0.001	0.0
P	4	18	5847.908	*0.015	0.5	P	4	17	5849.105	-0.014	0.8
P	4	16	5850.284	*0.010	1.0	P	4	15	5851.436	-0.014	0.8
P	4	14	5852.572	*0.012	0.0	P	4	13	5853.690	-0.008	0.8
P	4	12	5854.807	0.016	0.0	P	4	11	5855.867	0.004	0.0
P	4	10	5856.903	*0.012	0.5	P	4	9	5857.944	-0.002	0.0
P	4	8	5858.977	0.021	0.0	P	4	7	5859.940	-0.006	0.3
P	4	6	5860.924	0.009	0.0	P	5	33	5822.779	0.016	0.0
P	5	32	5824.291	0.033	0.0	P	5	31	5825.732	-0.001	0.3
P	5	30	5827.208	0.019	0.3	P	5	29	5828.643	0.018	0.3
P	5	28	5830.069	0.027	0.3	P	5	26	5832.844	0.030	0.5
P	5	25	5834.206	0.035	0.3	P	5	24	5835.537	0.029	0.3
P	5	23	5836.845	0.020	0.5	P	5	22	5838.146	0.025	0.3
P	5	21	5839.434	0.036	0.5	P	5	20	5840.690	0.036	0.0
P	5	19	5841.935	0.045	0.0	P	5	18	5843.120	0.014	0.3
P	5	17	5844.322	0.021	0.3	P	5	14	5847.780	0.015	0.3
P	5	13	5848.949	0.069	0.3	P	5	12	5849.979	0.006	0.0
P	5	11	5851.050	0.005	0.3	P	5	10	5852.139	0.041	0.0
P	5	6	5856.094	*0.004	0.3	P	5	7	5855.133	0.004	0.3
P	6	25	5828.439	0.021	0.3	P	6	24	5829.771	0.017	0.0
P	6	23	5831.885	0.015	0.3	P	6	22	5832.414	0.048	0.0
P	6	21	5833.640	*0.002	0.3	P	6	20	5834.891	-0.008	0.3
P	6	19	5836.189	0.054	0.0	P	6	18	5837.336	-0.015	0.3
P	6	17	5838.521	*0.026	0.3	P	6	16	5839.701	-0.022	0.3
P	6	15	5840.829	*0.049	0.3	P	6	11	5845.245	-0.049	0.3
P	6	10	5846.364	0.017	0.3	Q	1	1	5874.436	0.022	0.0
Q	1	2	5874.287	0.014	0.0	Q	1	3	5874.436	0.004	0.3
Q	1	4	5873.970	0.016	0.0	Q	2	6	5872.329	-0.012	0.0
Q	3	3	5869.954	0.005	0.3	Q	4	7	5865.706	-0.001	0.0

R	0	36	5890.448	*0.006	0.0	R	0	34	5890.448	0.011	0.0
R	0	32	5890.313	*0.012	0.3	R	0	26	5889.443	0.024	0.0
R	0	22	5888.314	*0.021	0.5	R	0	20	5887.642	-0.008	0.8
R	0	18	5886.867	*0.004	1.0	R	0	16	5886.005	0.008	0.5
R	0	14	5885.035	0.005	0.5	R	0	12	5883.981	0.009	0.5
R	0	10	5882.830	0.006	0.5	R	0	8	5881.578	-0.009	0.5
R	0	6	5880.276	0.014	0.0	R	0	4	5878.838	-0.014	0.0
R	0	2	5877.358	0.004	0.0	R	0	0	5875.776	0.002	0.0
R	1	30	5890.448	*0.013	0.3	R	1	29	5889.340	0.020	0.3
R	1	28	5890.064	0.003	0.3	R	1	26	5889.576	0.007	0.0
R	1	25	5888.477	0.004	0.8	R	1	24	5888.977	-0.009	0.5
R	1	23	5887.912	*0.002	0.5	R	1	22	5888.314	0.001	0.0
R	1	21	5887.288	0.020	0.5	R	1	20	5887.564	0.012	0.5
R	1	19	5886.555	0.022	0.5	R	1	18	5886.693	-0.010	0.8
R	1	17	5885.713	0.002	0.0	R	1	16	5885.773	0.004	0.5
R	1	15	5884.777	*0.024	0.0	R	1	14	5884.731	-0.017	0.0
R	1	13	5883.795	*0.009	0.5	R	1	12	5883.649	0.007	0.8
R	1	11	5882.725	0.006	0.5	R	1	10	5882.438	-0.014	0.0
R	1	9	5881.578	0.029	0.3	R	1	7	5880.276	-0.016	0.0
R	1	6	5879.816	*0.003	0.8	R	1	5	5878.947	-0.003	0.5
R	1	4	5878.365	*0.012	0.5	R	1	3	5877.516	-0.006	0.0
R	2	38	5890.064	0.014	0.0	R	2	36	5889.901	-0.008	0.3
R	2	35	5888.977	*0.010	0.0	R	2	34	5889.657	-0.023	0.0
R	2	32	5889.340	*0.024	0.3	R	2	31	5888.570	-0.012	0.3
R	2	30	5888.977	0.011	0.3	R	2	28	5888.477	-0.010	0.0
R	2	27	5887.821	0.004	0.5	R	2	26	5887.912	-0.017	0.3
R	2	25	5887.288	*0.013	0.0	R	2	24	5887.288	-0.005	0.3
R	2	23	5886.693	*0.005	0.5	R	2	22	5886.555	-0.026	0.0
R	2	21	5886.005	*0.004	0.5	R	2	20	5885.773	*0.020	0.0
R	2	19	5885.234	0.002	0.3	R	2	18	5884.919	-0.009	0.5
R	2	17	5884.370	0.000	0.5	R	2	16	5883.981	-0.006	0.5
R	2	15	5883.409	*0.012	0.5	R	2	14	5882.982	0.013	0.5
R	2	13	5882.387	0.000	0.0	R	2	12	5881.871	-0.001	1.0
R	2	11	5881.254	*0.015	0.3	R	2	10	5880.719	0.022	0.0
R	2	9	5880.061	*0.004	1.0	R	2	8	5879.440	-0.002	1.0
R	2	7	5878.780	0.003	0.3	R	2	6	5878.095	-0.011	0.3
R	2	5	5877.404	*0.001	0.3	R	3	31	5886.150	0.056	0.3
R	3	30	5886.005	0.035	0.5	R	3	29	5885.773	0.058	0.0
R	3	28	5885.577	0.044	0.5	R	3	27	5885.297	0.044	0.3
R	3	26	5885.035	0.018	0.8	R	3	25	5884.731	0.023	0.0
R	3	24	5884.447	0.026	0.3	R	3	23	5884.108	0.029	0.3
R	3	22	5883.795	0.050	0.3	R	3	21	5883.409	0.041	0.3
R	3	19	5882.592	0.018	0.5	R	3	18	5882.169	0.019	0.3
R	3	17	5881.700	0.003	0.5	R	3	16	5881.254	0.024	0.0
R	3	15	5880.754	0.016	0.0	R	3	13	5879.703	0.007	0.8
R	3	12	5879.164	0.021	0.0	R	3	11	5878.572	0.001	0.8
R	3	10	5877.972	*0.004	0.3	R	3	8	5876.724	-0.003	0.5
R	3	7	5876.063	*0.008	0.0	R	3	6	5875.391	-0.003	0.0
R	3	4	5873.970	*0.008	0.0	R	3	3	5873.255	0.016	0.0
R	4	28	5881.700	*0.041	0.3	R	4	27	5881.443	-0.052	0.3
R	4	26	5881.203	*0.027	0.0	R	4	25	5880.885	-0.058	0.8
R	4	24	5880.588	*0.050	0.5	R	4	23	5880.276	-0.034	0.0
R	4	22	5879.923	*0.040	0.5	R	4	21	5879.563	-0.033	0.5
R	4	19	5878.780	*0.019	0.3	R	4	18	5878.365	-0.005	0.3

R	4	17	5877.913	-0.008	0.3	R	4	15	5876.954	-0.006	1.0
R	4	14	5876.452	0.003	0.5	R	4	13	5875.904	-0.012	0.5
R	4	12	5875.367	0.004	0.3	R	4	11	5874.805	0.015	0.0
R	4	10	5874.204	0.008	0.3	R	4	9	5873.592	0.011	0.5
R	4	8	5872.973	0.026	0.3	R	4	7	5872.329	0.039	0.0
R	5	23	5875.537	0.027	0.3	R	5	22	5875.197	0.036	0.0
R	5	21	5874.805	0.013	0.3	R	5	20	5874.436	0.033	0.3
R	5	19	5874.027	0.034	0.3	R	5	18	5873.592	0.030	0.0
R	5	16	5872.676	0.035	0.0	R	5	15	5872.170	0.020	0.0
R	5	14	5871.665	0.027	0.3	R	5	13	5871.122	0.016	0.3
R	5	12	5870.571	0.019	0.0	R	5	11	5870.037	0.058	0.0
R	5	10	5869.459	0.074	0.3						

APPENDIX VI

FREQUENCIES FOR THE (3,0,1) BAND OF 14NO2

	K	N	OBS	O-P	WT		K	N	OBS	O-P	WT
P	0	36	5394.108	0.005	0.3	P	0	34	5397.253	-0.007	0.3
P	0	32	5400.336	0.019	0.0	P	0	30	5403.295	0.015	0.3
P	0	28	5406.159	0.008	0.5	P	0	26	5408.938	0.005	0.5
P	0	24	5411.633	0.005	0.8	P	0	22	5414.242	0.004	0.8
P	0	20	5416.768	0.003	0.5	P	0	18	5419.207	-0.002	0.3
P	0	16	5421.544	-0.028	0.0	P	0	14	5423.853	0.000	0.3
P	0	12	5426.042	-0.011	0.5	P	0	10	5428.168	-0.004	0.8
P	0	8	5430.207	-0.002	0.3	P	0	6	5432.159	-0.006	0.5
P	0	4	5434.032	-0.007	0.3	P	0	2	5435.832	0.001	0.5
P	1	32	5400.260	0.011	0.5	P	1	31	5401.863	0.005	0.8
P	1	30	5403.191	0.000	0.5	P	1	29	5404.783	-0.003	0.5
P	1	28	5406.046	0.000	0.8	P	1	27	5407.621	-0.003	1.0
P	1	26	5408.826	0.009	0.5	P	1	25	5410.366	-0.007	1.0
P	1	24	5411.504	-0.001	0.3	P	1	23	5413.029	-0.007	1.0
P	1	22	5414.109	-0.005	1.0	P	1	21	5415.599	-0.013	1.0
P	1	20	5416.643	0.001	1.0	P	1	19	5418.108	-0.003	1.0
P	1	18	5419.087	-0.003	1.0	P	1	17	5420.507	-0.003	1.0
P	1	16	5421.456	-0.004	1.0	P	1	15	5422.829	-0.004	1.0
P	1	14	5423.746	-0.003	1.0	P	1	13	5425.065	-0.006	1.0
P	1	12	5425.964	0.003	0.5	P	1	11	5427.218	-0.007	0.8
P	1	10	5428.103	0.010	0.3	P	1	9	5429.284	-0.010	0.8
P	1	8	5430.153	0.007	0.3	P	1	7	5431.272	-0.007	0.8
P	1	6	5432.122	0.003	0.0	P	1	5	5433.165	-0.014	0.3
P	1	4	5434.011	0.000	0.0	P	1	3	5434.979	-0.015	0.0
P	1	2	5435.832	0.008	0.5	P	2	35	5395.665	-0.011	0.3
P	2	34	5397.211	-0.005	0.3	P	2	33	5398.729	-0.041	0.0
P	2	32	5400.260	0.009	0.5	P	2	31	5401.749	-0.022	0.0
P	2	30	5403.191	-0.007	0.5	P	2	29	5404.626	-0.056	0.0
P	2	28	5406.046	-0.015	0.3	P	2	27	5407.547	0.041	0.0
P	2	26	5408.826	-0.015	0.5	P	2	25	5410.272	0.027	0.3
P	2	24	5411.542	0.003	0.3	P	2	23	5412.923	0.024	0.0
P	2	22	5414.160	0.003	0.3	P	2	21	5415.497	0.026	0.0
P	2	20	5416.698	0.005	0.5	P	2	19	5417.980	0.019	0.3
P	2	18	5419.151	0.004	0.5	P	2	17	5420.379	0.010	0.3
P	2	16	5421.522	0.002	0.5	P	2	15	5422.707	0.012	0.3
P	2	14	5423.822	0.011	0.3	P	2	13	5424.943	0.004	0.5
P	2	12	5426.042	0.022	0.3	P	2	11	5427.098	-0.004	1.0
P	2	10	5428.168	0.022	0.5	P	2	9	5429.184	0.001	0.8
P	2	8	5430.207	0.018	0.3	P	2	7	5431.189	0.007	0.8
P	2	6	5432.159	0.011	0.3	P	2	5	5433.109	0.011	0.3
P	2	4	5434.032	0.008	0.3	P	2	3	5434.919	-0.013	0.0
P	3	33	5398.622	0.037	0.0	P	3	32	5400.122	0.031	0.0

P	3	31	5401.596	0.019	0.3	P	3	30	5402.964	-0.074	0.0
P	3	29	5404.493	0.012	0.3	P	3	28	5405.905	0.007	0.3
P	3	27	5407.304	0.006	0.3	P	3	26	5408.674	0.001	0.5
P	3	25	5410.033	0.001	0.5	P	3	24	5411.366	-0.000	0.5
P	3	23	5412.687	0.003	0.5	P	3	22	5413.972	-0.005	0.0
P	3	21	5415.256	0.002	0.5	P	3	20	5416.506	-0.000	0.5
P	3	19	5417.735	-0.006	0.5	P	3	18	5418.949	-0.005	0.5
P	3	17	5420.141	-0.007	0.5	P	3	16	5421.316	-0.004	0.5
P	3	15	5422.470	-0.003	0.5	P	3	14	5423.599	-0.006	0.5
P	3	13	5424.707	-0.011	0.5	P	3	12	5425.805	-0.004	0.5
P	3	11	5426.868	-0.012	0.3	P	3	10	5427.917	-0.014	0.3
P	3	9	5428.959	-0.002	0.3	P	3	8	5429.972	0.002	0.0
P	4	23	5412.485	0.193	0.0	P	4	22	5413.779	0.196	0.0
P	4	21	5415.048	0.195	0.0	P	4	20	5416.298	0.186	0.0
P	4	19	5417.533	0.199	0.0	P	4	18	5418.737	0.192	0.0
P	4	17	5419.927	0.192	0.0	P	4	16	5421.095	0.189	0.0
P	4	15	5422.250	0.195	0.0	P	4	14	5423.375	0.190	0.0
P	4	13	5424.480	0.185	0.0	P	4	12	5425.576	0.192	0.0
P	4	11	5426.668	0.214	0.0	P	4	10	5427.665	0.162	0.0
P	4	9	5428.728	0.196	0.0	P	5	29	5404.056	-0.010	0.0
P	5	28	5405.469	-0.001	0.0	P	5	27	5406.861	0.007	0.0
P	5	26	5408.225	0.007	0.0	P	5	25	5409.556	-0.005	0.3
P	5	24	5410.874	-0.010	0.3	P	5	23	5412.190	0.002	0.3
P	5	22	5413.472	0.000	0.0	P	5	21	5414.734	-0.002	0.5
P	5	20	5415.967	-0.013	0.3	P	5	19	5417.221	0.017	0.5
P	5	18	5418.416	0.007	0.5	P	5	17	5419.592	-0.002	0.5
P	5	16	5420.754	-0.005	0.3	P	5	15	5421.902	-0.003	0.3
P	5	14	5423.024	-0.006	0.3	P	5	13	5424.140	0.005	0.3
R	0	30	5452.960	0.025	0.3	R	0	28	5452.626	0.014	0.8
R	0	26	5452.194	0.005	1.0	R	0	24	5451.628	-0.040	0.0
R	0	22	5451.065	0.013	1.0	R	0	20	5450.362	0.019	0.3
R	0	18	5449.557	0.016	0.3	R	0	16	5448.663	0.014	0.5
R	0	14	5447.682	0.016	0.5	R	0	12	5446.614	0.018	0.8
R	0	10	5445.451	0.013	1.0	R	0	8	5444.204	0.010	1.0
R	0	6	5442.869	0.005	1.0	R	0	4	5441.457	0.009	0.8
R	0	2	5439.975	0.028	0.3	R	0	0	5438.376	0.012	0.3
R	1	32	5454.280	0.012	0.8	R	1	31	5452.741	-0.013	1.0
R	1	30	5453.907	-0.020	0.8	R	1	29	5452.490	0.013	0.3
R	1	28	5453.474	-0.015	0.8	R	1	27	5452.116	0.012	0.3
R	1	26	5452.960	0.001	0.8	R	1	25	5451.628	-0.009	0.5
R	1	24	5452.328	-0.012	0.8	R	1	23	5451.065	-0.014	1.0
R	1	22	5451.628	-0.005	0.5	R	1	21	5450.426	-0.004	1.0
R	1	20	5450.844	0.003	1.0	R	1	19	5449.702	0.008	1.0
R	1	18	5449.965	0.001	1.0	R	1	17	5448.859	-0.010	1.0
R	1	16	5448.995	-0.010	1.0	R	1	15	5447.957	0.001	1.0
R	1	14	5447.957	-0.006	1.0	R	1	13	5446.958	0.000	1.0
R	1	12	5446.833	-0.007	1.0	R	1	11	5445.864	-0.009	1.0
R	1	10	5445.629	-0.006	1.0	R	1	9	5444.701	-0.000	1.0
R	1	8	5444.342	-0.005	1.0	R	1	7	5443.443	-0.001	1.0
R	1	6	5442.965	-0.015	1.0	R	1	5	5442.102	0.001	0.0
R	1	4	5441.512	-0.020	0.3	R	1	3	5440.664	-0.007	0.5
R	1	2	5439.975	-0.026	0.3	R	1	1	5439.130	-0.027	0.0
R	2	19	5450.053	0.011	0.8	R	2	18	5449.702	-0.010	0.8
R	2	17	5449.178	0.011	1.0	R	2	16	5448.781	0.017	0.8

R	2	15	5448.214	0.006	0.8	R	2	14	5447.758	0.009	0.5
R	2	13	5447.167	0.003	0.8	R	2	12	5446.614	-0.025	0.0
R	2	11	5446.035	-0.002	1.0	R	2	10	5445.451	-0.008	0.8
R	2	9	5444.827	0.000	0.8	R	2	8	5444.204	0.005	0.8
R	2	7	5443.528	-0.006	0.5	R	2	6	5442.869	0.010	1.0
R	3	24	5451.743	-0.006	0.3	R	3	23	5451.396	-0.010	0.5
R	3	22	5451.065	0.002	0.8	R	3	21	5450.683	0.000	0.3
R	3	20	5450.295	0.001	0.0	R	3	19	5449.873	-0.003	0.3
R	3	18	5449.444	0.000	0.3	R	3	17	5448.995	0.008	0.5
R	3	16	5448.513	-0.000	0.8	R	3	15	5448.019	0.003	0.0
R	3	14	5447.507	0.006	0.5	R	3	13	5446.958	-0.006	0.8
R	3	12	5446.425	0.017	0.0	R	3	11	5445.864	0.034	0.0
R	3	10	5445.255	0.022	0.0	R	3	9	5444.562	-0.053	0.0
R	3	7	5443.280	-0.037	0.0	R	4	21	5450.479	0.185	0.0
R	4	19	5449.702	0.222	0.0	R	4	16	5448.294	0.188	0.0
R	4	15	5447.804	0.195	0.0	R	4	13	5446.758	0.199	0.0

APPENDIX VII

FREQUENCIES FOR THE (3,0,1) BAND OF 15NO2

	K	N	OBS	O-P	WT		K	N	OBS	O-P	WT
P	0	32	5330.846	*0.007	0.3	P	0	30	5333.722	0.022	0.3
P	0	26	5339.166	*0.002	0.0	P	0	24	5341.770	-0.019	0.5
P	0	20	5346.825	0.022	0.0	P	0	18	5349.207	0.011	0.8
P	0	16	5351.508	*0.007	1.0	P	0	12	5355.908	-0.015	0.5
P	0	8	5360.826	*0.001	0.3	P	0	6	5361.966	0.000	0.3
P	0	4	5363.831	0.004	0.5	P	1	30	5333.407	-0.025	0.3
P	1	29	5335.104	0.010	0.5	P	1	25	5340.497	-0.003	0.5
P	1	24	5341.548	0.041	0.0	P	1	23	5343.091	0.001	0.3
P	1	22	5344.057	*0.001	0.8	P	1	21	5345.634	0.032	0.3
P	1	20	5346.563	0.026	0.0	P	1	19	5348.041	0.003	1.0
P	1	18	5348.946	0.003	0.8	P	1	17	5350.376	-0.019	0.8
P	1	16	5351.276	0.001	0.8	P	1	14	5353.519	-0.015	0.3
P	1	12	5355.719	0.001	0.5	P	1	11	5356.980	-0.016	0.3
P	1	10	5357.847	0.019	0.3	P	1	8	5359.867	0.005	0.5
P	1	7	5360.987	*0.014	0.3	P	1	5	5362.889	0.005	0.3
P	1	3	5364.682	*0.004	0.5	P	2	31	5331.772	-0.040	0.3
P	2	30	5333.157	0.022	0.3	P	2	29	5334.600	-0.020	0.5
P	2	28	5335.914	*0.000	0.3	P	2	27	5337.356	-0.004	0.5
P	2	25	5340.005	*0.025	0.5	P	2	24	5341.274	0.005	1.0
P	2	22	5343.834	*0.006	0.8	P	2	20	5346.356	0.018	0.3
P	2	19	5347.616	0.013	0.5	P	2	17	5349.983	0.006	0.5
P	2	16	5351.109	0.002	0.8	P	2	15	5352.275	-0.002	0.3
P	2	14	5353.342	*0.034	0.0	P	2	13	5354.495	-0.003	0.5
P	2	12	5355.564	*0.003	1.0	P	2	11	5356.650	0.007	0.3
P	2	10	5357.698	0.022	0.3	P	2	9	5358.704	-0.004	0.8
P	2	8	5359.697	*0.009	0.5	P	2	7	5360.688	-0.006	0.3
P	2	6	5361.637	*0.019	0.3	P	2	5	5362.588	-0.013	0.3
P	2	4	5363.504	*0.020	0.3	P	3	30	5331.369	0.018	0.3
P	3	29	5332.793	0.013	0.3	P	3	28	5334.199	0.017	0.3
P	3	27	5335.577	0.002	0.3	P	3	26	5336.924	-0.021	0.3
P	3	24	5339.643	0.008	0.3	P	3	23	5340.966	0.011	0.5
P	3	19	5346.027	*0.010	0.3	P	3	17	5348.445	-0.015	0.5
P	3	16	5349.632	*0.010	0.5	P	3	15	5350.783	-0.021	0.8
P	3	14	5351.916	*0.029	0.3	P	3	13	5353.064	-0.002	0.0
P	3	12	5354.120	*0.045	0.0	P	3	11	5355.225	-0.019	0.3
P	3	10	5356.295	*0.007	0.5	P	3	9	5357.346	0.007	0.3
P	3	8	5358.353	*0.002	0.5	P	3	7	5359.364	0.015	0.3
P	3	6	5360.322	0.001	0.3	P	3	5	5361.308	0.035	0.3
P	4	21	5335.395	*0.186	0.0	P	4	20	5336.738	-0.170	0.0
P	4	19	5337.976	*0.236	0.0	P	4	18	5339.397	-0.097	0.0
P	4	17	5340.734	*0.021	0.0	P	4	16	5341.966	-0.025	0.0
P	4	15	5343.227	0.021	0.0	R	0	24	5381.811	-0.006	0.3

R	0	22	5381.125	-0.013	0.0		R	0	20	5380.397	0.024	0.3
R	0	18	5379.490	-0.033	0.3		R	0	14	5377.572	0.003	0.3
R	0	12	5376.498	0.031	0.3		R	0	8	5374.029	0.014	0.3
R	0	6	5372.685	0.019	0.3		R	0	4	5371.253	0.016	0.3
R	0	2	5369.724	-0.004	0.3		R	1	31	5383.206	0.012	0.3
R	1	29	5382.814	0.020	0.5		R	1	27	5382.378	0.062	0.0
R	1	26	5383.053	-0.015	0.5		R	1	24	5382.378	0.003	0.3
R	1	23	5381.125	-0.001	0.3		R	1	22	5381.631	0.026	1.0
R	1	21	5380.394	-0.018	0.8		R	1	20	5380.744	-0.015	0.3
R	1	19	5379.645	0.026	0.3		R	1	18	5379.825	-0.012	0.8
R	1	16	5378.814	-0.025	0.0		R	1	15	5377.789	-0.001	0.3
R	1	14	5377.789	0.026	0.3		R	1	13	5376.737	-0.017	0.3
R	1	11	5375.605	-0.033	0.3		R	1	10	5375.374	-0.007	0.5
R	1	8	5374.023	-0.051	0.0		R	1	7	5373.150	-0.012	0.3
R	1	6	5372.685	-0.005	0.8		R	1	5	5371.819	0.016	0.3
R	1	4	5371.253	0.024	0.0		R	1	3	5370.359	-0.004	0.5
R	1	2	5369.724	0.034	0.0		R	2	29	5383.053	-0.041	0.3
R	2	28	5383.206	-0.007	0.5		R	2	27	5382.569	0.011	0.8
R	2	26	5382.569	0.002	0.8		R	2	22	5381.122	0.038	0.3
R	2	20	5380.248	0.005	0.5		R	2	19	5379.645	-0.035	0.3
R	2	18	5379.375	0.041	0.3		R	2	17	5378.814	0.043	0.0
R	2	15	5377.769	0.007	1.0		R	2	14	5377.298	-0.007	0.8
R	2	13	5376.737	0.021	0.3		R	2	12	5376.207	0.024	0.3
R	2	11	5375.605	0.034	0.3		R	2	10	5374.995	0.009	0.8
R	2	8	5373.710	-0.003	0.8		R	2	7	5373.028	-0.014	0.5
R	2	6	5372.370	0.008	0.5		R	2	5	5371.673	0.017	0.3
R	2	4	5370.929	-0.005	0.3		R	2	2	5369.417	-0.011	0.0
R	3	14	5375.785	-0.008	0.5		R	3	10	5373.575	0.009	0.3
R	3	9	5372.936	-0.022	0.0		R	3	8	5372.370	0.041	0.3
R	3	7	5371.673	-0.006	0.3		R	3	5	5370.359	0.044	0.3